

Rowan University

Rowan Digital Works

Theses and Dissertations

1-2-2023

INVESTIGATING THE ROLE OF VASOPRESSIN RECEPTOR 1A EXPRESSING NEURONS IN MOUSE DORSAL RAPHE

Tirth Nimishbhai Patel
Rowan University

Follow this and additional works at: <https://rdw.rowan.edu/etd>



Part of the [Neurosciences Commons](#)

Recommended Citation

Patel, Tirth Nimishbhai, "INVESTIGATING THE ROLE OF VASOPRESSIN RECEPTOR 1A EXPRESSING NEURONS IN MOUSE DORSAL RAPHE" (2023). *Theses and Dissertations*. 3178.
<https://rdw.rowan.edu/etd/3178>

This Dissertation is brought to you for free and open access by Rowan Digital Works. It has been accepted for inclusion in Theses and Dissertations by an authorized administrator of Rowan Digital Works. For more information, please contact graduateresearch@rowan.edu.

**INVESTIGATING THE ROLE OF VASOPRESSIN RECEPTOR 1A
EXPRESSING NEURONS IN MOUSE DORSAL RAPHE**

by

Tirth Nimishbhai Patel

A Dissertation

Submitted to the
Department of Cell Biology and Neuroscience
Rowan Virtua School of Translational Biomedical Engineering & Sciences
In partial fulfillment of the requirement
For the degree of
Doctor of Philosophy
at
Rowan University
June 21, 2023

Dissertation Chair: Daniel Chandler, Ph.D., Assistant Professor, Department of Cell
Biology and Neuroscience

Committee Members:

Benjamin Rood, Ph.D., Assistant Professor, Department of Cell Biology and
Neuroscience

Daniel Manvich, Ph.D., Assistant Professor, Department of Cell Biology and
Neuroscience

Barry Waterhouse, Ph.D., Full Professor and Department Chair, Department of Cell
Biology and Neuroscience

Joseph Lonstein, Ph.D., Professor, Department of Psychology, Michigan State University

© 2023 Tirth Nimishbhai Patel

Acknowledgements

I would like to express my sincere gratitude to all those who have been instrumental in the completion of this dissertation.

First and foremost, I would like to thank my mentor, Dr. Benjamin Rood, for his unwavering support and guidance throughout this academic journey. Your expertise, patience, and dedication to my growth as a scholar have been invaluable, and I am deeply grateful for the knowledge and wisdom you have shared with me.

I would also like to extend my heartfelt appreciation to my thesis committee members—Dr. Barry Waterhouse, Dr. Daniel Manvich, Dr. Joseph Lonstein, and Dr. Daniel Chandler—for their insightful advice and constructive criticism. Your collective expertise and commitment to excellence have played a pivotal role in shaping me into a critical thinker, a better writer, and a more skilled scientist.

To my friends, thank you for your unwavering support and encouragement. Your presence in my life has made this experience all the more meaningful.

Lastly, I want to express my deepest gratitude to my family. Your unconditional love, encouragement, and unwavering belief in my abilities have been the driving force behind my personal and professional growth. Your sacrifices and support have made it possible for me to pursue my academic goals, and for that, I am eternally grateful.

This dissertation would not have been possible without the contributions and support of all those mentioned above. I am truly fortunate to have had such a strong network of mentors, friends, and family members who have played a pivotal role in my success. Thank you for being a part of this incredible journey.

Abstract

Tirth Nimishbhai Patel
INVESTIGATING THE ROLE OF VASOPRESSIN RECEPTOR 1A EXPRESSING
NEURONS IN MOUSE DORSAL RAPHE

2022-2023

Daniel Chandler, Ph.D.
Doctorate in Cell Biology and Neuroscience

Human social interactions heavily impact our physical and mental wellbeing. Arginine-vasopressin (Avp) and serotonin have both been implicated in modulation of social behaviors ranging from affiliation to aggression. In male mice, Avp neurons in the bed nucleus of stria terminalis (BNST) show increased activity during prosocial behavior. BNST sends Avp afferents to the dorsal raphe (DR) in the midbrain, a home to a large portion of serotonin neurons in the mouse brain. Previous data suggests that DR is activated during male prosocial behavior with a female stimulus, and Avp indirectly excites serotonin neurons. We hypothesized that DR contains a population of vasopressin receptor 1a-expressing (Avpr1a) cells that may be involved in the regulation of social behavior. Our Fos expression data revealed that DR Avpr1a cells are active during an exposure to a female stimulus, suggesting that DR Avpr1a neurons may influence prosocial behavior. Using a novel Avpr1a-Cre mouse, we characterized the neuroanatomy of DR Avpr1a neurons. Then, hM4Di-mediated inhibition of DR Avpr1a neurons showed reduced social behavior, but unaltered nonsocial behavior, during interactions with a female stimulus in both male and female subjects. Interestingly, inhibition of DR Avpr1a neurons increased aspects of social behavior selectively in males exposed to a male stimulus. Overall, our studies provide insights into the role of DR Avpr1a cells during social behavior and establish a novel mouse model that is poised to accelerate research on the mouse Avp system.

Table of Contents

Abstract.....	iv
Chapter 1: Introduction.....	1
1.1 The Mental Health Crisis is a Global Issue.....	1
1.2 Social Behavior Impacts Human and Societal Health.....	1
1.3 Social Behavior has a Biological Basis.....	3
1.4 Arginine Vasopressin (Avp) is a Neuropeptide Produced in Several Major Brain Regions and Transported Widely throughout the Brain.....	4
1.5 Avp Receptors.....	6
1.6 Avp is Implicated in Human Social Behavior.....	7
1.7 Avp Binds to Avp Receptor 1a in Numerous Brain Regions to Facilitate Social Behaviors in a Variety of Species.....	9
1.8 Avp Nuclei in the Mouse Brain and Implications for Social and Anxiety-Like Behaviors.....	11
1.9 Serotonin, Social Behavior, and Dorsal Raphe.....	14
1.10 Case for a Functional Interaction between BNST Avp Neurons and DR Serotonin Neurons during Social Interactions.....	17
1.11 Summary.....	18
Chapter 2: Avpr1a-Cre Mouse & Dorsal Raphe Avpr1a Anatomy.....	20
2.1 Introduction.....	20
2.2 Rationale.....	21
2.3 Materials & Methods.....	23
2.3.1 Animals.....	23
2.3.2 Experiment 1: Assessing Cre Recombinase Efficacy and Specificity in Avpr1a-Cre::RC-PTom Mice.....	24
2.3.3 Experiment 2: Assessing TdTomato Expression in Avpr1a-Cre::RC-PTom, Avpr1a-Cre, and RC-PTom.....	27
2.3.4 Experiment 3: Assessing Cre Recombinase Efficacy in Adult Avpr1a-Cre Mice with Cre-Dependent Viral Vectors Injected to the Dorsal Raphe.....	28

Table of Contents (Continued)

2.3.5 Experiment 4: Characterize the Putative Avpr1a Cells throughout the Rostro-Caudal Extent of the Dorsal Raphe.....	30
2.4 Experimental Results	31
2.4.1 In Avpr1a-Cre::RC-Ptom Mice, Cre-Recombinase is Efficacious and Tdtomato Expression is Specific to Avpr1a-Positive Cells	31
2.4.2 Avpr1a-Cre::RC-Ptom, but not Avpr1a-Cre or RC-Ptom, Dorsal Raphe Sections Show Robust Tdtomato Staining.....	32
2.4.3 Assessing Cre Recombinase Efficacy in Adult Avpr1a-Cre Mice with Cre-Dependent Viral Vectors Injected to the Dorsal Raphe.....	33
2.4.4 Characterization of Putative Avpr1a Cells Throughout the Rostro-Caudal Extent of DR	35
2.5 Discussion	38
2.5.1 Cre Recombinase is Efficacious and Specific to Avpr1a-Expressing Cells	38
2.5.2 Distribution of Avpr1a Neurons in the DR	45
Chapter 3: Social Interactions and Dorsal Raphe	49
3.1 Introduction.....	49
3.2 Rationale	50
3.3 Materials & Methods	53
3.3.1 Animals	53
3.3.2 Social Interaction Test.....	53
3.3.3 Tissue Extraction.....	54
3.3.4 In Situ Hybridization and Image Acquisition	54
3.3.5 In Situ Hybridization Data Analysis	55
3.3.6 Behavior Video Analysis.....	56
3.3.7 Statistical Analyses	56
3.4 Experimental Results	57
3.4.1 Analysis of Non-Social and Social Behaviors	58

Table of Contents (Continued)

3.4.2 Male and Female Mice Have Greater Fos Positive DR Cells with Exposure to a Female Stimulus.....	59
3.4.3 Tph2 Positive Cells Do Not Show Increased Fos Positivity in Any Groups.....	60
3.4.4 Male and Female Mice Have Greater Fos Positive DR Avpr1a and Non-Serotonergic, Non-Avpr1a Neurons with Exposure to a Female Stimulus.....	60
3.5 Discussion	61
Chapter 4: Dorsal Raphe Avpr1a Neurons & Behavior	66
4.1 Introduction.....	66
4.2 Rationale	68
4.3 Materials & Methods	70
4.3.1 Animals and Surgery.....	70
4.3.2 Behavior.....	71
4.3.3 Virus Expression Verification	74
4.3.4 Statistical Analyses	75
4.4 Experimental Results	76
4.4.1 Histological Verification of Cre-Dependent Hm4di Virus Expression in DR.....	76
4.4.2 DREADD Inhibition of DR Avpr1a Cells Did Not Alter Sociability or Novelty Preference.....	77
4.4.3 In Male and Female Subjects, Chemogenetic Inhibition of DR Avpr1a Cells Decreased Prosocial Behavior When Exposed to a Female Stimulus in Social Interaction Test.....	79
4.4.4 Chemogenetic Inhibition of DR Avpr1a Neurons Increases Social Behavior In Male Mice Exposed to a Male Stimulus.....	83
4.5 Discussion	85
4.5.1 DR Avpr1a Neurons are Involved in Male-Female Interactions.....	86
4.5.2 DR Avpr1a Neurons May Decrease Male-Male Social Behavior.....	90
4.5.3 CNO Can Convert to Clozapine to Cause Off-Target Effects	92

Table of Contents (Continued)

Chapter 5: Summary and Conclusion 94

 5.1 Role of Dorsal Raphe in Social Interaction 94

 5.2 Multiple Sub-Types of Avpr1a-Expressing Neurons are Found in the Dorsal
 Raphe 98

 5.3 Summary and Future Directions 99

References 102

Appendix: Figures & Tables 121

Chapter 1

Introduction

1.1 The Mental Health Crisis is a Global Issue

Mental health is a critical aspect of our overall well-being as it affects how we think, feel, and ultimately behave. Mental illnesses are prevalent across various ages, sex, and race (*Figure A1. 1*). Approximately one in five adults in the U.S. experience mental illness each year, with the prevalence slightly higher among females (27.2% vs. 18.1%) than males (SAMHSA, 2022).

Globally, mental health has also emerged as a significant issue. According to the World Health Organization (WHO) report, mental health conditions affect approximately one in eight people globally. In 2019, approximately 970 million people globally were affected by a mental disorder, a figure that increased dramatically after the COVID-19 pandemic. In both males and females, two of the most common categories of mental health psychopathologies are anxiety and depressive disorders—with anxiety disorders more common in earlier age and depressive disorders more common in older adults (WHO, 2022).

1.2 Social Behavior Impacts Human and Societal Health

Social behavior is a major factor in the development of children and remains critical to mental health in adults. Studies show that the quality of social networks impacts health and development of adolescents (Ali & Dwyer, 2010; Haas & Schaefer, 2014; Hatzenbuehler et al., 2012; Hill et al., 2015). A positive interaction, such as thinking of a romantic partner, increases positive affect and blood glucose levels (Stanton et al., 2014).

Furthermore, an individual with a healthy social group has an increased probability of recovering from and decreased risk of developing depressive disorders (Hill et al., 2015). Just as positive social interactions are important for one's well-being, negative interactions like bullying in childhood increase the risk of developing somatic health issues as well as anxiety and depressive disorders (Gini & Pozzoli, 2009; Wolke & Lereya, 2014, 2015). In sum, social behavior and human mental health show a reciprocal relationship where a change in one inevitably alters the other.

Mental health disorders alter one's ability to think, feel, act, and interact with others. Such deviations from the norm in social behavior result in a poor quality of life and diminished ability to contribute to society. Since the onset of the 21st century, depressive and anxiety disorders were among the top ten causes of "global years" lived with disability, a metric used to measure disease burden on society. Moreover, approximately twelve billion workdays per year are lost due to poor productivity resulting from anxiety and depression alone (Chisholm et al., 2016). According to WHO, mental health conditions incurred a global economic loss of \$2.5 trillion in 2010, a figure expected to rise to \$6 trillion by 2030. This amount is greater than the projected cost of chronic respiratory disease, cancer, and diabetes combined. Therefore, improvement in the mental health of an individual is for the benefit of all. *Figure A1. 2* depicts multi-faceted benefits that can be derived from improving mental health (WHO, 2022).

Several studies have recommended organizational changes to ameliorate the societal burden caused by mental illnesses. For example, a Canadian study with ten companies showed that investment in workplace programs to improve mental health can yield positive results in as little as three years (Kangasniemi, 2019). Furthermore, a study

in Denmark showed that an increase in mental well-being is associated with lower cost of care, leading to a significant decrease in governmental welfare support (Santini et al., 2021). Recently, a systematic review concluded that systemic mental health interventions lead to improved economic outcomes related to education and employment (Lund et al., 2018). While interventions in the workplace and education systems are clearly helpful and necessary for one's psychological well-being, the neurobiology that underlies normal (and abnormal) social behavior should also be considered.

1.3 Social Behavior has a Biological Basis

As highlighted by the DSM-5 (APA, 2022), a standard clinical guide in psychiatric medicine, aberrant social behavior is a common symptom in numerous mental illnesses. Some examples of disorders that exhibit disrupted social behaviors are mood disorders, autism spectrum disorder, and schizophrenia. Conversely, disruption of social interaction, like the social isolation caused by the COVID-19 pandemic, can also be a contributing factor in causing mental illnesses like depressive and anxiety disorders. While environmental factors play a large role in social development, biological factors like genetics are also major determinants of normal and abnormal social behavior. Because social behavior is at the center of many psychiatric disorders, understanding the biological basis of social behavior is a critical first step in understanding the underpinnings of those same psychiatric disorders. This fact drives the imperative that we identify regions of the brain involved in social behavior and work to understand the complex neurophysiological networks that govern social behavior.

Current pharmacologic treatments provide some insight into the potential biological systems that go awry in mental disorders with dysfunctional social behavior. Selective monoamine (serotonin, norepinephrine, or dopamine) reuptake inhibitors are widely used to manage a variety of mood disorders (Caldwell et al., 2008; Egashira et al., 2007; Ferris et al., 1997; Lucki, 1998; Veenema, 2009), implicating the monoaminergic systems in regulation of mood. Further, psychotic disorders like schizophrenia that display a severe disturbance in social behavior are treated with antipsychotic drugs that primarily bind to receptors mediating serotonin and dopamine neurotransmission (Siafis et al., 2018). However, these drugs also display off target binding to a variety of neurotransmitter receptors including histaminergic (H1), adrenergic (α 1), and acetylcholinergic (M3) receptors (Correll et al., 2011; Guenette et al., 2013; Michl et al., 2014; Montastruc et al., 2015), which can induce many undesired side effects like dizziness, movement effects, weight gain, glucose intolerance, and dyslipidemia (Siafis et al., 2018). Such a diverse profile of side effects highlights the low specificity in targeting the responsible biological system, mainly due to a lack of a clear understanding for the neurobiological networks that govern normal social behavior.

1.4 Arginine Vasopressin (Avp) is a Neuropeptide Produced in Several Major Brain Regions and Transported Widely throughout the Brain

In addition to serotonin which has been a major focus of research studies investigating social behavior and anxiety, Avp has been implicated in modulation of social behaviors in many animal species including humans (Caldwell et al., 2008; Veenema, 2009). Avp is a nine amino acid peptide found throughout the central nervous system. Avp

is produced as a prepropeptide that is cleaved into and co-released as three distinct parts: Avp, neurophysin II, and Avp-associated glycopeptide (Gainer et al., 1977; Land et al., 1982). Avp functions similar to classical neurotransmitters: electron microscopy showed Avp within synapses in areas with Avp-immunoreactive (ir) fibers and its release is calcium dependent (Buijs & Swaab, 1979; Buijs & Van Heerikhuize, 1982). Avp exerts its actions by binding to one of three subtypes of Avp receptors: 1a (Avpr1a), 1b (Avpr1b), and 2 (Avpr2; a more detailed discourse of receptors follows below) (Lolait et al., 1992; Morel et al., 1992; Saito et al., 1995).

In most mammals, Avp is produced in three major hypothalamic nuclei: the supraoptic (SON), paraventricular (PVN), and suprachiasmatic (SCN) (De Vries & Panzica, 2006; Rood & De Vries, 2011). In mice, as in numerous other species, the BNST and medial amygdala (MeA) are two other major sites of Avp production (Correll et al., 2011; Rood & De Vries, 2011; Rood et al., 2013)). There are other discrete regions that produce Avp, like the anterior commissural and periventricular nucleus. Avp-producing cells (referred to throughout as “Avp cells”) are described to be magnocellular (large) in the PVN and SON, and parvocellular (small) in the SCN, BNST, and MeA (Castel & Morris, 1988; Rood & De Vries, 2011).

While there are five major Avp nuclei in the mouse brain, Avp-ir fibers are found throughout the mouse brain, ranging from the forebrain to spinal cord (see (Rood & De Vries, 2011) for a detailed discussion of Avp innervation of the mouse brain). Furthermore, (Rood et al., 2013) performed extensive studies to distinguish site of origin and sex differences in mouse Avp innervation. By leveraging the fact that BNST and MeA Avp production is gonadal steroid dependent (de Vries et al., 1984; De Vries et al., 1994; Mayes

et al., 1988), gonadectomies were used to eliminate steroid dependent Avp-ir fibers, which occurred largely in subcortical structures near the midline like the lateral septum (LS), mediodorsal thalamus (MD), or raphe nucleus (*Figure A1. 3*). BNST and MeA also contained a sexually dimorphic male-biased population of Avp-ir cells. Combination of gonadectomy and electrolytic lesion of SCN revealed a prevalence of widespread projection of Avp throughout the brain to both midline (e.g., periaqueductal gray) and lateral brain (e.g., mesencephalic reticular formation) structures, presumably from the PVN and SON.

1.5 Avp Receptors

As mentioned previously, Avp exerts its action through three known subtypes of Avp receptors: Avpr1a, Avpr1b, and Avpr2. Avp binding to Avpr2 receptor stimulates cyclic AMP system via Gs protein (Jard et al., 1987) to cause transduction of Avp in the renal collecting duct of the kidney (Bankir, 2001).

Next, while Avpr1b was originally described to be most prominent in the anterior pituitary where it potentiates adrenocorticotropin hormone release (Antoni, 1984; Yates et al., 1971), Avpr1b mRNA and Avpr1b-immunoreactive cell bodies have been found in regions like the olfactory bulb, septum, cerebral cortex, hippocampus, SCN, PVN, piriform cortical layer II, cerebellum, and red nucleus (Hernando et al., 2001; Lolait et al., 1995; Saito et al., 1995; Stemmelin et al., 2005; Vaccari et al., 1998). Furthermore, another study using in situ hybridization found prominent levels of Avpr1b mRNA in the hippocampal field CA2 pyramidal neurons (Young et al., 2006).

Of the three subtypes, Avpr1a has the most diverse expression profile within the CNS. Receptor autoradiography in the rat brain showed Avpr1a binding in neocortical layer IV, LS, hippocampal formation, amygdala, hypothalamus, ventral tegmental area (VTA), substantia nigra, superior colliculus, DR, nucleus of the solitary tract, and inferior olive (Johnson et al., 1993). In addition to these structures, mouse brain autoradiography also showed labeling in the ventral pallidum, medial septum, supramammillary nuclei, and periaqueductal gray (PAG) (Caldwell et al., 2008). In addition to the structures described in receptor binding studies, in situ hybridization showed Avpr1a expression in the rat olfactory bulb, lateral habenula, and locus coeruleus (Ostrowski et al., 1994; Szot et al., 1994). Since then, Avpr1a expression has been studied in many different species and the pattern of expression is strikingly similar, though differences do exist (Caldwell et al., 2008). Aside from the CNS Avpr1a localization, the receptors are observed in the liver and kidney as well as blood vessels peripherally (Caldwell et al., 2008) where they partake in vasoconstriction mediated blood pressure control (Demotes-Mainard et al., 1986; Oliver & Schafer, 1895). Lastly, both Avpr1a and Avpr1b function through Gq GTP binding protein. Therefore, Avpr1a and Avpr1b activate phospholipase C activity and in turn increase metabolism of inositol phospholipid which ultimately increases intracellular calcium levels (Shewey & Dorsa, 1988; Stephens & Logan, 1986).

1.6 Avp is Implicated in Human Social Behavior

Although Avp is well known to regulate blood pressure and volume peripherally (Turner & Pallone, 1997), Avp is produced in and transported to several different locations within the central nervous system (CNS) in humans, and its role in behavioral networks

within the CNS is less well understood. A few clinical studies have provided some link between Avp and human social behavior. In one study, intranasal administration of Avp caused males to respond agonistically and females to respond favorably when presented with neutral faces (Thompson et al., 2006). This study suggests two things about Avp in humans: Avp plays some role in social behavior and that it does so in a sex specific manner (Thompson et al., 2006). Moreover, association studies have found that variations in repetitive sequences within the 5' flanking region of Avpr1a contribute to increased risk for autism spectrum disorder (ASD) (Kim et al., 2002; Meyer-Lindenberg et al., 2011; Wassink et al., 2004; Yirmiya et al., 2006), possibly via the modulation of gene transcription (Knafo et al., 2008) or variable receptor distribution throughout the brain (Young et al., 1999). In healthy individuals, studies have found that individuals homozygous for the 334-base pair (bp) allele of RS3 (a type of promoter-region repetitive sequence) are associated with both decreased fidelity in men (Walum et al., 2008) and age of first sexual intercourse in men and women (Prichard et al., 2007), which are factors of a human social experience. While the mechanistic importance of RS3 polymorphism is not completely understood, (Knafo et al., 2008) found an association of higher Avpr1a human post-mortem hippocampal mRNA levels in individuals with 334-bp RS3 allele. Furthermore, a study conducted in healthy adults indicates a connection between the 334-bp RS3 allele and heightened activation of amygdala, a region recognized for its significance in pair-bonding behavior (Meyer-Lindenberg et al., 2009). Although correlative data linking Avp and its receptor to social behavior have begun to emerge from human studies, mechanistic data on Avp's effects in human social behavior is still elusive and difficult to study. Now the question is not whether Avp plays a role in social behavior, but how.

1.7 Avp Binds to Avp Receptor 1a in Numerous Brain Regions to Facilitate Social Behaviors in a Variety of Species

While human studies of Avp provide evidence of its potential role in pathologies with disrupted social behavior such as ASD (Kim et al., 2002; Meyer-Lindenberg et al., 2011; Wassink et al., 2004; Yirmiya et al., 2006), animal studies allow us to learn where Avp fits into the complex neurobiological networks that execute social behavior. Animal studies have suggested that Avp affects social behaviors like social memory, aggression, and affiliation. For example, (Dantzer et al., 1988) found that injection of Avp into the lateral septum of rats increases social memory. In contrast, injection of Avpr1a antagonists into the lateral septum decreases social memory in male rats, but not in female rats. In Avpr1a knock-out mice, which display impaired social recognition and reduced anxiety-like behaviors (Bielsky et al., 2004), re-expression of Avpr1a using viral injections to the lateral septum rescues social recognition (Bielsky et al., 2005). Additionally, (Ferris et al., 1997) injected Avp into the anterior hypothalamus of golden hamsters and observed reduced latency to bites and increased biting attacks (i.e., increased aggression).

Although these studies uncover a link between Avp in a brain region to specific social behaviors, more convincing evidence implicating Avpr1a in social behavior came from studying two evolutionary related vole species: monogamous, paternal prairie voles and promiscuous montane voles. Microinjection of Avp to the lateral septum of sexually naïve male prairie voles increases pro-social behaviors like grooming and crouching over pups (i.e., increased paternal response) (Wang et al., 1994). In contrast to the highly social and paternal prairie vole males (Bamshad et al., 1994; Wang et al., 1994), montane vole

males are not social, paternal, or monogamous (Shapiro & Dewsbury, 1990) and do not increase pro-social behaviors after Avp administration to the lateral septum (Young et al., 1999). Using autoradiography, (Young et al., 1999) showed a difference in distribution of Avpr1a within the brain between prairie and montane voles and predicted that differential expression of the Avp receptor 1a may play a role in producing such varied social behavior profile between the two closely related species. They, then, produced transgenic mice with Avpr1a gene with its regulatory elements from the highly social prairie vole species and observed prairie vole-like Avpr1a distribution and increased prosocial behavior after microinjections of Avp in the transgenic mice (Young et al., 1999). While social interaction includes complex patterns of behavior involving multiple factors, the studies discussed above suggest that some component of pro-social behavior is, in fact, affected by Avp, and more particularly by the distribution of Avpr1a within the brain.

Briefly, there are several accounts of Avpr1b mediated effects on social behavior. For example, Avpr1b knockout (KO) male mice display reduced social aggression and social memory preference, but no change to sexual behaviors (Wersinger et al., 2002). The reduced aggression in KO mice was rescued upon lentiviral delivery of the Avpr1b gene into the dorsal CA2 (Pagani et al., 2015). On the other hand, social memory is enhanced through optogenetic activation of Avp terminals in the dorsal CA2 during memory acquisition, an effect that is blocked by an Avpr1b antagonist (A. S. Smith et al., 2016). While Avpr1b is implicated in some social behaviors like aggression and social memory in mice, Avpr1a has been more widely implicated in social behaviors across many species.

1.8 Avp Nuclei in the Mouse Brain and Implications for Social and Anxiety-Like Behaviors

Another way to study the role of Avp in social behavior is to manipulate the distinct Avp cell groups. Rigney, Petrusis, and colleagues conducted several studies to study contributions of Avp cells from BNST, PVN, and SCN on mouse social behavior (reviewed in (Rigney et al., 2023a)). Using genetic techniques, they selectively ablated (caspase-9 mediated) Avp cells in each nucleus and investigated any potential ensuing behavioral deficits. Ablation of BNST Avp neurons in male mice decreased social investigation of a male stimulus in the three-chamber test and increased urine marking in response to a female stimulus, but did not alter ultrasonic vocalizations (USVs), aggression, mating behavior, anxiety-like behavior, investigation of a female, or olfactory discrimination. In female subjects, ablation caused slightly fewer male mounting attempts and increased latency to mount in a copulation test, but the rest of the behaviors described previously were unaffected. A potential reason for the observed sex-specific effects on social behavior may be the fact that BNST Avp neurons are sexually dimorphic, with males having a greater number of cells and denser projections (Rigney et al., 2019; Rood et al., 2013). Next, conducting the same battery of behavior tests following ablation of PVN Avp neurons caused an increase in anxiety-like behaviors in males and increased social investigation of both a male and female stimulus in females (Rigney et al., 2021).

While MeA Avp neurons are also sexually dimorphic (male > female) and gonadal steroid dependent like BNST Avp neurons, MeA Avp cells are less well studied in the context of social behavior. A few studies have looked at this Avp cell population in the context of predator odors in mice and reproductive behavior in rats. Ablation of MeA Avp

cells and overexpression of Avp in male mice increases and decreases aversion to cat odors respectively (Tong et al., 2021). More work is needed to study Avp population in the MeA in the context of other social behaviors as MeA at large has been implicated in aggression, social communication, and sexual behaviors (Raam & Hong, 2021). Similarly, SON Avp neuron population in mice is severely understudied in the context of social behavior despite evidence of modulation of aggression and social communication in rats and hamsters (Rigney et al., 2023a). Moreover, while SCN Avp cells are implicated in coordination of behavioral circadian rhythms (Mieda et al., 2015; Tsuji et al., 2017), ablation of Avp cells within the SCN does not directly affect social behavior but increases anxiety-like behavior (Whylings et al., 2021). In summary, studies manipulating the Avp cell groups indicate that among various Avp nuclei, BNST Avp neurons have the greatest impact on mouse social behavior.

While studies using Avp cell ablation have provided novel insights into the role of Avp cells in BNST, PVN, and SCN, this technique does not come without limitations. Each Avp nucleus has various projections that are simultaneously eliminated, making mechanistic interpretations difficult, if not impossible. Interpretations are further complicated by the fact that behavioral deficits seen after ablation of Avp cells cannot be attributed to Avp function alone since Avp cells may co-release other neurotransmitters unrelated to the Avp system. The need to study Avp function with more selective methods is underscored by the finding that downregulation of Avp expression in the BNST shows a decrease in male copulatory and aggressive behaviors, whereas ablation of Avp cells in BNST did not (Rigney et al., 2022). Furthermore, Ho and colleagues (Ho et al., 2010) performed resident-intruder and copulation experiments and found that Avp-producing

neurons (referred to throughout as “Avp neurons”) in the posterior part of the medial BNST show increased Fos (a neuronal activation marker) positivity during mating behavior and unchanged activity during aggressive behavior. More specifically, copulation increased Avp-Fos co-localization from a baseline 5% to 70% and non-aggressive male-male interaction increased the co-localization significantly to 11%, whereas aggressive male-male interaction did not significantly increase co-localization (Ho et al., 2010). *Figure A1.4* highlights potential roles of Avp nuclei on social behavior based on functional studies.

In sum, Avp cells from multiple nuclei have been implicated in various social behaviors in mice. However, of all Avp nuclei, the BNST presents as the most compelling region in control of mouse social behavior, especially in a sex-specific manner. This assertion is strengthened by the fact that BNST Avp cells are sexually dimorphic, with male mice having a significantly higher number than female mice, and sensitive to gonadal steroid hormones. BNST sends Avp projections to many regions that have been implicated in Avp-mediated regulation of social behavior such as social recognition and pair-bonding. However, aside from the lateral septum and anterior hypothalamus which have been extensively studied, other sites that receive innervation from BNST Avp neurons remain understudied. Particularly, there is a dearth of studies examining the physiological and functional attributes of Avp-responsive cells throughout the mouse brain, in part, due to lack of tools to adequately characterize, target, and manipulate Avp-responsive (i.e., Avp receptor-expressing) cells. Receptor autoradiography and in situ hybridization studies have provided us with a general accounting of where Avpr1a cells may exist throughout the brain; however, no studies, to our knowledge, have reported cellular resolution data on Avpr1a cells in the mouse CNS. Studying the role of Avp-responsive cells that receive

projections from BNST Avp neurons will increase our understanding of the mechanism of action of the Avp system in the regulation of social behavior.

1.9 Serotonin, Social Behavior, and Dorsal Raphe

The serotonin system has been shown to influence a diverse set of behavioral functions (Lesch, 2007; Lucki, 1998). Within the midbrain, the DR nucleus is distinguished for harboring the largest population of forebrain-projecting serotonin neurons (Lowry et al., 2008; Vertes & Crane, 1997). Initial indications of serotonin's behavioral impact stemmed from observations of remarkably reproducible motor manifestations like tremor, rigidity, and head shakes following the administration of L-5-hydroxytryptophan (a precursor molecule of serotonin) (Jacobs & Fornal, 1993). In cats, single-unit activity traces show that oral-buccal motor activity such as chewing or biting increases activity in approximately 25% of DR serotonin neurons (Jacobs & Azmitia, 1992). In addition to its influences on motor function, the serotonin system via the serotonin transporter (SERT), which regulates the availability of serotonin within the synaptic cleft and therefore its effect on the post-synaptic neuron, has been implicated in the regulation of emotional states like depression and anxiety (Collier et al., 1996; Langer et al., 1981; Lesch, 2007). SERT has also been identified as one of the binding sites of tricyclic anti-depressant drugs (Raisman et al., 1979). Furthermore, transgenic mice deficient in SERT, compared to wild type mice, spend less time in the open arm of an elevated plus maze, more time in the dark chamber of light-dark exploration test, and less time in the center of an open field—collectively signifying an overall increase in anxiety-like behaviors (Holmes et al., 2003).

Given its pivotal role in regulating mood and emotional states (Lesch, 2007; Lucki, 1998), it is unsurprising that the serotonin system exerts a significant influence over social behaviors encompassing maternal behavior, mating, and aggression. For example, maternal separation in rhesus monkeys causes a lasting impact on the serotonin system, demonstrated by low levels of 5-hydroxyindoleacetic acid (a metabolite of serotonin) in the cerebrospinal fluid (Lesch, 2007). Among rats, postpartum females with lesioned DR serotonin neurons are associated with increased pup mortality (Barofsky et al., 1983), perturbed nursing behavior patterns (e.g., reduced pup-licking), and attenuated maternal aggression (Holschbach et al., 2018). Additionally, global disruption in serotonin signaling in two distinct mouse lines displays aberrations in pup retrieval and nursing behaviors (Alenina et al., 2009; Lerch-Haner et al., 2008). Furthermore, male mice lacking tryptophan hydroxylase 2 (Tph2; transgenic mice referred to as Tph2-KO), an enzyme critical for serotonin biosynthesis, show a loss of sexual preference for female mice over male mice. Interestingly, following the injection of 5-hydroxytryptophan which circumvents the Tph2 deficiency to restore serotonin to wildtype level, Tph2-KO males prefer females over males, suggesting a role of serotonin signaling in male mating behavior (Liu et al., 2011). Central serotonergic function also influences aggression. Pharmacological studies suggest, in general, a reciprocal relationship between brain serotonin levels and predatory aggression in rats (Lucki, 1998; Miczek et al., 1989). In mice, administration of 3,4-methylenedioxymethamphetamine (MDMA), known to elevate monoamine but particularly serotonin levels, is associated with a dose-dependent decrease in inter-male aggression and increase in sociable acts (i.e., social sniffing and following) (Machalova et al., 2012). Employing intersectional genetic tools, (Niederkofler et al., 2016)

found that silencing a subset of DR serotonin neurons expressing the dopamine D2 receptor increases inter-male aggression in mice. While both global and DR specific evidence implicates the serotonin system in the regulation of social behavior, the precise neural mechanisms underpinning the effects of serotonin remain elusive. *Figure A1. 5* illustrates the anatomical divisions (from rostral to caudal) of the DR, differentiating the ventromedial (VMDR), dorsomedial (DMDR), and lateral wing (LWDR) clusters of serotonin neurons as well as the lateral DR which contains glutamate and GABA neurons. *Figure A1. 5* also identifies the general location and inputs from BNST Avp neurons and summarizes major projection profiles of serotonin subfields.

Given the well-documented effects of BNST Avp and the DR serotonin system on social behavior (Ho et al., 2010; Lucki, 1998; Rigney et al., 2019), coupled with the dense innervation of the DR by BNST Avp (Rigney et al., 2023b; Rood et al., 2013), the DR serotonin system is strategically positioned to receive information from BNST Avp neurons that may affect social behavior. However, although the DR nucleus is often thought to be synonymous with the serotonin system, the DR encompasses diverse groups of neurons distinguished by their chemical composition and projection profiles. In addition to serotonin neurons, DR is also comprised of neurons that synthesize neurotransmitters like GABA, glutamate, dopamine, or nitric oxide (Beitz et al., 1983; Johnson & Ma, 1993; Reichling & Basbaum, 1990; Simpson et al., 2003) and neuropeptides like enkephalin, neurotensin, cholecystokinin, substance P, and somatostatin (Beitz et al., 1983; Li et al., 1990; Moss et al., 1983; Shipley et al., 1987). Moreover, serotonin neurons have been observed to co-synthesize the aforementioned neurotransmitters and neuropeptides (an exhaustive exploration of DR chemoarchitecture is available in (Lowry et al., 2008)). In

addition to the chemical diversity, the serotonin system displays a topographic organization in many species like lobster (Ma et al., 1992), fish (Lillesaar, 2011) and mammals (Azmitia & Segal, 1978; Bobillier et al., 1976; Jacobs & Azmitia, 1992; Muzerelle et al., 2016; Ren et al., 2018; Waterhouse et al., 1993). For example, in rats, the ventral part of the DR projects mainly to cortical areas like the sensorimotor cortex (Waterhouse et al., 1986), visual cortex (Waterhouse et al., 1993; Waterhouse et al., 1986), and ventrolateral orbital cortex (Coffield et al., 1992). In contrast, the dorsal part projects largely to subcortical areas associated with stress- and anxiety-related behaviors (Lowry et al., 2005) such as the hypothalamus (Commons et al., 2003), BNST (Commons et al., 2003; Petit et al., 1995), and amygdala (Li et al., 1990; Ottersen, 1981) (*Figure A1. 5*).

1.10 Case for a Functional Interaction between BNST Avp Neurons and DR Serotonin Neurons during Social Interactions

We have noted that both BNST Avp and DR serotonin systems impact prosocial behaviors in mice. Given that DR receives a dense BNST Avp innervation, it would make sense logically if the Avp and serotonin systems functionally interact to regulate prosocial behaviors in mice. In fact, previous pharmacological studies have observed functional interactions between serotonin and Avp in the regulation of social behavior (Ferris et al., 1997; Terranova et al., 2016). For instance, Avp application to the anterior hypothalamus of male Syrian hamsters increases in territorial aggression. However, this response is inhibited when the hamsters are pre-treated with a selective serotonin reuptake inhibitor (Ferris et al., 1997). More specifically for the DR, a patch clamp study in mice showed that bath applied Avp increases glutamatergic excitatory post-synaptic currents in DR serotonin

neurons (Rood & Beck, 2014), suggesting that glutamatergic Avp-responsive neurons are situated in or around the DR and that Avp increases serotonin neuron activity.

In 2010, Ho and colleagues found that BNST Avp neurons are activated (as measured by Fos quantification) in male mice during mating encounters but not during male-male aggressive interactions (Ho et al., 2010). Given that BNST Avp neurons react to prosocial mating cues, BNST Avp neurons innervate the DR, Avp administered to the DR induces an excitatory glutamate mediated excitatory response in serotonin neurons, and serotonin neurons are implicated in the regulation of prosocial behaviors, we hypothesize that DR Avp-responsive neurons will be active during prosocial interactions and perturbing their function will decrease social behavior.

1.11 Summary

Both BNST Avp and DR serotonin systems are implicated in mouse social behaviors like mating and aggression. The DR contains a large majority of the serotonin neurons found in the CNS, and serotonin appears to play a role in promoting pro-social behavior. Likewise, the BNST Avp system is implicated in pro-social behaviors, and, important to our hypothesis, the DR is densely innervated by the BNST Avp neurons. Therefore, the DR is a likely site for Avp to influence social behavior. To effectively study the role of DR Avp-responsive neurons in social behavior, we introduce a novel transgenic Avpr1a-Cre mouse model which will allow for selective control over the putative Avpr1a cell population (validation in Chapter 2 and application in Chapter 4). Following validation of our new mouse model, we present data definitively showing neural activation of DR Avpr1a neurons in response to social interactions (Chapter 3). Then, we employ our new

mouse model to test the impact of inhibiting DR Avpr1a neurons on social interaction
(Chapter 4).

Chapter 2

Avpr1a-Cre Mouse & Dorsal Raphe Avpr1a Anatomy

2.1 Introduction

Vasopressin (Avp) has been implicated in regulation of multiple social behaviors in many species. For example, Avp impacts social memory in rats and mice (Bielsky et al., 2005; Bielsky et al., 2004; Dantzer et al., 1988), paternal behavior in voles and mice (Bamshad et al., 1994; Wang et al., 1994; Young et al., 1999), and aggression in golden hamsters (Ferris et al., 1997). In mice, BNST Avp neurons and, less often, those in the PVN have been implicated in regulation of social behavior (Rigney et al., 2021; Rigney et al., 2019). Loss-of-function studies in mice have indicated that BNST Avp is important for male-male social communication and male mating behavior (Rigney et al., 2019; Rigney et al., 2022), and correlative studies in hamster and mice have noted increased BNST Avp neuronal activation during prosocial, but not antagonistic, interactions (Kollack-Walker & Newman, 1995) and male mating behavior (Ho et al., 2010). Similarly, the DR serotonin system has been implicated in the regulation of social behaviors like mating and aggression (discussed in detail in Chapter 1). Because the DR receives a dense innervation from BNST Avp neurons, the serotonin system is an ideal target for the relay of social signals conveyed by BNST Avp neurons. While some BNST Avp projection sites like the lateral septum have been extensively studied, less is known about DR Avp-responsive neurons and their possible influence on social behavior.

2.2 Rationale

In mice, Rood and colleagues (Rood & De Vries, 2011) performed extensive experiments to describe the distribution of Avp-ir fibers and cell bodies throughout the mouse CNS. Then, they conducted several more experiments to delineate the sites of origin of various Avp-ir fibers (Rood et al., 2013). Because Avp nuclei seem to divide into three functionally distinct groups (Rood et al., 2013), anatomical accounting of Avp neuron projection targets provides foundational knowledge for hypothesis generation when studying a particular brain region innervated by Avp (Patel et al., 2022). While the anatomy, morphology, and projection sites of Avp neurons are well studied, the accounting of Avp-responsive neurons throughout the brain is less clear. Methods like receptor autoradiography and in situ hybridization have provided us with a general picture of where Avp binding or Avpr1a mRNA expression occurs, but detailed maps of Avpr1a and Avpr1b are lacking and data on the phenotype of these cell populations is limited (see section 1.5 Avp receptors for more detail). Immunohistochemical staining methods could provide a refined picture of the morphology and distribution; but, to our knowledge, clear demarcation of Avpr1a cells is not possible with current tools (e.g., antibodies). Characterizing neurons expressing Avpr1a has been technically challenging.

Recent advances in transgenic mouse models have been groundbreaking in providing access to previously inaccessible subtypes of neurons. One example of such technology is the integration of site-specific recombinase (SSR) enzyme systems into transgenic mouse models. While a thorough discussion of transgenic mouse models that utilize SSR technology is beyond the scope of this Chapter, a brief background on SSRs is warranted. “Cre-LoxP” system consists of “Cre”, one of several SSRs, that catalyzes

recombination between specific target sites named “LoxP”. Depending on the orientation of the target sites, Cre-mediated recombination can result in either splicing out or inversion of the intervening DNA sequence (*Figure A2. 1*; see (Branda & Dymecki, 2004) for a complete discussion of SSR technology and mouse genetics).

One usage example that exploits the Cre-LoxP system is a model in which Cre expression is induced in a cell-type of interest by inserting a transgene using cell-type specific promoters and encoding the Cre gene into mice. Then using a viral strategy or breeding strategy with another transgenic mouseline, an effector gene (functionally relevant gene such as a fluorescent protein) can be unlocked by the DNA editing action of the Cre-recombinase. Using such a strategy in which a fluorescent reporter gene is expressed in a Cre-dependent manner, we can exploit this technology to visualize Avpr1a-expressing neurons throughout the mouse brain. Because no Cre-recombinase model using Avpr1a regulatory sequences existed, we contracted Cyagen (Santa Clara, CA) to make a BAC transgenic Avpr1a-Cre mouse (C57BL/6J background) in which Cre recombinase expression is driven by the regulatory sequences of Avpr1a gene (*Figure A2.2A*). Presumably, in this mouse, Cre recombinase is present in the nucleus of cells that also express Avpr1a. Ai14 (also referred to as RC-PTom) is a reporter mouse line that contains a LoxP-flanked “STOP” cassette preventing transcription of a red fluorescent protein variant (TdTomato) gene inserted into the Rosa26 locus (*Figure A2.2B*; JAX stock #007908, (Madisen et al., 2010)). When a Avpr1a-Cre mouse is bred with a RC-PTom mouse, resulting progeny carrying both transgenes (referred to as “Avpr1a-Cre::RC-PTom”) should have Cre-mediated excision of the STOP cassette within cells that express

an active *Avpr1a* promoter, and the transcription of TdTomato reporter gene should be unlocked allowing for visualization of the red fluorescent protein (*Figure A2. 2C*).

While the Cre-LoxP system may help characterize the *Avpr1a* neurons within the dorsal raphe (and in other regions of the brain), several important quality control questions must be answered. How strictly is Cre expression confined to *Avpr1a* cells? Is Cre recombinase functional? Is there a basal level of TdTomato protein expression independent of Cre-mediated recombination events? In this chapter, we have designed several experiments to answer the above questions. We will assess the specificity of Cre expression within *Avpr1a* cells and efficacy of Cre-mediated recombination. Then, we will use this double transgenic mouse model to perform immunohistochemistry to visualize the red fluorescent protein (RFP, i.e., putative *Avpr1a* neurons) and *Tph2* (i.e., Serotonin neurons), and describe the anatomical distribution of DR *Avpr1a* neurons, with respect to serotonin neurons, through the rostral to caudal extent of the DR.

2.3 Materials & Methods

2.3.1 Animals

For all experiments conducted in this chapter, adult (>postnatal day 60) male and female mice of C57BL/6J (WT), *Avpr1a*-Cre, RC-PTom, and *Avpr1a*-Cre::RC-PTom genetic backgrounds were used. The transgenic lines have undergone more than 10 generations of backcrossing to the C57BL/6J strain. The animals used in these studies were produced through breeding pairs residing in the animal care facility at Rowan University School of Medicine (Rowan SOM). Animals were group housed under a 12:12 light/dark

cycle (lights on at 06:00 am) in ventilated cages with ad libitum access to food and water. All animals were used in accordance with the National Institutes of Health guide for the care and use of laboratory animals, and all experiments were approved by the Institutional Animal Care and Use Committee of Rowan University.

2.3.2 Experiment 1: Assessing Cre Recombinase Efficacy and Specificity in Avpr1a-Cre::RC-PTom Mice

To use the Avpr1a-Cre mouse to gain access to Avpr1a neurons in a cell-specific manner, Cre expression must be efficacious in mediating recombination events and highly specific to cells that contain Avpr1a. To verify these assumptions, we designed an in situ hybridization experiment to assess the co-localization of Avpr1a and TdTomato mRNA in Avpr1a-Cre::RC-PTom mice.

2.3.2.1 Tissue Collection. Avpr1a-Cre::RC-PTom double transgenic adult mice (n = 2 per sex) were decapitated following isoflurane anesthesia, and brains were harvested, and flash frozen in dry ice chilled 2-methyl butane. Brains were stored at -80°C until sectioning. Next, brains were sectioned at 20 μ M thickness, mounted directly on to SuperFrost Plus slides, and stored foil-wrapped at -80 °C.

2.3.2.2 In Situ Hybridization. In situ hybridization was performed on every third section (20 μ M thickness) through the dorsal raphe (AP -4.24 mm to -4.92 mm from bregma), using the fresh frozen workflow and materials found in RNAscope fluorescent multiplex assay version 2 (Advanced Cell Diagnostics or ACD). The workflow consists

of several sequential steps (see ACD document # UM 323100 for a detailed protocol). Initially, sections are fixed for about 15 minutes in ice-chilled 4% paraformaldehyde (PFA, in 0.1 M PBS) and then dehydrated using ethanol for approximately 20 minutes. Following dehydration, 10 min of RNAscope hydrogen peroxide is applied to the sections, which are then subjected to a 30 min incubation step in RNAscope Protease IV to permeabilize cell membranes. The hybridization of probes (C1, C2, or C3) is the next step and is conducted over 2 hours. To amplify the signal for sufficient detection, there are serial incubation steps with RNAscope Multiplex FL v2 AMP 1 (30 minutes), RNAscope Multiplex FL v2 AMP 2 (30 minutes), and RNAscope Multiplex FL v2 AMP 3 (15 minutes). Each probe (C1, C2, or C3) development includes three stages: the horseradish peroxidase (HRP) step, the fluorophore step, and the HRP blocker step. RNAscope Multiplex FL v2 HRP-C1 (-C2, or -C3) is applied for approximately 15 minutes. Then, the 1st Opal Dye fluorophore is applied for 30 minutes, followed by RNAscope Multiplex FL v2 HRP blocker for approximately 15 minutes. These steps are repeated for all probes used in the experiment. Finally, the workflow concludes with application of DAPI-containing FluoromountG (Electron Microscopy Sciences, Hatfield, PA) to detect nuclei and coverslipping to preserve the tissue. In this experiment, probes used included Avpr1a (#418061-C1) and TdTomato (#317041-C3), paired with Opal dye 520 (Akoya Biosciences, SKU FP1487001KT) and opal dye 620 (Akoya Biosciences, SKU) respectively.

2.3.2.3 Image Acquisition and Data Analysis. Keyence BZ-X710 fluorescent microscope was used to acquire 20x images of the entire dorsal raphe in multiple

channels (DAPI, Avpr1a, and TdTomato). Images were stitched together using Keyence BZ-X710 analyzer software.

DAPI channel images were used to draw an image mask (REGION) to capture the DR region. DAPI images were brightened in ImageJ to reduce background and maximize foreground and then fed into MATLAB nucleiSegmentationBot program ((Cicconet et al., 2017); Resize Factor = 0.5, Fragmentation = 0.9, Background Threshold = 0.3, and Grow = +2)) to create image masks of cells using watershed outlines of identified nuclei (CELLS). For all probe images (PROBE), ImageJ was used to make a duplicate image on which a median filter with radius of 2 pixels was applied, then the duplicate image was subtracted from the original image to reduce background signal and maximize foreground signal. Image sets of REGION, CELLS, and PROBES (Avpr1a and TdTomato) were used in a Cell Profiler (Carpenter et al., 2006) pipeline to identify cell objects (using CELLS image masks) within the dorsal raphe (using REGION masks), count mRNA puncta for each probe (using PROBES images) by thresholding, and relate puncta counts to the identified cell objects; resulting data consisted of a table of all “parent” cells and associated “child” puncta for each probe. Next, the output data was imported into R software (version 4.2.2) to count and categorize cells based on phenotype marker (Avpr1a or TdTomato). Based on counts from negative control slides, a minimum threshold of 5-or-more puncta was required to classify a cell to be “positive” for mRNA detection. Then, positive cells were further phenotyped based on the type of puncta in each cell (Avpr1a, TdTomato, or co-localized).

2.3.3 Experiment 2: Assessing TdTomato Expression in Avpr1a-Cre::RC-PTom, Avpr1a-Cre, and RC-PTom

To use TdTomato signal as indirect evidence of Cre-mediated recombination, it is important to control for any possible endogenous or Cre-independent RFP expression in Avpr1a-Cre or RC-PTom mouse lines respectively.

2.3.3.1 Tissue Collection and Immunohistochemistry. Adult Avpr1a-Cre::RC-PTom double, Avpr1a-Cre single, and RC-PTom single transgenic mice (n = 2/genotype) were used in this project. Mice were anesthetized with isoflurane and underwent intracardiac perfusion with 0.9% saline followed by 4% PFA. Next, brains were harvested and stored in 4% PFA at 4 °C for overnight fixation. Thereafter, brains were stored in 30% sucrose at 4 °C until sectioning. Tissue was sectioned at a thickness of 40 µM and stored in cryoprotectant (30% sucrose and 30% ethylene glycol in 0.1M PB) until further processing.

A series containing every third section was used for immunohistochemistry. Tissue was washed 3x for 10 min in PBS (in mM: NaH₂PO₄ 17, Na₂HPO₄ 83, NaCl 154) prior to incubation in PBST-BSA (PBS with 0.5% Triton-X100 and 0.04% bovine serum albumin) for 30 minutes. Next, tissue was incubated in PBST-BSA containing the primary antibody (rabbit anti-RFP, 1:2000, Rockland) overnight. Then, tissue was washed 3x for 10 min in PBST-BSA followed by incubation in PBST-BSA containing the secondary antibody (donkey anti-rabbit Alex Fluor 594, 1:250, Invitrogen) for 4 hours. Tissue was washed 3x in PBS for 10 min each time and stored free-floating in PBS at 4 °C and covered to avoid light exposure. Tissue was mounted onto SuperFrost Plus slides and coverslipped

using DAPI-containing FluoromountG mounting medium. Stained slides were stored at 4°C until image acquisition.

2.3.3.2 Image Acquisition. Keyence BZ-X710 Fluorescent Microscope was used to capture 10x images of anatomically matched slices from each animal representing several key brain regions (i.e., LS, MD, and DR). Images were processed in ImageJ to optimize contrast and adjust pseudocoloring for presentation, and in Adobe Illustrator to annotate brain regions. Imaging data was analyzed qualitatively to describe the presence of TdTomato positive (or putative Avpr1a) cells in brain regions known to contain Avp-immunoreactive fibers in each of the three genotypes.

2.3.4 Experiment 3: Assessing Cre Recombinase Efficacy in Adult Avpr1a-Cre Mice with Cre-Dependent Viral Vectors Injected to the Dorsal Raphe

Given that TdTomato expression in Avpr1a-Cre::RC-PTom mice may be induced by Cre-mediated recombination at any point in development, it is important to rule out the possibility that a population of TdTomato positive neurons in the region of interest is not a result of conditional Cre-expression during development.

2.3.4.1 Stereotaxic Injections. Adult WT and Avpr1a-Cre mice (n = 6 per genotype) received stereotaxic injections of one of three Cre-dependent viral vectors (n = 2 per genotype): 1) pAAV-FLEX-TdTomato (TdTomato; Addgene #28306-AAV1, $\geq 1 \times 10^{13}$ vg/ml), 2) pAAV-hSyn-DIO-hM3D(Gq)-mCherry (hM3Dq; Addgene #44361-AAV2, $\geq 6 \times 10^{12}$ vg/ml), or 3) pAAV-hSyn-DIO-hM4D(Gi)-mCherry (hM4Di; Addgene

#44362-AAV2, $\geq 5 \times 10^{12}$ vg/ml). Animals were anesthetized using isoflurane (4% induction, 2% maintenance) to deliver Cre-dependent viral vectors into the Dorsal raphe by targeting the following bregma coordinates (Franklin & Paxinos, 2008): AP -4.48 mm, ML 0 mm, DV -3.15 mm. 150 nl of virus was injected at the rate of 50 nl / min. After injection, the needle remained undisturbed in the brain for 5 min to allow for virus dispersion. Finally, the needle was removed slowly (1 mm / min) to minimize leaking of the virus up the needle track. After the surgical procedure, post-operative care included administration of analgesia (2 mg/kg meloxicam every 24 hours for 3 days) for pain and assessment of the surgical site including observation of posture, hydration, and appetite. Staples were removed 7-10 days after the procedure.

2.3.4.2 Tissue Collection, Immunohistochemistry, and Image Acquisition.

Three weeks after surgery, tissue was extracted and then used to perform immunohistochemistry (as described previously in section 2.3.3.1) to detect the presence of mCherry or TdTomato (RFP; primary: rabbit anti-RFP, 1:2000, Rockland; secondary: donkey anti-rabbit Alex Fluor 594, 1:250, Invitrogen) and green fluorescent protein (GFP; primary: chicken anti-GFP, 1:1000, Abcam; secondary: goat anti-chicken Alex Fluor 488, 1:250, Invitrogen). Keyence BZ-X710 fluorescent microscope was used to capture 10x representative images in multiple channels, and exposure time for each channel was kept consistent across sections from different animals (WT vs. Avpr1a-Cre) infused with different viruses (TdTomato, hM3Dq, hM4Di). ImageJ was used to adjust brightness/contrast to optimize images for best visualization.

2.3.5 Experiment 4: Characterize the Putative Avpr1a Cells throughout the Rostro-Caudal Extent of the Dorsal Raphe

Because our data indicates a role of DR Avpr1a neurons in social behavior, and previous data indicates an interaction of Avp with the DR serotonin system, DR Avpr1a neurons might display a characteristic neuroanatomical distribution with respect to the DR serotonin neurons. Knowing this relationship can be useful in generation of circuit-level hypotheses.

2.3.5.1 Tissue Collection, Immunohistochemistry, and Image Acquisition.

Adult Avpr1a-Cre::RC-PTom mice (n = 7; 3 male, 4 female) were euthanized, brains were extracted, and resultant tissue used to performed immunochemistry (as described previously in section 2.3.3.1 Tissue collection and immunohistochemistry) to detect the presence of RFP (primary: rabbit anti-RFP, 1:2000, Rockland; secondary: donkey anti-rabbit Alexa Fluor 594, 1:250, Invitrogen) and Tph2 (primary: goat anti-Tph2, 1:500, Abcam; secondary: donkey anti-goat Alexa Fluor 488, 1:250, Invitrogen). Keyence BZ-X710 was used to capture 10x images of the stained sections in multiple channels. Images were analyzed qualitatively to characterize the anatomical position of putative Avpr1a cells throughout the rostro-caudal extent of the DR defined by the Tph2 stained serotonin cells. Using ImageJ, representative images of the dorsal raphe were optimized to maximize foreground and minimize background. Adobe Illustrator was used to annotate anatomical boundaries and label regions.

2.4 Experimental Results

2.4.1 In Avpr1a-Cre::RC-PTom Mice, Cre-Recombinase is Efficacious and TdTomato Expression is Specific to Avpr1a-Positive Cells

To effectively utilize Avpr1a-Cre mouse model to target Avpr1a cells specifically, we need to confirm specificity of Cre expression within cells expressing Avpr1a. Given the genetic construct in Avpr1a-Cre mouse, we predict that Cre-recombinase is present in Avpr1a cells (*Figure A2. 2*). However, it might be possible to observe Avpr1a, but not Cre, expression, which would curtail the effectiveness of the model when using Cre-mediated recombination to target Avpr1a cells. In contrast, it may also be possible to observe Cre expression in cells without Avpr1a expression, which could be an indication of ectopic expression of Cre recombinase and would reduce the ability to target Avpr1a cells specifically.

Given that Cre expression should be specific to Avpr1a expressing cells, we hypothesize that TdTomato and Avpr1a mRNA will be largely co-localized. To test this hypothesis, we performed in situ hybridization (ISH) using probes against Avpr1a and TdTomato mRNA in tissue acquired from double transgenic Avpr1a-Cre::RC-PTom mice (*Figure A2. 3A*). Representative images of the periaqueductal gray, median raphe, and dorsal raphe (*Figure A2. 3B*) illustrate that signal from Avpr1a and TdTomato puncta is colocalized (blue arrow) in a majority of neurons; however, Avpr1a (yellow arrow) or TdTomato (magenta) puncta alone are also sparingly observed. Quantification of cell counts by phenotype (colocalized, Avpr1a or TdTomato alone) from 6025 “positive” cells (defined by 5 or more total puncta in a given cell; see section 2.3.3.2 Image acquisition for

rationale) across four animals (2 females and 2 males) indicates that approximately 64% of cells contain both Avpr1a and TdTomato puncta, and percentage of cells that contain Avpr1a or TdTomato puncta alone are approximately 25 and 11 respectively (*Figure A2. 3C*). When this data is separated for each animal in the experiment, male subjects seem to have a greater percentage of colocalized cells than female subjects (67.29% vs. 58.15%; *Figure A2. 3D*). Furthermore, males show a larger percentage of cells that express TdTomato alone (14.88% vs. 4.56%) but a smaller percentage of cells that express Avpr1a alone (17.84% vs. 37.30%) when compared to females (*Figure A2. 3D*). Although this data may hint toward sex differences in specificity of Avpr1a-Cre model, this study is not powered to draw any statistical conclusion.

2.4.2 Avpr1a-Cre::RC-Ptom, but not Avpr1a-Cre or RC-Ptom, Dorsal Raphe Sections Show Robust Tdtomato Staining

While section 2.4.1 discusses the efficacy and specificity of Cre recombinase within Avpr1a neurons using the Avpr1a-Cre::RC-PTom double transgenic mouse, it is based on the assumptions that RC-PTom and Avpr1a-Cre single transgenic mice do not express TdTomato independently. Furthermore, it is important to test the efficacy of this model in different regions of the brain, as Cre-recombinase activity has been documented to differ between different tissue and regions (Gofflot et al., 2011).

To verify that the RFP expression is specific to Cre function and to rule out the possibility of endogenous RFP expression in RC-PTom mice or Avpr1a-Cre mice alone, we performed immunohistochemistry to detect RFP expression in sections from single transgenic Avpr1a-Cre and RC-PTom mice and double transgenic Avpr1a-Cre::RC-PTom

mice. Assuming efficacious Cre-recombinase enzyme is present in cells with active Avpr1a promoter region, we hypothesized that we would observe robust RFP expression only in tissue from the Avpr1a-Cre::RC-PTom double transgenic, but not Avpr1a-Cre or RC-Tom single transgenic mouse lines. *Figure A2. 4* shows IHC data from dorsal raphe sections from the three mouse lines. In the Avpr1a-Cre::RC-PTom mouse, RFP signal is robust and specific in regions known to contain Avp-immunoreactive fibers/terminals (Rood & DeVries, 2011) and/or Avpr1a cells (Patel et al., 2022), including the LS (*Figure A2. 4A''*), thalamus (*Figure A2. 4B''*), DR (*Figure A2. 4C''*), ventrolateral PAG (VLPAG, *Figure A2. 4C''*), and median raphe (MR, *Figure A2. 4D''*). Importantly in Avpr1a-Cre and RC-PTom mice that lack TdTomato and Cre respectively, we observe no RFP positive cells in any region [LS (*Figure A2. 4A, A'*), thalamus (*Figure A2. 4B, B'*), DR (*Figure A2. 4C, C'*), VLPAG (*Figure A2. 4C, C'*), or MR (*Figure A2. 4D, D'*)]. This data suggests that Cre recombinase in the Avpr1a-Cre::RC-PTom mouse model carries out a recombination event at LoxP sites on the RC-PTom allele and induces reliable and robust TdTomato expression for specific visualization of Avpr1a cells.

2.4.3 Assessing Cre Recombinase Efficacy in Adult Avpr1a-Cre Mice with Cre-Dependent Viral Vectors Injected to the Dorsal Raphe

In Avpr1a-Cre::RC-PTom mouse model, expression of TdTomato protein is unlocked within cells that had a transient activation of Avpr1a promoter at some point during development. Therefore, it is possible that a population of TdTomato positive cells may not have Avpr1a expression in adulthood, and thus present as “false positives”. To rule out this mechanism as a major driver for expression of TdTomato protein in the genetic

model, we injected Cre-dependent viral vectors into the dorsal raphe of adult Avpr1a-Cre mice. In Avpr1a-Cre mice, Cre recombinase would be present in cells with active Avpr1a promoter (*Figure A2. 5A*). We hypothesize that viral vectors with Cre-dependent genes will express in adult cells that have functional Cre-recombinase enzyme in Avpr1a-Cre, but not wildtype mice. To test this hypothesis, we stereotaxically injected virus with Cre-dependent TdTomato, hM3Dq-mCherry, and hM4Di-mCherry to the dorsal raphe of Avpr1a-Cre and WT (negative control) mice (*Figure A2. 5B*).

Eleven of twelve animals that underwent stereotaxic surgery survived and recovered from the procedure with no noticeable functional change. Thus, group numbers for TdTomato, hM3Dq-mCherry, and hM4Di-mCherry injections were 4 (2 Avpr1a-Cre, 2 WT), 3 (2 Avpr1a-Cre, 1 WT), and 4 (2 Avpr1a-Cre, 2 WT) respectively. Using immunohistochemistry, we visualized the expression of RFP and GFP (to detect Cre-GFP fusion protein). Five of six AAV injections in Avpr1a-Cre mice produced RFP positive cells in the DR (n = 1 TdTomato, 2 hM3Dq-mCherry, and 2 hM4Di-mCherry). One TdTomato AAV injection in Avpr1a-Cre mouse missed the DR but did display RFP positive cells in the MR (data not shown), which harbors RFP positive cells in the Avpr1a-Cre::RC-PTom mice (*Figure A2. 4*) and Avp-immunoreactive (-ir) fibers (Rood & De Vries, 2011). One hM3Dq-mCherry AAV injection in Avpr1a-Cre mouse showed RFP cells in the VLPAG (data not shown), as well as the DR, both locations known to contain Avp-ir fibers (Rood & De Vries, 2011) (Patel et al., 2022) and RFP positive cells in Avpr1a-Cre::RC-PTom mice (*Figure A2. 4*). In the DR sections from a TdTomato AAV injected animal, RFP positive cells are located bilaterally surrounding the midline (*Figure A2. 5D*), a pattern observed in DR sections from Avpr1a-Cre::RC-PTom mice (*Figure A2. 4C*). Furthermore,

RFP-positive fibers (*Figure A2. 5D*) are penetrating the midline where serotonin cells are typically located (data not shown), lending anatomical support to the hypothesis that BNST Avp neurons send signals to DR serotonin neurons through a distinct population of Avpr1a neurons in or near the DR. Importantly, injection of Cre-dependent viral vectors into the dorsal raphe of wildtype mice did not display RFP-positive cells in any of the five injections (n = 2 TdTomato, 1 hm3dq, 2 hm4di; *Figure A2. 5E*).

2.4.4 Characterization of Putative Avpr1a Cells Throughout the Rostro-Caudal Extent of DR

Because the topography of neurons within brain regions is often intimately linked to their function at a circuit level (Simpson et al., 2003; Waterhouse et al., 1993; Waterhouse et al., 1986), it is important to characterize the anatomical distribution of neurons within a given region of interest. The DR contains the majority of serotonergic neurons in the brain and generates the most serotonergic innervation of the rodent forebrain. The DR serotonin system has been associated with regulation of mood, anxiety, and social behaviors (Lucki, 1998; Rood & Beck, 2014). Recent studies in mice have revealed topographically distinct serotonin neuron clusters within the DR that have distinct projection sites with opposite function (Muzerelle et al., 2016; Ren et al., 2018). Given that the DR Avpr1a neurons potentially act as intermediate nodes relaying signals from BNST Avp neurons to DR serotonin neurons (Rood & Beck, 2014), it is important to characterize the neuroanatomical distribution of DR Avpr1a neurons. To examine the location of Avpr1a neurons in relations to the topography of serotonin neurons, we performed immunohistochemistry to visualize TdTomato and Tph2, an enzyme involved in serotonin

production and exclusive to serotonin neurons, in dorsal raphe sections from Avpr1a-Cre::RC-PTom mice.

Tissue from seven mice (4 females, 3 males) displayed a consistent pattern of RFP-positive cells within the DR but also in other regions expected to contain Avpr1a-expressing cells like the PAG. *Figure A2. 6* shows representative images of the rostral to caudal extent of the DR ranging from anterior-posterior (AP) coordinates of -4.36 to -4.84 mm from bregma. Maps of the DR were drawn using images from the DAPI channel. For the dorsal raphe, regional borders were drawn based on the cell density changes that mark borders of the DR (Franklin & Paxinos, 2008). Specifically, cells in the DR cluster in a highly cell dense region at the midline ventral to the cerebral aqueduct (Aq) and dorsal to medial longitudinal fasciculus (MLF). DR extends bilaterally to a less dense region marking the borders along the VLPAG (*Figure A2. 6* left column).

Serotonin neurons in the DR form 3 distinct clusters often described in the literature as the dorsomedial DR, ventromedial DR, and lateral wings of the DR. In some descriptions the serotonin neurons spreading down between the right and left medial lateral fasciculus are described separately as the interfascicular cluster. In our typical workflow, we identify 5 distinct relatively evenly spaced sections (domains ~ 120 μm apart) that reflect distinct changes in serotonin neuron topography from rostral to caudal (*Figure A2. 6A-E* middle and right columns). In far rostral DR (AP -4.36 mm), serotonin cells concentrate along the midline between the cerebral aqueduct and medial longitudinal fasciculus in the dorsal-ventral (DV) axis. At this AP location, most Avpr1a cells are located lateral and adjacent to the dorsal two-thirds of serotonin neurons. In lower quantity, some Avpr1a cells are interspersed at the midline with the serotonin cells and a few sparingly extend laterally

towards the border of VLPAG (*Figure A2. 6A*). At around AP -4.48 mm from Bregma, DR serotonin neurons divide into two distinct subregions, dorsomedial DR (DMDR) and ventromedial DR (VMDR). At this point, most Avpr1a cells bilaterally flank the DMDR, and a moderate number of Avpr1a cells are in the gap between DMDR and VMDR. A smaller number of Avpr1a neurons are located in and around the VMDR (*Figure A2. 6B*). Moving further caudally, at around AP -4.60 mm from Bregma, serotonin cells begin to slightly spread out laterally towards borders of VLPAG forming the first hint of the lateral wings of the DR. Avpr1a cells are more interspersed with serotonin cells laterally, and, medially, there are only a few Avpr1a cells remaining at the midline in DMDR and even fewer in VMDR. Overall, the number of Avpr1a cells decreases compared to more rostral sections (*Figure A2. 6C*). In a more caudal section (AP -4.72 mm from Bregma), serotonin cells just below the aqueduct continue to spread out laterally and slightly dorsally toward VLPAG, segregating into a bilateral subdomain, lateral wing dorsal raphe (LWDR) (*Figure A2. 6D*). Here, some Avpr1a cells are located within the LWDR bilaterally, with cells still found within the DMDR, and in a smaller number in the VMDR. Of all rostro-caudal sections of the DR, *Figure A2. 6D* region seems to house the fewest number of Avpr1a cells, and in general, most of the Avpr1a cells in DR are found in rostral and far caudal sections of DR. In caudal DR (AP -4.84 mm from Bregma, *Figure A2. 6E*), serotonin cells are found more tightly at midline in a single continuous column bridging the gap between DMDR and VMDR like that in far rostral section (*Figure A2. 6A*). The LWDR serotonin cells extend farther laterally and dorsally. Overall number of serotonin cells decrease drastically compared to other rostral DR sections (*Figure A2. 6A-D*). As for the Avpr1a cells, most are seen within the LWDR, with very few found in DMDR and VMDR at

midline. Above, we describe the distribution of Avpr1a neurons that are in the closest proximity and appear to be within the anatomical borders ascribed to the dorsal raphe. While the DR contains distinct populations of Avpr1a cells, Avpr1a neurons are also found in varying amounts in regions surrounding the DR like the VLPAG, lateral PAG (LPAG), dorsolateral PAG (DLPAG), and dorsomedial PAG (DMPAG) (*Figure A2. 6A-E* middle panel). Of the subregions of PAG, VLPAG and DMPAG seem to contain the majority of PAG Avpr1a cells and DLPAG contains the least. In contrast to the regional patterns seen of DR Avpr1a cells, PAG Avpr1a cells increase in number in caudal sections compared to rostral sections (*Figure A2. 6A-E* middle panel). In caudal sections of the DR, there is a distinct cluster of Avpr1a neurons that forms somewhat separated from the VMDR and LWDR serotonin neurons; this region appears to correspond with the dorsal tegmental nucleus.

2.5 Discussion

2.5.1 Cre Recombinase is Efficacious and Specific to Avpr1a-Expressing Cells

The integration of Cre-Lox system into mouse genetics has revolutionized the study of behavioral neuroscience. The Cre-Lox system has enabled scientists to access select cell types of interest within specific brain regions using tools to characterize anatomy using reporter proteins or to alter neuronal activity and assess the impact on behavior. One way the Cre-Lox system is employed is through the creation of transgenic mouse models that express Cre recombinase under the control of a promoter specific to a cell type of interest. In the studies presented above, we validated a novel Avpr1a-Cre mouse in which Cre

expression is driven by the regulatory sequences of *Avpr1a* (*Figure A2. 2*). Upon breeding this mouse to a Cre-dependent reporter line like RC-PTom, RFP can be expressed within cells that express *Avpr1a* enabling easier anatomical characterization of *Avpr1a* cells throughout the mouse brain.

While conceptually sound, this system must be validated to ensure reliable and reproducible results. First, Cre enzyme should be functional such that it recognizes and recombines DNA containing LoxP sites to, for example, excise the STOP cassette within the RC-PTom allele to induce TdTomato expression (*Figure A2. 2*). Second, Cre-recombinase expression should be specific, expressed primarily within expected cell-types such as *Avpr1a* in our case. Last, to use RFP as a proxy signal for putative *Avpr1a* neurons, endogenous RFP expression without Cre-mediated recombination event must be minimal or, preferably, absent. We performed several experiments in this chapter to assess the validity of the above stated assumptions.

Several different experiments indicate that Cre-recombinase in the *Avpr1a*-Cre mouse is efficacious. First, ISH (*Figure A2. 3*) performed on DR sections from *Avpr1a*-Cre::RC-PTom mice displays a robust TdTomato signal, indicating a high level of TdTomato expression following a Cre-mediated recombination event. The immunohistochemistry data (*Figure A2. 4*) in tissue from *Avpr1a*-Cre:RC-PTom, but not *Avpr1a*-Cre and RC-PTom mice, shows bright RFP signal in several brain regions that contain *Avp*-ir fibers (Rood & De Vries, 2011) and *Avpr1a* neurons (Patel et al., 2022). Lastly, injections of viral vectors containing a Cre-dependent reporter in the DR of *Avpr1a*-Cre, but not wild type, mice show robust reporter expression (*Figure A2. 5*). In contrast, it is noteworthy to mention that GFP immunostaining fails to detect Cre-recombinase

directly. We separately performed ISH using probes to detect Cre and GFP mRNA (data not shown) which also showed no signal. A likely reason for this finding is that Cre-GFP might be expressed at a level that is suboptimal for detection via the methodologies employed. Similarly, a study using OxtR-Cre transgenic mice failed to directly detect Cre recombinase using immunohistochemistry but did report that Cre recombines at LoxP sites as expected (Inoue et al., 2022). Together, it is reasonable to conclude that even though Cre-GFP is produced at a sub-detection level (as indicated by the absence of Cre or GFP staining) in Avpr1a-Cre mice, Cre enzyme is highly efficacious in mediating a recombination event at loxP sites, whether they are found on a chromosome or are virally delivered.

To assess the specificity of Cre expression, in situ hybridization to detect Avpr1a and TdTomato mRNA was conducted in dorsal raphe sections from Avpr1a-Cre::RC-PTom mice. We observed that approximately 64% of cells with positive puncta signal had both Avpr1a and TdTomato puncta (i.e., colocalized signal), 25% contained Avpr1a signal alone, and 11% contained TdTomato puncta alone. Furthermore, the data shows that 71.9% of all Avpr1a positive cells colocalize TdTomato signal whereas 85.3% of all TdTomato positive cells also display Avpr1a signal. In other words, the transgenic model appears to capture a majority of Avpr1a neurons, but may miss a quarter to a third of cells, and the potential for transgene expression in non-Avpr1a neurons (i.e. ectopic expression) is relatively low at about 15%.

Observation of Avpr1a signal alone could be due to several reasons. First, if Avpr1a promoter is not highly active, then Cre recombinase in some Avpr1a cells may not be expressed in sufficient quantity to catalyze efficient recombination at LoxP target sites. In

fact, our in situ hybridization data suggest that *Avpr1a* is indeed expressed at quite low levels based on the number of *Avpr1a* puncta observed per cell, especially when compared to other expressed genes such as *TdTomato*, discussed above, or mRNAs related to glutamate and GABA phenotypes (Patel et al., 2022). Second, it could also be due to less than 100% efficiency of Cre in mediating the recombination event. Cre recombinase performs excision at LoxP sites in 80-100% of the cells in which Cre is transiently expressed (Gagneten et al., 1997; Sauer, 1993). Furthermore, the expression of native *Avpr1a* may be modulated by distant regulatory sequences (e.g., enhancers and repressors) that are not near enough the *Avpr1a* gene to be included in the contig used to generate the BAC transgenic *Avpr1a*-Cre mouse, which would likely result in more limited expression from the transgene. We believe the limitations of the BAC method may be the most likely reason for the number of observed *Avpr1a*-only cells. A knock-in mouse line, in which Cre expression would be driven by native regulatory sequences of target gene, may have shown a more efficient expression of the trans gene (Gofflot et al., 2011). Next, recombination efficiency can be dependent on the locus of the target sites and has been documented to differ based on the reporter line used (Gofflot et al., 2011; Vooijs et al., 2001). Because the location of recombination event (i.e., LoxP sites on RC-PTom allele) in the double transgenic mouse model is within the chromosomal DNA, efficiency can also depend on differences in the chromatin structure, DNA methylation, and transcriptional activity at the locus of interest (Gofflot et al., 2011). While the state of chromatin structure or DNA methylation may explain the less than perfect efficiency, it is unlikely to be the transcriptional activity of the promoter since *TdTomato* expression in the RC-PTom allele is driven by a highly active, ubiquitous CAG promoter (Madisen et al., 2010).

Our data shows a small percentage of TdTomato-only (14.7%) suggesting a small amount of off-target TdTomato expression. TdTomato signal without Avpr1a signal could represent a population of cells with ectopically expressed Cre-recombinase; we demonstrated that the RC-PTom mouse line itself does not have expression in the absence of Cre. An alternative explanation for observing TdTomato-only cells is that Avpr1a expression is below detectable levels. Although unlikely given our own results suggesting no expression of TdTomato in the absence of Cre, other studies using the RC-PTom mouse line have noted a low level of TdTomato expression independent of Cre-mediated recombination (Madisen et al., 2010). Due to the high sensitivity of RNAscope in situ hybridization, cells exhibiting minimal levels of Cre-independent TdTomato expression could be identified as TdTomato-only cells. Despite the low level of leaky expression of TdTomato, we only observe 14.7% TdTomato-only cells. In fact, RFP immunohistochemistry data from the double transgenic mouse model shows a robust expression of TdTomato protein in a pattern closely aligned to that seen in studies of Avpr1a fibers and putative Avpr1a cells from Avpr1a-GFP mice (Patel et al., 2022; Rood & De Vries, 2011). TdTomato protein expression is absent in anatomically matched regions in tissue from Avpr1a-Cre and RC-PTom mouse. In the latter single transgenic mouse, a faint, non-specific signal is observed in certain regions like the caudate putamen, which could be due to a low level of TdTomato expression independent of Cre recombinase, as mentioned earlier. However, the noticeable enhancement in TdTomato signal following the Cre-mediated recombination event is very robust as described by other studies (Madisen et al., 2010). Finally, it is worth noting that a portion of the TdTomato-only cells could be attributed to potential transient expression of Cre during development. Though,

developmental transient activation is a less likely explanation because the pattern of RFP-positive cells (*Figure A2. 4* and *Figure A2. 6*) is remarkably restricted to regions that in adulthood are known to contain Avp-ir fibers (Rood & De Vries, 2011) and putative Avpr1a neurons (Patel et al., 2022) like the lateral septum, thalamus, and raphe nucleus. Use of a virally delivered Cre-dependent effector gene revealed that there is sufficient Cre-expression to drive recombination and unlocking of fluorescent reporters and other effector genes. While this finding does not eliminate the potential for a fate-mapping problem (i.e., cells express Cre developmentally, but not in adulthood), the expression of virally delivered effector proteins suggests the problem is limited at least for the dorsal raphe, which is the focus of experiments described in Chapters 3 and 4.

Performing electrophysiology studies to verify Avp-induced responses in the majority, if not all, RFP-positive cells will offer further support for precise Cre expression in Avpr1a cells and reduce the likelihood of ectopic RFP expression. In Avpr1a-GFP mice, a transgenic mouse model with a similar construction to that of the Avpr1a-Cre mouse, patch clamp study showed that 10 out of 12 GFP+ cells were responsive to Avp (Patel et al., 2022).

Examination of Cre line validations presented in the literature reveals substantial variability in the quantity and quality of evidence presented. Further, evidence presented is often exclusively qualitative, and a consensus regarding the threshold of evidence deemed acceptable for evaluating a mouse line's utility remains elusive. For example, in a Vill1-CreERT2 mouse line, Cre expression is directed to the epithelium of intestinal crypts. A study bred Vill1-CreERT2 to a reporter line to analyze the specificity of Cre recombinase to intestinal epithelium and qPCR analysis found that the excised allele was detected at a

relative proportion of 15% to 30% instead of the predicted 50% (50% floxed allele and 50% WT allele), far from a perfect Cre recombinase efficiency (Gofflot et al., 2011). Further, (Zhuang et al., 2005) produced both DAT-Cre (dopamine neuron specific) and SERT-Cre (serotonin neuron specific) lines and provided extensive validation data. Upon crossing both lines to the Cre-dependent YFP reporter line, the authors noted that 92% of YFP cells in the VTA also colocalized TH and 99% of YFP cells in the raphe colocalized Tph2. Our data shows that of all TdTomato positive cells, 85.3% also colocalize Avpr1a signal in the DR. While studies on other DAT-Cre lines (Backman et al., 2006; Turiault et al., 2007) and OxtR-Cre (oxytocin receptor) line (Inoue et al., 2022) demonstrate primarily overlapping cell-specific markers with Cre-dependent reporter proteins, there are also instances of single-labeled cells. Unfortunately, these studies did not provide quantitative data regarding the percentage of cells exhibiting colocalization versus single labeling. Overall, analysis of Cre line validation studies exposes significant variability in presented evidence, with no established consensus on the acceptable evidence threshold for assessing a mouse line's utility. Given the variation in Cre-recombinase efficiency reported across regions, tissues, and cell types of interest in the literature (Gofflot et al., 2011) and our focus largely on the DR, quality control experiments to assess specificity and efficacy should be performed for other brain regions of interest when using the Avpr1a-Cre mouse.

In summary, Cre expression in our Avpr1a-Cre and Avpr1a-Cre::RC-PTom mice is highly efficacious and specific to Avpr1a cells in the dorsal raphe. First, the IHC study in Avpr1a-Cre::RC-PTom mice shows that Cre recombinase is highly efficacious in recombining LoxP sites on the RC-PTom allele to allow the expression of TdTomato protein in an anatomical pattern like that found for Avp-ir fibers (Rood & De Vries, 2011;

Rood et al., 2013) and Avpr1a cells (Patel et al., 2022). Second, we show a similar pattern of RFP expression in the DR with a viral delivery of Cre-dependent reporter in Avpr1a-Cre mice. Third, the ISH study in Avpr1a-Cre::RC-PTom mice displays that 71.9% of all Avpr1a positive cells also show TdTomato signal and 85.3% of all TdTomato positive cells colocalize Avpr1a. While data suggests a 14.7% ectopic expression rate for TdTomato protein in the Avpr1a-Cre::RC-PTom mice, there are multiple potential factors that could account for the expression of TdTomato in the absence of Avpr1a including leaky expression of stop-Loxed TdTomato in RC-PTom. Because we can utilize Cre-dependent viral construction in the Avpr1a-Cre mouse, the possibility of leaky expression from the RC-PTom presenting as a confounding variable is avoided altogether, further increasing the utility of the single transgenic line. Furthermore, because we observe a remarkable increase in intensity of fluorescence following Cre-dependent recombination on the RC-PTom allele, Avpr1a-Cre::RC-PTom mice provide a convenient means of visualizing putative Avpr1a-expressing neurons in the dorsal raphe, facilitating the examination of the anatomical distribution of this cell population and enabling future investigations into the electrophysiological and gene expression profile of DR Avpr1a neurons. Having observed efficacious and specific expression of Cre during the validation of the Avpr1a-Cre mouse model, we believe it represents a pioneering tool in the field of vasopressin research, offering access to Avpr1a cells across the entire mouse brain.

2.5.2 Distribution of Avpr1a Neurons in the DR

While the validation of the Avpr1a-Cre mouse was the major goal of work presented in this chapter, we also provide a careful analysis of Avpr1a neuron distribution in the DR

as this neuron population is the focus of projects described in subsequent chapters. In general, Avpr1a neurons were more numerous rostrally, but were present at all rostral to caudal levels of the DR. In rostral areas, Avpr1a neurons mostly clustered lateral to serotonin neurons, which were visualized by staining for Tph2. Moving caudally, Avpr1a cells tended to cluster in the midline separation between the VMDR and DMDR to insert sparsely amongst the clusters of serotonin neurons. Avpr1a cells interspersed with Tph2 cells were more common in caudal sections of the dorsal raphe. In describing the location of Avpr1a neurons in relation to serotonin neurons and in delineating the raphe in figures, we have largely used the terms ventromedial, dorsomedial, and lateral wings of the DR. These terms are most often applied in reference to the 3 distinct clusters of serotonin neurons in mice and rats. Many Avpr1a neurons lay outside of the actual serotonin neuron clusters. As indicated in our drawing the DR, we characterize the dorsal raphe as the cell dense region below the aqueduct and above the medial lateral fasciculus. The lateral edges are defined by an area of slightly lower cell density. When viewed with Tph2, the lateral extent of the defined region starts at the dorsal edge of Tph2 staining and travels down and outward meeting the ventral edge of the gray matter about where the medial lateral fasciculus ends laterally. The region encapsulates many neurons that are not serotonergic, which may generate question about nomenclature.

The serotonin system exhibits a topographical arrangement across various species including mammals (Azmitia & Segal, 1978; Bobillier et al., 1976; Jacobs & Azmitia, 1992; Lillesaar, 2011; Ma et al., 1992; Muzerelle et al., 2016; Ren et al., 2018; Waterhouse et al., 1993). *Figure A2. 7* depicts DR serotonin neurons' efferent topography in mice. For instance, DMDR and VMDR serotonin neurons exhibit stark differences in their efferent

projections, with the former favoring subcortical areas (e.g., the hypothalamus, BNST, and central amygdala (CeA)) and the latter projecting to cortical areas like the orbitofrontal cortex (OFC) (Commons et al., 2003; Muzerelle et al., 2016; Ren et al., 2018). This suggests the possibility of at least two functionally distinct serotonin systems within the DR. In fact, Ren and colleagues (Ren et al., 2018) found that chemogenetic activation and conditional Tph2 depletion in DMDR serotonin neurons projecting to the CeA increases and decreases anxiety-like behaviors respectively. In contrast, chemogenetically activating OFC-projecting serotonin neurons located largely in the VMDR promotes escape behavior in the forced swim test while conditional Tph2 depletion in the same cell population shows the opposite effect, implying a role of subset of VMDR serotonin neurons in active coping (Ren et al., 2018). Since the putative Avpr1a neurons are found mainly surrounding the DMDR compared to the VMDR, DR Avpr1a neurons may be more likely to play a role in anxiety-like behaviors than in active coping, an area that should be further explored in future studies. Lastly, there are other groups of Avpr1a cells in the DR that are unlikely to interact with serotonin neurons, particularly in the caudal DR, based on the electrophysiological data (Rood & Beck, 2014). Together, these data hint at the presence of functionally distinct populations of Avpr1a neurons that may interact with different neurotransmitter systems along the rostral to caudal extent of the DR. Using the Avpr1a-Cre::RC-PTom mouse, we can design novel studies to distinguish between clusters of Avpr1a cells that might differ phenotypically within the DR, which may enhance our understanding of the Avp system and behavior.

The distribution of Avpr1a neurons in the DR reported here matches closely to the location of Avp-ir fibers identified previously in the DR, and Avpr1a fibers (i.e., RFP

positive fibers) are found highly dispersed surrounding the DR serotonin cells (*Figure A2. 7*), further giving credence to the hypothesis that DR Avp impacts serotonin systems through intermediate neurons expressing Avpr1a. Next, most Avp-responsive serotonin neurons (*Figure A2. 8*) were found in rostral areas similar to where we see the largest numbers of Avpr1a cells in the present experiments (*Figure A2. 7*).

Chapter 3

Social Interactions and Dorsal Raphe

Note: This chapter is adapted from:

Patel, T. N., Caiola, H. O., Mallari, O. G., Blandino, K. L., Goldenthal, A. R., Dymecki, S. M., & Rood, B. D. (2022). Social Interactions Increase Activation of Vasopressin-Responsive Neurons in the Dorsal Raphe. *Neuroscience*, 495, 25-46.

<https://doi.org/10.1016/j.neuroscience.2022.05.032>

Author Contributions: T.N.P. and B.D.R. designed projects. T.N.P., H.O.C., O.G.M., K.L.B., and B.D.R. performed research. T.N.P., H.O.C., and B.D.R. analyzed data. S.M.D. guided some projects. B.D.R. wrote the paper.

3.1 Introduction

Social interactions are part of our everyday life. They are fundamental to our maturation, and maintenance of healthy lifestyles as adults. Broadly, social networks are the backbone of a functional society. Therefore, mental illnesses that disrupt social behavior are not only cumbersome to the individuals affected but also society at large. Despite the overwhelming importance of social behavior, our understanding of the neurobiological mechanisms that drive social behaviors or their disruptions in psychopathologies remains incomplete. Multiple brain regions and neurotransmitter systems across many species are implicated in the regulation of social behaviors. In this Chapter, we explore small population of vasopressin (Avp)-responsive (Avpr1a-expressing) neurons in the dorsal raphe (DR) and their potential role in the regulation of prosocial behavior.

3.2 Rationale

As discussed extensively in Chapter 1, Avp has been implicated in the regulation of social behaviors like parental care, mating, and aggression in a variety of species. In contrast, manipulations of suprachiasmatic nucleus Avp neurons have implicated Avp in non-social behaviors like locomotion especially in reference to circadian rhythms (Delville et al., 1998). Overall, data suggest three functionally distinct Avp systems at play in the mouse brain: paraventricular and supraoptic nuclei for the regulation of physical and psychosocial stress; bed nucleus of the stria terminalis (BNST) and medial amygdala (MeA) for the regulation of social behavior; and suprachiasmatic nucleus for circadian rhythms (Rood et al., 2013). While Avp nuclei have been studied at length in the last decade (Rigney et al., 2023a), the role of Avp-responsive neurons remains less well studied. We believe that to obtain a mechanistic understanding of the Avp system and its effects on social behavior, it is equally important to study the role of Avp-responsive cells (i.e., downstream targets of Avp), specifically cells that express *Avpr1a*.

A projection of both BNST and MeA Avp neurons, the DR in the midbrain is particularly interesting as it houses a large group of forebrain-projecting serotonin neurons (Lucki, 1998; Rood & Beck, 2014). The serotonin system is well-known to play a role in mood regulation. For example, many current treatments for mood and behavior-altering psychiatric disorders focus on altering the serotonin system within the brain (Berman et al., 1997; Lucki, 1998). In addition, numerous studies have indicated a role for serotonin in modulating aggression. In rats, electrolytic lesion of the DR increases levels of aggression (Jacobs & Cohen, 1976). Near complete reduction of brain serotonin production by knockout of the *Tph2* gene (Mosienko et al., 2012), disruption of serotonin neuron

differentiation and maturation by knockout of the transcription factor Pet-1 (Hendricks et al., 2003), and chemical silencing of serotonin neurons using genetically controlled expression of the neurotransmitter release-inhibiting tetanus toxin light chain (Niederkofler et al., 2016) all result in elevated levels of aggression in mice. Mounting evidence suggests that subtypes of serotonin neurons may be selectively critical for aggression or perhaps regulate different types or aspects of aggression. Silencing of a relatively small subset (~500 neurons) of DR serotonin neurons that express the dopamine D2 receptor results in elevated aggression similar to that produced by silencing of the entire DR (Niederkofler et al., 2016), and knocking out D2 receptors in this neuron population alters social dominance interactions (Lyon et al., 2020). Because disruptions to serotonin neuron function result in elevated aggression, increasing excitation of DR serotonin neurons could potentially help promote a more affiliative or prosocial pattern of behavior.

Several studies have noted functional interactions between Avp and serotonin systems (Ferris et al., 1997; Terranova et al., 2016). Rood and colleagues (Rood & Beck, 2014) performed patch clamp studies of DR serotonin neurons and found that bath application of Avp increased excitatory post synaptic currents (EPSCs) in serotonin neurons. Because application of the AMPA/kainate glutamate receptor antagonist DNQX and tetrodotoxin eliminated the EPSCs, an intermediate glutamate neuron functioning in an action potential-dependent manner must be involved. It is likely that this intermediate neuron linking Avp to serotonin neurons expresses Avpr1a, as the response was eliminated with application of Avpr1a antagonists (Rood & Beck, 2014). Together, these data indicate that glutamatergic, Avp-responsive neurons are present in ex-vivo slices containing the DR and that these neurons increase the activity of serotonergic neurons in response to Avp and

may, therefore, be associated with decreased aggression or increased prosocial behaviors. Further, studies from Chapter 2 more clearly identify the presence of Avpr1a neurons in the DRL bilaterally surrounding the DR serotonin neurons at the midline.

In addition, because Ho and colleagues (Ho et al., 2010) found that mating behavior in male mice is associated with increased Fos-positive Avp neurons in the BNST (see section 1.8 for a detailed discussion), and because BNST Avp neurons project to the DR (Rood et al., 2013), it is possible that mating behaviors may increase Fos positivity in the DR. To test this hypothesis, Rood and colleagues conducted a similar social interaction assay to that in (Ho et al., 2010) by exposing male mice to a sexually-receptive female stimulus or unfamiliar male and measuring Fos activity in the DR using immunohistochemistry (Patel et al., 2022). Males exposed to a female stimulus, compared to those exposed to a male stimulus and homecage or handling controls, show an increased number of Fos-positive cells in the DR (*Figure A3. 1*). Further analysis of Fos positive neurons by subregions of the DR showed that most Fos-expression occurred in DRL bilaterally surrounding the Tph2 positive cells in the DMDR where putative Avpr1a neurons are located (*Figure A3. 1*; see *Figure A2. 7* for an anatomical schematic of DR subfields).

Overall, a discrete population of neurons in the DR is active when male mice are exposed to sexually receptive females (i.e., mating behavior), a finding like that of BNST Avp neurons (Ho et al., 2010). Because Avp indirectly activates DR serotonin neurons through Avpr1a suggesting the presence of DR Avpr1a neurons (Rood & Beck, 2014) and the fact that DR neurons were activated in response to a female stimulus, we predicted that if Avpr1a neurons play a role in prosocial behaviors, then DR Avpr1a neurons would be

among those activated in response to social stimuli. To test this, we replicated the experiment by (Ho et al., 2010) with some modifications allowing us to assess Avpr1a and Tph2 phenotypes in additions to Fos activation.

3.3 Materials & Methods

3.3.1 Animals

Adult (> postnatal day 60) male and female wildtype C57BL/6J mice were used as both subjects and stimulus animals. The animals used were bred and maintained in the animal care facility at Rowan SOM. Experimental subjects (n = 5 per sex per group) were single housed seven days prior to test day. Stimulus animals were group housed prior to behavior testing. Both subject and stimulus mice were housed in filter top mouse cages (7 in x 15 in x 5 in) under a 12-hour light/dark cycle (lights on at 6:00 am) with ad libitum access to food and water. All animal procedures were conducted in accordance with the guidelines outlined in the National Institutes of Health's guide for the care and use of laboratory animals and were approved by the Institutional Animal Care and Use Committee of Rowan University.

3.3.2 Social Interaction Test

Subject mice were habituated to the behavior room two hours/day for three days leading to the test day. An interaction test consisted of a twenty-minute session of a subject mouse in a homecage (7.25 in x 11.625 in x 4.875 in) exposed to one of four stimulus conditions: opposite sex, same sex, handling control, or no stimulus homecage control.

Subject animals in the handling control group received a simulation of placement and removal of a stimulus animal at the beginning and end, respectively, of the 20 min test. Subjects in the homecage control were euthanized without any testing. For social and handling conditions, behavior during the 20-minute test period was video recorded for later analysis.

3.3.3 Tissue Extraction

Seventy minutes after the onset of the behavior test, the subject mice were anesthetized using isoflurane (Covetrus, Inc., Portland, ME), euthanized by decapitation, and brains were extracted and flash frozen in dry ice-chilled 2-methyl butane (Thermo Fisher Scientific, Inc.). Frozen brains were stored at -80 °C until sectioning. Using a cryostat, the DR region (AP coordinates from approximately bregma -4.24 mm to -4.92 mm) of each brain was sectioned at 16 µm thickness and tissue was directly mounted onto SuperFrost Plus slides (VWR) and stored at -80 °C until processing.

3.3.4 In Situ Hybridization and Image Acquisition

Every third tissue section was subjected to in situ hybridization using the fresh frozen tissue workflow of RNAscope fluorescent multiplex assay according to the manufacturer's instructions (Version 1, Advanced Cell Diagnostics (ACD)). Workflow for version 1 kit (ACD document # 320293-USM for a detailed protocol) is similar to the one for version 2 kit (as described in section 2.3.2.2 In situ hybridization), with a few exceptions mentioned below. Version 1 used in this experiment did not use opal dyes for fluorescence labeling, hence the hydrogen peroxide, HRP, opal dye fluorescence, and HRP

blocker incubation steps found in the Version 2 workflow were omitted. Instead, in version 1, fluorescence is coupled with a fourth AMP step (~15 min) using a specific AMP solution (A, B, or C). Probes recognizing Avpr1a (probe #418061-C2), Tph2 (probe #318691-C1), and cfos (probe #316921-C3) mRNA were fluorescently labeled using AMP 4 Alt A solution (C1-Alexa 488, C2-Atto 550, C3-Atto 647). DAPI-containing FluoromountG (Electron Microscopy Sciences, Hatfield, PA) was used to detect nuclei and preserve tissue following coverslipping. Keyence BZ-X710 fluorescent microscope was used to acquire 20x images of the entire dorsal raphe in multiple channels to accommodate different fluorophores. Images were stitched together using Keyence BZ-X analyzer software.

3.3.5 In Situ Hybridization Data Analysis

DAPI channel images were used to draw an image mask (REGION) to capture the DR region. Borders of the DR were defined by the aqueduct dorsally, medial longitudinal fasciculus ventrally, and more cell-dense regions of the ventrolateral periaqueductal gray laterally. DAPI images were brightened in ImageJ to reduce background and maximize foreground and then fed into MATLAB nucleiSegmentationBot program ((Cicconet et al., 2017); Resize Factor = 0.5, Fragmentation = 0.9, Background Threshold = 0.3, and Grow = +2)) to create image masks of cells using watershed outlines of identified nuclei (CELLS). For all probe images (PROBE), ImageJ was used to make a duplicate image on which a median filter with radius of 2 pixels was applied, then the duplicate image was subtracted from the original image to reduce background signal and maximize foreground signal. Image sets of REGION, CELLS, and PROBES (Avpr1a, Tph2, and cfos) were used in a Cell Profiler (Carpenter et al., 2006) pipeline to identify cell objects (using CELLS

image masks) within the dorsal raphe (using REGION masks), count mRNA puncta for each probe (using PROBES images) by thresholding, and relate puncta counts to the identified cell objects; resulting data consisted of a table of all “parent” cells and associated “child” puncta for each probe. Next, the output data was imported into R software (version 4.2.2) to count and categorize cells based on phenotype marker (Avpr1a, Tph, or cfos). Based on counts from negative control slides, a minimum threshold of 5-or-more puncta was required for classification.

3.3.6 Behavior Video Analysis

Twenty-minute video recordings of social interactions or handling controls were manually scored by a trained experimenter using ANY-Maze software (Stoelting Co.). Bouts and durations of the following behaviors were recorded: digging, grooming, exploring, rearing, investigating, allogrooming, chasing (referred to as “following” in chapter 4), fighting, and mounting. Following the end of the interaction test, subjects were allowed to explore the homecage for another fifty minutes, and locomotor activity was measured using the motion tracking feature of ANY-Maze.

3.3.7 Statistical Analyses

Data summaries and graphs were generated, and statistical tests were performed using Statistica software (TIBCO). Graphs and tables were annotated using Adobe Illustrator. Behavioral data were expressed as mean \pm SEM in figures and text and analyzed using a two-way ANOVA with SEX (male or female) and TREATMENT (For non-social behaviors: same sex, opposite sex, handling control, or homecage control; social behaviors:

same sex or opposite sex) as between-subject factors. Where appropriate, multiple comparisons were adjusted using a SNK post-hoc test, with a p value ≤ 0.5 considered significant. Relevant statistics are also outlined in the figure legends and results section.

3.4 Experimental Results

Given the finding from (Ho et al., 2010) that BNST Avp neurons are activated in response to mating behaviors, we hypothesized that mating behaviors may also activate neurons in the DR, which receives projections from BNST and/or MeA Avp neurons (Rood et al., 2013). Our lab previously simulated a similar behavioral paradigm to the (Ho et al., 2010) study and exposed male mice to either an ovariectomized and hormonally primed female (sexually receptive) or male stimulus animal. Immunohistochemistry performed on brain sections of the male subject mice revealed increased Fos-positive cells in the DR, particularly the rostral dorsomedial DR, following exposure to a female, but not a male stimulus animal (Patel et al., 2022).

Based on the finding from our first experiment, we hypothesize that the Avpr1a-expressing neurons in the DR also increase Fos positivity in response to mating behaviors (i.e., male subjects exposed to female stimulus, and possibly, female subjects exposed to male stimulus). To test this hypothesis, we performed a similar behavioral paradigm, with the addition of female subjects (see 3.3.2 Social interaction test for more details), and performed in situ hybridization using probes against Avpr1a, cfos, and Tph2 (serotonin marker) mRNA on sections of the rostral DR.

3.4.1 Analysis of Non-Social and Social Behaviors

Non-social (*Table A3. 1*) as well as social (*Table A3. 2*) behavior was scored manually, and behavior duration and bouts were measured. ANOVA of SEX (male or female) and TREATMENT (opposite sex, same sex, handling or homecage control) as independent factors and overall activity (sum of all active behaviors) as a dependent factor revealed a main effect of TREATMENT ($F_{2,24} = 3.52$, $p = 0.046$) with handling group displaying less overall activity than the same sex group (1029.78 ± 25.41 sec vs. 1130.61 ± 27.73 sec; SNK post-hoc tests, $p \leq 0.05$). Additionally, opposite sex group did not differ from handling or same sex group.

Time spent engaged in non-social behaviors (sum of digging, grooming, exploring, and rearing) were significantly higher in the handling group compared to other groups (TREATMENT: $F_{2,24} = 7.89$, $p = 0.002$; SNK post-hoc, $p \leq 0.05$). In contrast, for social behaviors, there were no observed significant main effects of or interactions between SEX or TREATMENT in duration or latency to start of social behaviors (sum of investigating, allogrooming, chasing, fighting, and mounting). Lastly, analysis of general activity in the post-test period showed less overall activity in handling group (661.89 ± 173.06 sec) than both opposite sex (1362.31 ± 198.74 sec) and same sex groups (1573.02 ± 251.98 sec; TREATMENT: $F_{2,24} = 6.24$, $p = 0.007$; SNK post-hoc, $p \leq 0.05$).

Analysis of digging, exploring, and rearing showed no differences between groups or sex; however, there was a main effect of TREATMENT in grooming time ($F_{2,24} = 11.07$, $p \leq 0.001$) with handling group spending more time grooming than the other groups (*Table A3. 1*; SNK post-hoc, $p \leq 0.05$). Next, analysis of social behaviors individually revealed no significant main effects or interactions (*Table A3. 2*). Conspecific investigation (sniffing)

and chasing were observed in all tests and did not differ between groups. Allogrooming was observed at low levels across both groups and did not differ. Fighting mainly occurred in male–male interactions and still did not significantly differ between groups. Fighting behavior was also observed at low levels, with two out of five male–male interactions engaging in no bouts of fighting. Similarly, mounting was also a low frequency behavior in male–female interactions (6 out of 10 interactions) and nonexistent in male-male or female-female interactions. In summary, social behaviors were not significantly different between groups.

3.4.2 Male and Female Mice Have Greater Fos Positive DR Cells with Exposure to a Female Stimulus

Because immunohistochemistry of tissue from male mice exposed to female stimulus showed increase DR Fos activity within the rostral regions, we chose sections from the rostral DR (*Figure A3. 1*) for the in situ hybridization analysis (*Figure A3. 2*). Data from two animals (a male from same sex group and a female from opposite sex group) were excluded from the analysis due to the lack of acceptable anatomically matched sections, resulting in a sample size of four for the Male - Same Sex and Female - Opposite Sex groups. All other groups had a sample size of five. The analysis of total cfos expression irrespective of cell phenotype using a two-factor ANOVA (*Figure A3. 2C*) revealed a significant main effect of TREATMENT ($F_{3,30} = 6.2, p = 0.002$) and an interaction between TREATMENT and SEX ($F_{3,30} = 3.7, p = 0.023$). Further SNK post-hoc tests ($p \leq 0.05$) revealed that for female mice, a female stimulus induced significantly more Fos expression compared to females from Homecage and Handling groups; similarly in males, exposure

to a female stimulus induced more Fos expression than those from Homecage control with other groups being intermediate (*Figure A3. 2C*). These results replicate male data from our previous experiment (*Figure A3. 1*) and show that females have increased Fos expression in response to Same Sex, not Opposite Sex, stimuli.

3.4.3 Tph2 Positive Cells Do Not Show Increased Fos Positivity in Any Groups

Next, we used Tph2 and Avpr1a puncta to differentiate between serotonergic and Avpr1a neurons, respectively. We found that ~ 20% of Tph2 cells (n = 6525) contained puncta for Avpr1a (n = 1346). However, most Avpr1a cells in the DR do not contain Tph2, with only about 10% of Avpr1a neurons (n = 11,058) containing Tph2 (n = 1346). Together, this data suggests a definitive subpopulation of serotonin neurons that contain Avpr1a mRNA. As for Fos expression, Tph2 and Tph2 + Avpr1a cells contained a low quantity of Fos signal across all groups (~ 0 to 15 cells across all subjects, *Figure A3. 2D*). ANOVA with TREATMENT (opposite sex, same sex, handling, or homecage control) or SEX (male or female) as factors revealed a main effect of TREATMENT ($F_{3,30} = 4.6$, $p = 0.009$), with both opposite and same sex groups having higher Fos + Tph2 cells than the homecage control (SNK post-hoc, $p \leq 0.05$), but not handling control. As for Fos + Tph2 + Avpr1a cells, there were no differences across the groups.

3.4.4 Male and Female Mice Have Greater Fos Positive DR Avpr1a and Non-Serotonergic, Non-Avpr1a Neurons with Exposure to a Female Stimulus

Counts of Fos puncta in non-serotonergic cells were substantially higher than those in serotonergic cells, ranging from 0 to 236 Fos positive cells. The pattern of Fos expression

in response to different stimuli was similar in Avpr1a cells and Fos-only (i.e., non-Avpr1a, non-Tph2 positive) cells (*Figure A3. 2 E & F*), and largely mirrored the pattern seen in all Fos positive cell (*Figure A3. 2C*). Two-factor ANOVA displayed a significant main effect of TREATMENT (Fos + Avpr1a: $F_{3,30} = 5.8$, $p = 0.003$; Fos-only: $F_{3,30} = 4.9$, $p = 0.007$) and interaction between SEX and TREATMENT (Fos + Avpr1a: $F_{3,30} = 3.9$, $p = 0.018$; Fos-only: $F_{3,30} = 3$, $p = 0.048$). Female mice that interacted with a same sex stimulus had greater Fos + Avpr1a cells than those in homecage and handling control groups, and male mice exposed to an opposite sex stimulus had more Fos + Avpr1a cells than those in homecage control group (*Figure A3. 2E*, SNK post-hoc, $p \leq 0.05$). Post-hoc analyses (SNK, $p \leq 0.05$) for Fos-only cell data revealed that exposure of male mice to an opposite sex conspecific and female mice to a same sex conspecific had greater positive cells than males and females in homecage control group respectively (*Figure A3. 2F*).

3.5 Discussion

The studies in this chapter were designed to investigate the mouse dorsal raphe in the context of prosocial and aggressive behavior. Moreover, we aimed to confirm the presence of Avpr1a-expressing neurons in the DR and investigate whether cells in the DR, like BNST Avp neurons (Ho et al., 2010), activate during prosocial behavior (i.e., male–female interactions) but not aggressive encounters (i.e., male–male interactions). Preliminary work by others indicated that male mice exposed to a sexually receptive female do show increased Fos-positive cells mainly in DMDR in the rostral extent of the DR (*Figure A3. 1*).

Our in situ hybridization data suggest the presence of a discrete population of Avpr1a-expressing cells within the DR (*Figure A3. 2A*) that show increased cfos mRNA colocalization in male and female subjects exposed to a female stimulus animal (*Figure A3. 2E*). Furthermore, we also observed cells expressing cfos, but not Avpr1a or Tph2, mRNA that are active during interactions with a female stimulus, indicating another population with unknown phenotype that may play a role in social behavior (*Figure A3. 2F*). Lastly, the homecage control group showed fewer Tph2 + Fos cells than either opposite or same sex groups, but the same vs. opposite sex did not differ from one another (*Figure A3. 2D*).

Surprisingly, our hypothesis that females, like males, would show heightened Fos expression when presented with an animal of the opposite sex (i.e., strictly mating group) turned out to be incorrect. Instead, female subjects exhibited heightened neural activity when exposed to another female, but not to a male. The similarity in the response of both male and female subjects to a female stimulus may be due to several possibilities. One explanation could be that DR cells, including those that express Avpr1a, may play a role in detection of a female, regardless of the sex of the subject. Or perhaps certain aspects of behavioral interaction that are comparable between female-female and male-female as opposed to female-male and male-male interactions are regulated by the DR.

Simple sex discrimination is unlikely to be the sole function of DR Avpr1a-neuron signaling to serotonin neurons. Sex specific cue detection beginning at the main olfactory bulb and vomeronasal organ is quickly distributed across multiple targets including the BNST and MeA and is integrated with numerous other inputs (Dong et al., 2001; Kunkhyen et al., 2017; Lin et al., 2005; Pankevich et al., 2004). Studies examining neural activation

in response to odor cues suggest that olfactory bulb neurons as well as neurons in olfactory processing regions such as MeA and BNST respond to male and female odor cues. However, there are subtle and complex differences with multiple studies suggesting the presence of differential responding based on factors such as sex, estrous cycle in females, or hierarchical social status in males (Aste et al., 2003; Borelli et al., 2009; Kang et al., 2009; Veyrac et al., 2011). Disruption of higher-order target areas appears to disrupt stimulus-specific behavior while leaving olfactory discrimination of sex-specific cues intact. For example, female Syrian hamsters with excitotoxic lesions of the principal nucleus of the BNST (BNSTpr) maintain the ability to discriminate between male and female urine but will scent mark indiscriminately in response to male or female stimuli (Martinez & Petrulis, 2011). In mice, chemogenetic activation of aromatase-expressing BNSTpr neurons disrupts the patterning of male mating behavior toward a female and greatly increases mounting attempts directed toward a male stimulus animal (Bayless et al., 2019). Critical to our data, the BNSTpr is where BNST Avp neurons are located. The BNST to DR signal is likely influenced by the sex of the stimulus animal. However, sex discrimination is not dependent on the BNST, and BNST modulation leads to complex changes in behavior suggesting the BNST signal likely carries more information than sex alone. There are limited data for the impact of olfactory cues or social interactions on DR neural activation in mice, although multiple studies using rats suggest that various social interactions impact DR Fos expression (Paul et al., 2011; van Kerkhof et al., 2014).

If sex specific cues are not a likely explanation for the Fos response observed in the DR of male and female mice exposed to a female stimulus, then perhaps some aspect or quality of the behavioral interaction should be considered. A simple explanation of time

spent interacting is not likely as latency to interact and time spent interacting were not different between any social behavior groups. General activity itself may have had some impact on Fos expression as the Handling group tended to be intermediate between social stimulation and Homecage groups. Our data suggest that in both male and female mice, exposure to a female most strongly induced Fos expression in the DR overall and specifically in Avpr1a neurons. However, it is important to note that significant differences revealed by post-hoc tests were in comparison to the no stimulation (Homecage) groups. In some cases, exposure to Handling or to a male resulted in an intermediate level of responding such that subjects did not differ from female exposed animals or Homecage controls. It is possible that there was a low level of Fos activation induced by handling or a male stimulus, but the female stimulus definitively induced the most robust levels of Fos expression. The study was limited by a low sample size, and it is possible that a larger number of subjects could resolve group differences further. Fos expression also does not appear to be due to overall activity or the amount of social behavior as there were no differences in latency to interact or duration of social interaction or in any of the specific behaviors recorded (i.e., allogrooming, chasing, investigation, and fighting) except for mounting which only occurred in male–female pairings. Mating alone is unlikely to be the cause of higher Fos expression as females had higher Fos expression in female-female pairings, where there were no mounting attempts. As noted previously, handling groups consistently showed intermediate levels of Fos expression, and so in future studies, it would be interesting to see if lower general activation versus stimulus-specific activation recruited different cell types in the DR or just more of each cell type. An important next step for investigating DR Avpr1a neurons is to functionally manipulate them in behaving mice.

However, it has been a difficult task for the Avp field to gain access to Avpr1a neurons. To address this, we validated an Avpr1a-Cre mouse line that allows selective control over the putative Avpr1a cells (hereafter referred to as Avpr1a cells or neurons) throughout the mouse brain. In Chapter 4, we use this mouse line to express inhibitory chemogenetic receptors specifically in Avpr1a neurons of the DR allowing us to disrupt the function of Avpr1a cells and assess the impact on social behavior.

Chapter 4

Dorsal Raphe Avpr1a Neurons & Behavior

4.1 Introduction

The role of Avp in social behavior has been extensively studied for decades (see Chapter 1). In one of the earliest studies of Avp function, peripheral administration of Avp alone restored a conditioned response in neurohypophysis-removed rats that exhibit a shuttle-box avoidance response (De Wied, 1971). While this study demonstrated a definitive behavioral impact of Avp, the peripheral injection approach lacked the ability to pinpoint brain regions involved. With the emergence of specific Avp receptor agonists and antagonists, researchers were able to target specific brain regions to study behavioral effects of Avp. For example, (Ferris & Potegal, 1988) used a guide cannula to deliver Avpr1a antagonist d(CH₂)⁵Tyr(Me)Avp to the anterior hypothalamus of adult male hamsters and observed a reduction in aggressive behavior when subjects were exposed to smaller “intruder” hamsters in a resident-intruder paradigm. In prairie voles, injections of Avp and Avp receptor antagonists into the lateral septum of male voles increased and decreased paternal behaviors (i.e., grooming, crouching, over, contacting, and retrieving pups) respectively (Wang et al., 1994). Electrolytic lesions of discrete Avp nuclei have also added valuable insight into our understanding of the contributions of different Avp nuclei to the control of social behavior. For example, (Delville et al., 1998) electrolytically lesioned the SCN in golden hamsters and found that although removal of SCN disrupted the circadian rhythm of locomotion (as determined by wheel running), flank-marking behavior (i.e., a type of social communication / territorial behavior that involves scent

marking objects often the test arena itself with glands located near the animal's flank) was not affected, and thus must be regulated by Avp from regions other than SCN.

Advances in genetic tools have created new approaches to delve into the mechanisms by which Avp impacts social behavior and other processes. For instance, knock-out (KO) mouse lines with Avpr1a or Avpr1b genes removed have contributed to our understanding of overall action of Avp through these receptors. For example, Avpr1b-KO but not Avpr1a-KO mice display a significant impairment in expression of aggression (longer latency and fewer attacks) compared to controls (Wersinger, Caldwell, Christiansen, et al., 2007; Wersinger, Caldwell, Martinez, et al., 2007; Wersinger et al., 2002; Wersinger et al., 2004). Avpr1a-KO mice display impaired social recognition and reduced anxiety-like behaviors (Bielsky et al., 2004). Together these data suggest that Avp may affect distinct social behaviors, in part, through different Avp receptors. While numerous techniques and approaches have contributed greatly to our understanding of Avp and its role in social behavior, each new method has its limitations as in, for example, determining the spread of microinjected compounds, the unintended damage to fibers of passage in lesion studies, or the unknown role of compensatory mechanisms during development in phenotypes of constitutive gene knock-out models.

New chemogenetic and optogenetic techniques allow for transient modulation and predictable spatial and temporal control over regions of interest. As such, they may serve as an alternative or complementary approach to conventional methods for gain- and loss-of-function studies. Further, cell-type specific control of effector expression can be achieved by using gene-specific promoters, which in the living organisms are the mechanism of cell-type specific expression (Kim et al., 2017; K. S. Smith et al., 2016).

Recently, Avp-Cre transgenic mice, in which Cre expression is driven by the promoter of the Avp gene, in combination with Cre-dependent viral constructs that cause caspase-mediated cell death were used to study the effects of loss of Avp containing neurons in distinct regions like PVN, BNST, and SCN of adult mice (Rigney et al., 2021; Rigney et al., 2019; Whylings et al., 2021). There are several advantages of this combinatorial approach. Methods like Cre-dependent caspase-mediated cell death or chemogenetics in Cre transgenic mice are minimally invasive during behavior testing and achieve cell-type specificity. Chemogenetic or optogenetic manipulations are acute, temporary, and lessen the effects of compensatory mechanisms that may be involved in other methods that cause permanent alterations to cells of interest. While optogenetic approaches offer a better temporal control over the neurons of interest, chemogenetics confers less damage to surrounding brain structures (i.e., no lasting track damage like in optogenetics) and is a more suitable approach for experiments where multiple animals are simultaneously tested (e.g., social interaction test). Because of the advantages highlighted above, in this chapter, our goal is to utilize chemogenetics to temporarily inhibit the DR Avpr1a neurons in behaving mice and monitor for behavioral changes.

4.2 Rationale

The DR region in the midbrain is of particular interest when it comes to social behavior. DR houses a large population of serotonergic cells, and serotonin is known to play a role in mood regulation and social behaviors, including aggression. Studies have shown that manipulating serotonin levels or disrupting serotonin neuron function leads to increased aggression in rodents (Mosienko et al., 2012; Niederkofler et al., 2016). Given

the link between decreased serotonin neuron function and aggression, increasing the excitation of DR serotonin neurons may work in the opposite direction and promote prosocial behaviors. The DR receives projections from Avp cells in the BNST and MeA, which are also implicated in a variety of prosocial behaviors. Previous work in patch clamp studies demonstrated that Avp bath applied to a slice containing the DR indirectly activated patch clamped serotonin neurons. Further characterization of the response demonstrated that Avp invoked an increase in glutamate mediated excitatory post-synaptic currents in some serotonin neurons and that the response was dependent on the Avpr1a receptor and required the Avp-responsive cell to be in the same slice as the patched serotonin cell (response was sensitive to tetrodotoxin) (Rood & Beck, 2014). In work presented here and published in (Patel et al., 2022), we found that the DR contains Avpr1a expressing cells that are activated (as measured by fos expression), in both male and female mice, during an exposure to a female stimulus (Chapter 3), a finding similar to that of the BNST Avp neurons observed in male mice exposed to a female subject. We also confirmed the existence of DR Avpr1a neurons in an Avpr1a-Cre mouse model through the detection of TdTomato protein in DR of Avpr1a-Cre::RC-PTom mice and the recombination of an AAV encoding a Cre-dependent TdTomato gene injected into the DR of Avpr1a-Cre mice. Furthermore, in situ hybridization data shows that TdTomato mRNA is highly colocalized with Avpr1a mRNA in the DR of Avpr1a-Cre::RC-PTom mice (Chapter 2). Together, these data indicate a distinct population of neurons expressing Avpr1a in the mouse dorsal raphe which may have some role in social behaviors, specifically prosocial behavior. However, it is not clear what aspect of an interaction with a female stimulus seems to drive the increased activation in DR Avpr1a neurons and whether DR Avpr1a neurons are

functionally necessary for any part of an interaction with a female stimulus. Therefore, in this chapter our goal is to study the functional effects of silencing DR Avpr1a cells during tests of social behavior, especially in response to a female stimulus. We predict that chemogenetic inhibition of the DR Avpr1a neurons will decrease prosocial, and possibly increase aggressive behavior in mice. We will test this hypothesis using a battery of behavior tests that allow for the assessment of various aspects of 1) social behaviors including sociability (i.e., propensity of an organism to be social), novelty preference, following a conspecific, sniffing, huddling, mating, and fighting, and 2) non-social behaviors like grooming, rearing, exploring, and general locomotion.

4.3 Materials & Methods

4.3.1 Animals and Surgery

Adult Avpr1a-Cre (~8-16 weeks; male = 17, female = 19) and WT (stimulus animals) mice were used in this study. The Avpr1a-Cre mouse line has undergone more than 10 generations of backcrossing to the C57BL/6J strain, and all animals used were bred in the animal care facility at Rowan School of Osteopathic Medicine (Stratford, NJ). Animals were group housed in a 12-h light/dark cycle (lights on at 06:00 am) with ad libitum access to water and food. We targeted DR Avpr1a neurons by injecting an AAV that encodes Cre-dependent hM4Di-mCherry, a modified G-protein coupled receptor protein that can decrease neuronal excitability temporarily when activated by an exogenous ligand, clozapine-N-oxide (CNO) (Alexander et al., 2009; Armbruster et al., 2007; Krashes et al., 2011). Avpr1a-Cre mice underwent stereotaxic surgery during which they received

injections of AAV encoding Cre-dependent hM4Di-mCherry (pAAV-hSyn-DIO-hM4D(Gi)-mCherry; Addgene #44362-AAV2, $\geq 5 \times 10^{12}$ vg/ml) into the dorsal raphe at coordinates AP -4.48 mm, ML 0 mm, DV -3.15 mm (described in detail in Section 2.3.4.1). All animals were used in accordance with the National Institutes of Health Guide for the Care and Use of Laboratory Animals, and all materials and procedures were approved by the Institutional Animal Care and Use Committee of Rowan University.

4.3.2 Behavior

After surgery, subject animals were single-housed and given three weeks to recover allowing time for expression of hM4Di-mCherry. Following recovery, subjects were tested in a three-chamber social behavior test, an opposite-sex social interaction test, and a same-sex social interaction test over a 3-week period (*Figure A4. 1*). All behavior testing was conducted using a within-subject design, with each subject tested twice (one time per day for two consecutive days), receiving CNO (1 mg/kg) or vehicle (0.9% NaCl). The order of CNO and vehicle administration was randomized and counterbalanced. Although stimulus animals were used in multiple behavior tests, subjects only interacted with a specific stimulus animal once (i.e., stimulus animals were different each test day for a given subject).

4.3.2.1 Three-Chamber Social Behavior Test. The 3-chamber social behavior test (*Figure A4. 2*) has become a staple in the study of social behavioral deficits observed in animal models of autism spectrum disorder (Kaidanovich-Beilin et al., 2011; Moy et al., 2004) and social behavior in general. There are two distinct parts to this test: sociability /

social interest and social memory / social novelty preference. The apparatus consists of 3 distinct chambers made with transparent Plexiglas, with two doors separating the middle chamber from the side chambers on each side. Subject mice were habituated to the apparatus for 15 mins each day for 3 days prior to the first social behavior test. On test day, the subject was placed in the middle chamber and allowed 5 minutes to acclimate. During this period, entry to side chambers was blocked by clear Plexiglas barrier (*Figure A4. 2A*). After the acclimation period, an unfamiliar stimulus, a diestrus female, was placed in a wire cage in one of the two side chambers and the wire cage in the opposite chamber was left empty (*Figure A4. 2B*). Then, the barriers between the side chambers were removed and the subject animal was able to explore the entire apparatus for 10 mins. This part tested for animal's "sociability", which is defined by the animal's preference to spend more time with the stimulus animal than in the empty cage chamber (Kaidanovich-Beilin et al., 2011). Following a brief intermission in which the animal was returned to the closed middle chamber, a second round of testing was conducted in which a second unfamiliar diestrus female was placed in the previously empty wire cage (*Figure A4. 2C*). Mice generally prefer to investigate a novel over familiar stimulus requiring them to remember the stimulus animal from the first 10 min. of the test (i.e., spend more time in the second stimulus chamber); (Kaidanovich-Beilin et al., 2011; Moy et al., 2004)). Therefore, this second part tests a preference for social novelty or social memory. For both parts of the test, behavior was videotaped and videos were analyzed using motion tracking features of ANY-Maze behavior analysis software (Stoelting Co.). Measurements included time spent within each chamber and time in which subject's head was within 3cm of and pointed at the stimulus cage. Other general behavioral data such as activity measures, number of

entries into each chamber, and latency measures were also recorded. One potential advantage of the 3-chamber test comes from the fact that the stimulus animals are surrounded by wired cages. This still allows for auditory, olfactory, and visual investigation between the subject and stimulus while eliminating some extreme social interactions like sexual and/or aggressive encounters (Moy et al., 2004). However, we were also interested in tests with direct social interaction, which are described below.

4.3.2.2 Opposite Sex Social Interaction. A subject mouse was placed in a novel cage, which had the same dimensions as the home cage but did not contain bedding. Animals were allowed to acclimate to and explore the new cage for 10 min. Thereafter, an unfamiliar stimulus of the opposite sex was placed in the cage, and the mice were allowed to interact freely for 20 min. Female stimuli animals were only included in the test if they were in diestrus stage of estrus cycle to minimize any confounding effects of estrus females. The interaction was video recorded for manual scoring of social and non-social behaviors using ANY-Maze keylogging features. Social behaviors scored included sniffing anogenital region (head-to-rear sniffing), head-to-head sniffing, following, allogrooming, huddling, mounting, fighting, and lateral attacks. Non-social behaviors observed and scored included grooming (i.e., self-grooming), rearing, and exploring. ANY-Maze output included number of bouts, total duration, and latency to first occurrence of each behavior scored.

4.3.2.3 Same Sex Social Interaction. This test was run just like the opposite sex social interaction test, with one difference—the sex of the stimulus animal in this test was

the same as that of the subject. Behavior was recorded and manually scored for the same set of behaviors scored in the opposite sex test.

4.3.2.4 Activity Assay. Before opposite and same sex interaction tests, each subject was allowed to acclimate and explore the novel cage for 10 min before the stimulus animal was placed in the cage. Activity during this period was recorded and automated motion tracking analyses using ANY-Maze were calculated to get general activity measures including distance travelled and average speed of movement.

4.3.3 Virus Expression Verification

Following the end of behavior testing, mice were euthanized by intracardiac perfusion with 0.9% saline followed by 4% paraformaldehyde in phosphate buffered saline and brains were collected and stored in 4% paraformaldehyde overnight followed by a 30% sucrose solution until sectioning. Tissue was sectioned at 40 um on a cryostat, and every 3rd section was stained using immunohistochemistry procedures similar to those described in Section 2.3.3.1 to visualize mCherry (primary: rabbit anti-RFP, 1:2000, Rockland; secondary: donkey anti-rabbit Alexa Fluor 594, 1:250, Invitrogen) as a proxy for viral spread, and Tph2 (primary: goat anti-Tph2, 1:500, Abcam; secondary: donkey anti-goat Alexa Fluor 488, 1:250, Invitrogen) to identify serotonin neurons.

A Keyence BZ-X710 with a 10x objective was used to capture images of dorsal raphe sections. Multi-panel images of entire brain sections were acquired and then stitched using an ImageJ macro utilizing Grid/Collection Stitching plugin (Preibisch et al., 2009). DAPI and Tph2 images were used to visualize the anatomy of each section including the

location of serotonin neurons, and a region map encapsulating the dorsal raphe was drawn (according to boundaries shown in *Figure A2. 6*; Mouse Brain Atlas (Franklin & Paxinos, 2008)). RFP images were then used in conjunction with the region map to quantify the RFP positive cells in and around the dorsal raphe.

To optimize images for cell counting, each RFP image was modified using ImageJ. First the RFP image was duplicated, converted to 8-bit, and passed through a gaussian blur filter (sigma = 20) and the resulting image was subtracted from the original; this process removes background pixel information creating better contrast of image foreground pixels, in other words, RFP cell bodies. The Otsu method was then used to threshold cell bodies creating a mask image, a watershed filter was applied to separate clustered cells, and, finally, the analyze particle feature (size = 30-500 pixels², circularity = 0.2-1) was used to quantify cells, which were then assigned to appropriate anatomical regions.

4.3.4 Statistical Analyses

R software (version 4.2.2; RCoreTeam, 2022) was used for all data analyses. Data summaries were generated using the tidyverse package (version 2.0.0), statistical tests were performed using the rstatix package (version 0.7.2), and plots were graphed using the ggplot2 package (3.4.1). Figures, graphs and tables were annotated as needed using Adobe Illustrator.

Behavioral data were expressed as means \pm SEM in figures and text. Data were analyzed using a two-way mixed-model ANOVA with SEX (male or female) as a between-subjects factor and DRUG (CNO or Saline) as a within-subjects factor. Post hoc tests were performed to study the effect of DRUG (within-subject factor) on social behaviors that are

substantially different between the two sexes. Where appropriate, Benjamini-Hochberg method (False Discovery Rate, 5%; (Benjamini & Hochberg, 1995)) was used to control multiple comparisons. The criterion for statistical significance was set at $p \leq 0.05$. Relevant statistics are also outlined in the figure legends and results sections.

4.4 Experimental Results

To test the hypothesis that Avpr1a-expressing cells in the DR modulate social behavior, we designed an experiment in which we could examine the impact of chemogenetic inhibition of DR Avpr1a cells on multiple aspects of social behavior displayed in the three-chamber social behavior test, opposite sex social interaction test (mating), and same sex social interaction test (resident-intruder).

4.4.1 Histological Verification of Cre-Dependent Hm4di Virus Expression in DR

For chemogenetic inhibition of DR Avpr1a neurons, Avpr1a-Cre mice ($n = 36$) underwent stereotaxic injections of Cre-dependent hM4Di-mCherry virus into the DR. Confirmation of target accuracy was accomplished by qualitative and quantitative analyses of immunofluorescent detection of mCherry (*Figure A4. 3*). Of the 36 animals receiving injections, 29 mice (12 males, 17 females) displayed accurate viral expression centered in the DR; seven mice had off-target injections and were excluded from further analyses. Of the seven missed injections, three (1 male, 2 females) displayed no mCherry expression. The remaining four had injections centered in the median raphe (one male), periaqueductal gray (one male), inferior colliculus (one male), or superior colliculus (one male). Quantification of DREADD-mCherry expressing cells in the DR revealed an average of

263 labeled cells per animal (272 for males, 257 for females), with a minimum and maximum of 96 and 542 respectively (*Figure A4. 3H*). It is important to note that every 3rd section was collected for histology, thus actual impacted cell number would be ~3X higher than reported. We further characterized the rostro-caudal spread of the viral infection by dividing the DR into five prominent regions based on patterns of serotonin neurons: Bregma A) -4.36 mm, B) -4.48 mm, C) -4.60 mm, D) -4.72, and E) -4.84 mm (*Figure A4. 3B-G*) and quantified mCherry positive cells within each of the five anatomically matched rostro-caudal (A – E) regions. We found that most animals displayed viral spread throughout most of the DR regions (average number of mCherry positive cells: 30 in A, 30 in B, 25 in C, 42 in D, 37 in E; *Figure A4. 3H*).

4.4.2 DREADD Inhibition of DR Avpr1a Cells Did Not Alter Sociability or Novelty Preference

To analyze behavioral data including the three-chamber test here and interaction with male and female stimulus animals in an open arena presented in subsequent sections, we employed a two-factor mixed model ANOVA with the between-subjects factor SEX (male or female) and the within-subjects DRUG treatment (CNO or saline). For the sociability test, we first examined the percent time spent in the stimulus chamber versus empty chamber ($[\text{time spent in stimulus chamber} / (\text{time spent in stimulus chamber} + \text{time spent in empty chamber})] * 100$). There was a significant main effect of SEX ($F_{1,27} = 14.795$, $p = 0.0007$) with male mice spending a greater percentage of time in the stimulus chamber ($65.8 \pm 2.0\%$ vs. $55.7 \pm 1.6\%$) compared to female subjects (*Figure A4. 4A*). There was no significant main effect of DRUG ($F_{1,27} = 0.088$, $p = 0.77$) or interaction between

SEX and DRUG ($F_{1,27} = 0.049$, $p = 0.83$). We also examined percent time spent investigating the stimulus animal (time spent investigating stimulus animal / (time spent investigating stimulus animal + time investigating empty cup) * 100); investigating was defined as being within 3 cm of the stimulus cup. We again found a significant effect of SEX ($F_{1,27} = 12.670$, $p = 0.001$) with males, compared to females, spending a greater percent time investigating the stimulus animal ($67.0 \pm 2.4\%$ vs. $55.9 \pm 1.9\%$, *Figure A4. 4B*), but we did not observe main effect of DRUG ($F_{1,27} = 0.162$, $p = 0.691$) or an interaction between SEX and DRUG ($F_{1,27} = 0.165$, $p = 0.688$).

Next, we examined the percent of entries into the stimulus chamber (entry into the stimulus chamber / (entry into the stimulus chamber + entry into the empty chamber) * 100) and percent of stimulus investigation bouts (bouts of stimulus investigation / (bouts of stimulus investigation + bouts of empty cup investigation) * 100). Interestingly, CNO treatment ($F_{1,27} = 5.287$, $p = 0.029$) significantly increased the percent of entries into the stimulus chamber ($58.6 \pm 2.3\%$ vs. $50.6 \pm 2.5\%$) compared to saline treatment irrespective of sex (SEX: $F_{1,27} = 2.375$, $p = 0.135$; SEX x DRUG: $F_{1,27} = 0.654$, $p = 0.426$; *Figure A4. 5*). Male mice had a greater percentage of stimulus investigation bouts than females ($64.6 \pm 2.4\%$ vs. $55.2 \pm 2.2\%$; $F_{1,27} = 7.540$, $p = 0.011$) but no differences in response to treatment for either males or females (treatment: $F_{1,27} = 0.595$, $p = 0.447$; sex and treatment: $F_{1,27} = 2.365$, $p = 0.136$).

Lastly, we examined the activity level of animals by measuring the distance traveled during the test. There were no significant main effects (SEX: $F_{1,27} = 1.819$, $p = 0.189$; DRUG: $F_{1,27} = 0.534$, $p = 0.471$) or interactions ($F_{1,27} = 0.067$, $p = 0.798$) in distance traveled during the sociability stage of the test (*Figure A4. 6*).

In the second stage of the three-chamber test, the same animal from the sociability test remains in one stimulus cup and an unfamiliar/novel mouse is placed in the previously empty cup. The interval between sociability and novelty tests can be increased to tax social memory, but here we used a short interval of ~5 min. We tested the effects of silencing DR Avpr1a neurons on novelty preference. First, we examined effects of sex or treatment on percent time spent in the novel chamber ($\text{time in novel chamber} / (\text{time in novel chamber} + \text{time in familiar chamber}) * 100$) as well as percent time spent investigating the novel animal ($\text{time investigating novel animal} / (\text{time investigating novel animal} + \text{time investigating familiar animal}) * 100$). We observed no significant effects of SEX ($F_{1,27} = 0.00054$, $p = 0.982$) or DRUG ($F_{1,27} = 1.15$, $p = 0.293$) nor any interaction between SEX and DRUG ($F_{1,27} = 0.045$, $p = 0.834$) on time spent in the novel chamber (*Figure A4. 7A*). Males and females spent approximately $53.7 \pm 2.2\%$ and $53.8 \pm 2.3\%$ time respectively in the chamber with a novel animal, whereas CNO and saline treated subjects spent $55.6 \pm 2.2\%$ and $51.9 \pm 2.4\%$ time in the novel chamber. Similarly, there were no SEX or DRUG main effects or interactions in percent entry into the novel chamber (*Figure A4. 7B*), time investigating (*Figure A4. 7C*), or bouts of investigation (*Figure A4. 7D*) of the novel animal.

4.4.3 In Male and Female Subjects, Chemogenetic Inhibition of DR Avpr1a Cells Decreased Prosocial Behavior When Exposed to a Female Stimulus in Social Interaction Test

In our previous experiments, both male and female mice exposed to a female stimulus mouse had more cells with colocalized Avpr1a and Fos compared to exposure to

male mouse or non-social controls. Therefore, we hypothesized that chemogenetic silencing of DR Avpr1a cells might decrease prosocial behaviors in male and female mice exposed to a female stimulus animal in a social interaction test.

First, we analyzed locomotion as a general measure of activity during the 10-min acclimation period before introducing a social stimulus into the test cage. For distance traveled, two-way ANOVA with SEX (between-subject) and DRUG treatment (within-subject) as factors revealed a main effect of SEX ($F_{1,27} = 7.955$, $p = 0.009$), with males traveling a greater distance (15.483 ± 1.124 m vs. 12.172 ± 0.819 m) than females (*Figure A4. 8A*), but no significant effect of DRUG ($F_{1,27} = 2.273$, $p = 0.143$) or interactions between SEX and DRUG ($F_{1,27} = 0.005$, $p = 0.945$). Similarly, males, compared to females, displayed a greater mobile time (368.7 ± 16.6 sec vs. 303.3 ± 18.6 sec; SEX: $F_{1,27} = 7.176$, $p = 0.012$) irrespective of CNO treatment (DRUG: $F_{1,27} = 2.761$, $p = 0.108$; SEX x DRUG: $F_{1,27} = 0.509$, $p = 0.482$; *Figure A4. 8B*).

Next, we examined social (*Table A4. 1*) and non-social behaviors (*Table A4. 2*) of male and female subjects exposed to a female stimulus. Recorded social behaviors included behaviors readily displayed by both sexes sniffing (by the subject; head-to-head and head-to-rear), following, allogrooming (by subject and stimulus animal), and huddling behaviors as well as behaviors displayed predominantly by males: mounting and fighting. For total social behavior (summarized in *Table A4. 1*), the summation of individual behaviors (excluding male-predominant behaviors, i.e., mounting and fighting), we found a significant main effect of DRUG with subjects receiving CNO spending less time engaged in social behaviors ($F_{1,27} = 8.971$, $p = 0.006$). There were no SEX or SEX by DRUG interactions (*Figure A4. 9*). While not statistically significant, there was a trend toward

decreased number of bouts of social behavior following CNO treatment (225.379 ± 14.144 vs. 246.448 ± 16.125 ; treatment: $F_{1,27} = 3.436$, $p = 0.075$), but there was a main effect of SEX with males having significantly more displays of social behavior than females (274.292 ± 16.27 vs. 208.824 ± 12.438 ; sex: $F_{1,27} = 6.572$, $p = 0.016$). The interaction was not significant (SEX x DRUG: $F_{1,27} = 1.442$, $p = 0.240$).

Head-to-rear sniffing and following behaviors were both highly impacted by CNO treatment (*Table A4. 1* and *Figure A4. 10*). For head-to-rear sniffing, CNO reduced the time subjects spent sniffing (DRUG: $F_{1,27} = 8.636$, $p = 0.007$), and males spent more time engaged in sniffing than did females (SEX: $F_{1,27} = 7.715$, $p = 0.01$); the interaction was not significant. For following behavior time, there were significant main effects of SEX ($F_{1,27} = 27.554$, $p = 1.56 \times 10^{-5}$) and DRUG ($F_{1,27} = 5.969$, $p = 0.021$) as well as a significant interaction ($F_{1,27} = 4.469$, $p = 0.044$).

Females overall displayed very little following behavior. Subgroup analysis suggests that the effect of DRUG is largely driven by a decrease in following time in males given CNO, whereas females had similarly low following times. Post hoc test of DRUG separated by SEX showed that, within male subjects, CNO treatment causes a strong trend towards reducing following behavior (BH, $t_{11} = 2.09$, $p = 0.061$). Next, the number of bouts of head-to-rear sniffing were significantly decreased in response to CNO treatment (DRUG: $F_{1,27} = 8.636$, $p = 0.044$) and males subjects showed more bouts of behavior than females (SEX: $F_{1,27} = 13.624$, $p = 0.001$). Further, the number of bouts of following behavior showed a trend towards a reduction in response to CNO treatment (DRUG: $F_{1,27} = 3.383$, $p = 0.08$) with males displaying a higher frequency of the behavior (SEX: $F_{1,27} = 14.087$, $p = 0.00085$). Huddling behavior (*Table A4. 1*) was more prevalent in female

subjects (SEX: $F_{1,27} = 10.13$, $p = 0.004$) as male subjects showed very low levels of huddling during interactions with a female stimulus, with a mean huddling time of 21.82 sec, and mean huddling bouts of 5.6 (collapsed across treatment). There was a strong trend suggesting that CNO reduces huddling time in female-female interactions ($t_{16} = 2.01$, $p = 0.0618$), but not huddling bouts (30.6 ± 4.4 vs. 36.3 ± 4.2 ; $t_{16} = 1.02$, $p = 0.322$) with CNO treatment.

Head-to-head sniffing, allogrooming, mounting, and fighting behavior time or bouts did not differ in response to DRUG (behavior time displayed in *Table A4. 1*). In general, allogrooming, mounting, and fighting behaviors were observed at very low levels, with CNO (vs. saline) treated animals displaying an average of approximately 6.69 (vs. 6), 10.3 (vs. 12.8), and 0.7 (vs. 0.3) bouts respectively. Additionally, head-to-head sniffing, allogrooming, and fighting behavior did not differ between sex (*Table A4. 1*). Mounting behavior time and bouts showed a significant main effect of sex, but female subjects, unsurprisingly, displayed no mounting behavior (*Table A4. 1*).

Non-social behavior measures included grooming, rearing, and exploring behaviors, which were summed to obtain total non-social behavior times. For non-social behavior time, no significant main effects or interactions were found (*Table A4. 2* and *Figure A4. 11A*). However, males displayed more bouts of non-social behaviors than females (304 ± 14.5 vs. 242.4 ± 12.5 ; SEX: $F_{1,27} = 6.670$, $p = 0.016$), but CNO treatment had no observable impact (DRUG: $F_{1,27} = 0.458$, $p = 0.504$; SEX x DRUG: $F_{1,27} = 0.086$, $p = 0.772$). Analysis of individual nonsocial behaviors revealed that CNO treatment had no impact on time grooming, rearing, or exploring, but there were differences in these

behaviors depending on the sex of the animal, with males exploring and rearing more and females grooming more (*Table A4. 2*).

4.4.4 Chemogenetic Inhibition of DR Avpr1a Neurons Increases Social Behavior In Male Mice Exposed to a Male Stimulus

Because our Fos experiment data showed that male and female subjects exposed to a female stimulus show increased Avpr1a + Fos mRNA positive cells in the DR, we hypothesized that chemogenetic silencing of this population of cells may cause a reduction in social behavior. We did, in fact, observe a decrease in social behavior in CNO treated male and female subjects exposed to a female stimulus. In contrast, our Fos experiment did not show activation of DR Avpr1a neurons in male and female subjects exposed to a male stimulus. Our interpretation of the Fos experiment was that perhaps DR Avpr1a cells are active during pro-social behaviors for both sexes (i.e., male and female subjects exposed to a female stimulus). Because it seems that an exposure to a male stimulus is antagonistic or not pro-social, we hypothesized that chemogenetic inhibition of DR Avpr1a neurons would decrease pro-social behaviors overall and potentially even increase aggression in male-male interactions.

For social behavior time, an outlier test (box-plot method) identified two male subjects (during saline treatment) with social behavior time of 690.4 sec and 666.6 sec that were removed from further analysis of social behavior time (n = 10 males). A similar analysis on social behavior bouts showed one male (treated with saline) to be an outlier (473 bouts) and was also removed from further analysis (n = 11 males). Next, we examined total social behavior time and bout number as well as individual social behaviors. Time

spent engaged in social behaviors are summarized in *Table A4. 3*, with two-factors ANOVA with SEX as a between-subjects factor and DRUG as a within-subjects factor. There was an effect of SEX (male: 319.7 ± 26.2 s > female: 219.6 ± 17.1 s), DRUG (CNO: 283.8 ± 23.2 s > Sal: 229.5 ± 20.6 s), and an interaction between the two on social behavior time (*Table A4. 3*; *Figure A4. IIB*), with the analysis of DRUG by SEX showing that within male subjects CNO treatment increased social behavior time (BH adj, $p = 0.036$; *Figure A4. II*).

Similarly, analysis of bouts of social behaviors revealed that male, compared to female, subjects engaged in a significantly higher number of social behavior encounters (258.1 ± 14.8 vs. 136.0 ± 8.6) with a male stimulus ($F_{1,26} = 45.78$, $p = 3.52 \times 10^{-7}$), and CNO treatment, though not significant, showed a trend towards increasing bouts of social behavior (male-CNO: 284.5 ± 18.3 > male-Sal: 231.6 ± 21.0) in males but not females (SEX x DRUG: $F_{1,26} = 6.618$, $p = 0.016$; BH post-hoc for male-CNO vs. male-Sal: $p = 0.07$, *Figure A4. IID*). Together, this data may indicate stimulus sex-specific function of DR Avpr1a neurons as treatment of CNO seemed to decrease social behavior in response to a female and increase social responding to male stimulus animal. Further, male subjects, in general, spent significantly more time engaging in head-to-head sniffing, head-to-rear sniffing, following, allogrooming, huddling, and fighting (*Table A4. 3*). Female subjects exposed to a male stimulus showed a minimal engagement in following, allogrooming, huddling, mounting, and fighting behaviors (*Table A4. 3*). Males did not engage and females scarcely participated in mounting behaviors (*Table A4. 3*). Fighting behavior was entirely seen in male subjects (*Table A4. 3*), though at low levels as only 6 out of 12 males from the CNO and saline groups engaged in more than 5 bouts of fighting behavior.

Therefore, although CNO treatment in males trended toward decreasing fighting time and bouts, paired t-test to compare male-CNO to male-Sal for fighting time ($t_{11} = 1.63$, $p = 0.132$) and bouts ($t_{11} = 1.34$, $p = 0.209$) showed no statistical differences.

Total non-social behavior time did not differ between groups (*Table A4. 4*; *Figure A4. 11*), but there was a significant main effect of sex for number of bouts of non-social behavior ($F_{1,27} = 6.656$, $p = 0.016$; *Figure A4. 11*), with males, compared to females, engaging in more non-social behavior events (315.5 ± 21.1 vs. 235.4 ± 15.6). There were no DRUG or SEX differences or any interactions in time spent grooming or rearing (*Table A4. 4*). Exploring behavior did not show any SEX or DRUG differences but did reveal an interaction between the two (*Table A4. 4*). Post hoc comparisons by SEX revealed that female, but not male, subjects spent less time exploring with CNO treatment (BH adjustment, $p = 0.02$, *Table A4. 4*). As for bouts, rearing behavior showed no effect of SEX, DRUG, or any interaction; in contrast, male mice displayed more grooming behavior (48.8 ± 4.9 vs. 34.6 ± 2.1 ; SEX: $F_{1,27} = 6.794$, $p = 0.015$) and exploring (203.5 ± 15.5 vs. 136.3 ± 10.7 ; SEX: $F_{1,27} = 9.086$, $p = 0.006$) events than females, and CNO treatment reduced bouts of exploration in female but not male mice (SEX x DRUG: $F_{1,27} = 4.859$, $p = 0.036$; BH adj, $p = 0.029$).

4.5 Discussion

We designed the experiments described above based on the finding that dorsal raphe Avpr1a neurons are active in male and female mice when exposed to a female, but not male, stimulus animal. Though active, as measured by Fos expression, it is not known whether DR Avpr1a neurons play a role or are functionally necessary for any aspect of

social interaction. To examine the functional role of DR Avpr1a neurons, we used a transgenic mouse model, Avpr1a-Cre, that allows for genetic access to cells that express Avpr1a. AAV injections resulted in expression of the inhibitory DREADD receptors in putative DR Avpr1a neurons. We then examined the impact of chemogenetically inhibiting the DR Avpr1a neurons on different aspects of mouse social behavior like social investigation and novelty preference in the three-chamber test, and social interactions with a male stimulus and female stimulus in a social interaction assay. Because our Fos data indicated that DR Avpr1a neurons seem to be active during an interaction with a female stimulus in both male and female mice, we predicted that chemogenetic inhibition of DR Avpr1a neurons will decrease prosocial behaviors with a female stimulus, and possibly increase aggressive behavior in male-male interactions.

4.5.1 DR Avpr1a Neurons are Involved in Male-Female Interactions

Our results indicate that chemogenetic inhibition causes a decrease in social, but not non-social, behaviors in male and female mice during interactions with a female stimulus. This is the first study that functionally implicates DR Avpr1a neurons in the regulation of social behavior during interactions with a female stimulus. Specifically, we identified that there was a significant reduction in male-female (subject-stimulus) head-to-rear sniffing behavior in a social interaction assay. In male mating behavior, a characteristic sequence of behaviors includes head-to-rear sniffing, following, and mounting attempts (Grant & Mackintosh, 1963; Terranova & Laviola, 2005). This sequence is usually repeated until successful mounting and ejaculation is achieved. In our data head-to-rear sniffing was significantly decreased after chemogenetic inhibition of DR Avpr1a neurons. Additionally,

following behavior showed a strong trend towards decreasing, but mounting attempts were unaffected. These results are in line with what we know about the role of BNST Avp neurons in male mating behaviors, where copulatory, but not aggressive, behavior increases Fos expression (Ho et al., 2010) and shRNA-mediated knockdown of Avp reduces number of intromissions and ejaculations (Rigney et al., 2022). Together, the data suggest that both BNST Avp neurons and, one of their targets, DR Avpr1a neurons are important for components of male mating behaviors (i.e., a prosocial behavior).

For female-female interactions, head-to-rear sniffing is part of normal pattern of investigation of a conspecific but does not typically lead to mounting behavior as confirmed in our study. Because our data indicate a significant main effect of treatment on head-to-rear sniffing, it is possible that regardless of the end goal (mating for male subjects, and social affiliation/huddling for female subjects) during an interaction with a female stimulus, DR Avpr1a neurons may promote or facilitate head-to-rear sniffing behavior. In addition, it is important to note that alternations in head-to-rear sniffing and following behaviors are stimulus specific (i.e., female stimulus) as they were unaltered in interactions with a male stimulus. Female rodents often display prosocial behaviors like huddling (Bowen & McGregor, 2014) and allogrooming (Li et al., 2021). Though not statistically significant, our data indicates that chemogenetic inhibition of DR Avpr1a neurons caused a strong trend toward reducing female-female huddling ($p = 0.06$). As for allogrooming, we did not see any differences, though it is worth noting an already low baseline level of allogrooming behavior in saline treated subjects. In fact, studies that examine allogrooming behavior in female rodents often do so in the context of “consolation” where the conspecific is stressed prior to interaction with the subject, increasing the baseline level of

allogrooming (Li et al., 2021). Our study design did not utilize such interventions, which may explain the low baseline level of allogrooming. As with allogrooming, huddling behavior is often studied in some specific context such as defensive aggregation in response to a predator threat, like cat odor (Bowen & McGregor, 2014). Using contexts that boost female-female interactions could potentially amplify the impact of silencing DR Avpr1a neurons in specific female-female prosocial interactions. While certain social behaviors were affected during female stimulus interactions where animals were able to physically interact, general sociability is unaffected in both male and female mice as the time spent in the stimulus chamber or directly investigating the stimulus in the three-chamber test was unaffected by the treatment of CNO. These findings are, in fact, in line with a pharmacological study in which (Rigney et al., 2020) applied an Avpr1a antagonist to the dorsal raphe and found that social investigation in the three-chamber test is not altered in male or female mice when exposed to a female stimulus. Similarly, novelty preference is also unaltered. One important observation was that although baseline novelty preference level is above 50%, it is quite lower than the expected value (~ 60-70%) based on previous studies (Kaidanovich-Beilin et al., 2011; Moy et al., 2004) possibly indicating a flaw in our experimental design. In fact, a recent study from (Liu et al., 2023) indicates that while social isolation in mice, as for our mice post-surgery, promotes higher social “need,” it simultaneously eliminates the preference for novel over familiar mice compared to that observed in group-housed subject mice.

Lastly, there were significant sex differences in many of the behaviors we tested that are previously unreported in the field, in part, due to the lack of female subjects in experiments. In the three-chamber test with a female stimulus, our data indicates that male

subjects display a higher level of sociability and novelty preference as compared to females. (Rigney et al., 2020) included male and female stimuli for female subjects in the three-chamber test and saw that female subjects displayed an even lower level of activity when the stimulus was a male compared to a female. Furthermore, male (vs. female) subjects tend to exhibit higher levels of social behaviors in interaction assays. Irrespective of sex of the stimulus animal, male subjects engaged in head-to-rear sniffing and following behavior far more than female subjects. In interactions with a male stimulus, male subjects spent more time exhibiting head-to-head sniffing, huddling, social behavior, and allogrooming compared to female subjects. When exposed to a female stimulus, male (vs. female) subjects displayed a higher level of rearing and exploring whereas female (vs. male) subjects spent more time grooming and huddling. The seemingly more robust impact of silencing DR Avpr1a neurons on expression of social behaviors by male subjects could partly be explained due to higher level of activity in male subjects, but could also depend on sex differences in physiology of the BNST Avp system. BNST Avp neurons are more numerous in the BNST of male mice (Rood et al., 2008) and Avp-ir fiber density is greater in the dorsal raphe of male mice (Rood et al., 2013). Our results also highlight a need for more research of female specific behavior in tests of social behavior and the special consideration of factors that specifically impact female specific social behavior. We noted that huddling and possibly allogrooming, using interventions to raise the baseline levels of said behavior (described in (Bowen & McGregor, 2014) for huddling and (Li et al., 2021) for allogrooming), are robustly displayed by female subjects with a female stimulus. In summary, our data suggest that DR Avpr1a neurons are involved in male-female social interactions and specifically impact head-to-rear sniffing and possibly following a

conspecific but are not necessary for the expression of preference for a social (vs. avoidant) or novel (vs. familiar) stimulus. Furthermore, DR Avpr1a neurons likely play a role in female-female prosocial behaviors as well.

4.5.2 DR Avpr1a Neurons May Decrease Male-Male Social Behavior

In mice and many other mammals, male–male interactions often result in displays of aggressive behaviors like fighting, biting, and chasing. DR serotonin neurons are highly implicated in regulation of aggressive behavior in mice with most studies suggesting that serotonin neurons reduce aggression (Ferris et al., 1997; Hendricks et al., 2003; Jacobs & Azmitia, 1992; Lucki, 1998; Niederkofler et al., 2016). Because downregulation of DR serotonin tends to increase aggression for the most part, and because Avp indirectly activates DR serotonin neurons (Rood & Beck, 2014), we speculated that Avpr1a neuronal action on serotonin neurons may potentially lower aggression. In theory, then, chemogenetic silencing of DR Avpr1a neurons may cause an increase in aggressive behaviors, and possibly a reduction in prosocial behaviors. Surprisingly, our data indicated the opposite. We found that chemogenetic inhibition of DR Avpr1a neurons significantly increased social behaviors in male-male interactions, possibly indicating that DR Avpr1a neurons normally may be important in male mice to limit interactions with other males. In fact, a previous study (Rigney et al., 2020) has reported that Avpr1a antagonism in the DR reduces urine marking in male mice exposed to another unfamiliar male, indicating a role of DR Avpr1a neurons in male-male competitive but not aggressive behavior. Our data also indicates that fighting behavior was mostly unaltered with a weak trend toward a reduction in response to chemogenetic inhibition of DR Avpr1a neurons; though, it is important to

note the already low levels of fighting behavior in most male subjects. Therefore, interventions to increase intermale aggression like combination of sexual experience and isolation (Rigney et al., 2020) prior to loss-of-function studies might be helpful in teasing apart any potential effects on aggression.

It is likely that DR Avpr1a neurons only influence a subset of DR serotonin neurons. Perhaps, then, the manipulation of DR Avpr1a neurons may not adequately perturb the DR serotonin system involved in modulation of aggressive behavior. This explanation for why aggressive behavior is unaffected by chemogenetic inhibition of the DR Avpr1a neurons is further supported by the studies in Chapter 2, which show that most DR Avpr1a neurons are organized mainly in the DRL bilaterally surrounding the serotonin neurons in the DMDR within rostral-mid DR levels. Moreover, electrophysiological data suggest that most DR serotonin cells that respond to Avp bath application are located mainly in the DMDR and dorsal part of VMDR within rostral-mid DR (Rood & Beck, 2014). DR serotonin neurons also exhibit topographic organization within the subfields of DR that have efferent connections to functionally distinct regions (Lowry et al., 2008; Muzerelle et al., 2016; Ren et al., 2018; Waterhouse et al., 1993). Therefore, it is plausible that the DR Avpr1a neurons have limited or no connections to the serotonin neurons involved in the regulation of aggression, and therefore the DR Avpr1a neurons may instead exert a more nuanced influence on male-male social interactions.

Our data indicate that inhibiting DR Avpr1a neurons decreases social interaction in male subjects exposed to a female but increases social responding in response to a male stimulus. In contrast, female social interaction toward another female is reduced when DR Avpr1a neurons are silenced, but no changes in social behavior are detected with a male

stimulus. These findings present an unexpected yet interesting potential role of the DR Avpr1a neurons in accentuating or differentiating responses in a stimulus specific manner dependent on both the sex of the subject and the sex of the stimulus.

4.5.3 CNO Can Convert to Clozapine to Cause Off-Target Effects

A limitation in our study is the lack of experimental groups to control potential CNO off-target effects. In brief, CNO, originally thought to exclusively bind to DREADDs, can convert to clozapine in the peripheral circulation (Gomez et al., 2017; Manvich et al., 2018), and then cross the blood brain barrier to bind many endogenous receptors (Schotte et al., 1993) to confound DREADD studies. Neurochemical side effects of CNO administration in Wistar rats, regardless of DREADDs, include increased extracellular levels of glutamate and dopamine (Rodd et al., 2022). Furthermore, low doses of CNO (as low as 1 mg/kg) can reduce startle and amphetamine-induced locomotion in rats (MacLaren et al., 2016).

Despite these findings, we believe that there are several reasons our interventions are unlikely to be off-target effects of CNO. First, since 1 mg/kg but not lower dose of clozapine has been known to alter locomotor behavior, plasma clozapine concentration in our experiments is likely far below levels needed to affect locomotion (Gomez et al., 2017). Accordingly, we see no effects of CNO on locomotion in any of our tests and CNO dose of 1 mg/kg has been used successfully without any documented off-target effects in experiments that study social behaviors (Li et al., 2021; Ren et al., 2018). Furthermore, the effects on male-female social behavior we see after chemogenetic inhibition of the DR Avpr1a neurons are aligned with data from 1) a Fos study of DR Avpr1a neurons (Patel et

al., 2022), 2) a Fos study of BNST Avp neurons (Ho et al., 2010), and 3) shRNA-mediated downregulation of BNST Avp neuronal function (Rigney et al., 2022), adding credence that our data is not a result of CNO impact on endogenous receptors.

Chapter 5

Summary and Conclusion

The studies in this dissertation were designed to test the role of dorsal raphe (DR) vasopressin (Avp)-responsive neurons in the regulation of social behavior in male and female mice. Lacking tools to directly access and thereby manipulate Avpr1a neurons, we worked to validate a new mouse model that carries a BAC transgene encoding Cre recombinase under the control of Avpr1a gene regulatory elements (Chapter 2). Having determined that the DR contains a distinct population of cells expressing Avpr1a, we demonstrated that DR Avpr1a neurons are activated in both male and female subjects exposed to a female, but not a male, stimulus (Chapter 3). Confident with our new transgenic mouse model, we then used AAVs to deliver inhibitory DREADD receptors to the dorsal raphe resulting in a region and cell-type specific expression of DREADDs. Now with genetic access to DR Avpr1a neurons, we were able to demonstrate that silencing these neurons resulted in a decrease in aspects of prosocial interaction in both male and female subjects toward a female stimulus, and counter-intuitively, increased aspects of prosocial behavior between males (Chapter 4). Below, we discuss our findings within the context of the broader literature and identify how our findings enhance our understanding of the Avp system and its impact on social behavior.

5.1 Role of Dorsal Raphe in Social Interaction

Recently, electrophysiological data showed that DR Avpr1a neurons are excited by Avp (Patel et al., 2022) and serotonin neurons have increased glutamatergic excitatory post-

synaptic currents in response to Avp (Rood & Beck, 2014). In theory, BNST Avp activation should activate a subset of DR serotonin neurons via Avpr1a neurons.

What role do serotonin neurons play in social interaction? In Tph2-KO mice, which exhibit depletion of brain serotonin, the ability of mice to differentiate between male or female odors is intact (Angoa-Perez et al., 2015), but male mice show altered sexual behavior patterns (Liu et al., 2011). While WT mice typically prefer a female over male mouse, Tph2-KO males lose this preference, which is rescued following the rescue of brain serotonin to WT levels by administration of 5-hydroxytryptophan which circumvents the Tph2 step in serotonin biosynthesis (Liu et al., 2011). However, in another study, Tph2-KO males maintain their preference for a female over male (Angoa-Perez et al., 2015). Furthermore, Tph2-KO males show aggression toward both males and females, whereas WT males are only aggressive toward the male stimulus (Angoa-Perez et al., 2015). In another study with constitutively silenced serotonin neurons using genetically controlled expression of the neurotransmitter release-inhibiting tetanus toxin light chain, male mice show higher levels of aggression compared to controls (Niederkofler et al., 2016). While female mice typically show low levels of aggression, (Angoa-Perez et al., 2015) found that both Tph2-KO and WT males had more successful mounting attempts with Tph2-KO females than WT females suggesting that disruption of the serotonin system made female mice more permissive (i.e., more amenable to male subjects). These data suggest that under normal conditions, there may be a more antagonistic response by females in response to males in mating tests. In fact, antagonistic behavior patterns are well documented in the rodent sex behavior literature where research shows that, if able to, female rats and mice will control the pattern of mating by escaping from and returning to the male between

mounting attempts, and if the apparatus is constrained to prevent escape, female mice tend to “reject” (i.e. bite or turn away from) the male (Erskine, 1985; Johansen et al., 2008). Therefore, although the female–male (subject–stimulus) pairing is traditionally viewed as a prosocial interaction, parts of the interaction for the female subject may be antagonistic. Overall, it seems that serotonin is important for normal sexual behavior and aggression in males and possibly aggression in females under certain conditions.

Taken together all these data suggest that the DR may be important in driving or modifying stimulus specific responses so that behavioral output matches stimulus input. Fos expression occurred in the DR in males and females exposed to females, interactions that lead to prosocial behaviors from the perspective of the subject, whereas the reverse groupings lead to more antagonistic encounters. While sex specific cues are likely integrated in the BNST-to-DR signal, that signal may also convey information about the valence (i.e., positive or negative value) of the perceived stimulus. In support of this hypothesis, recent studies suggest that DR serotonin neurons are critical for social reward. Fiber photometry data from male mice shows that DR 5HT neurons Ca^{2+} signals slightly increase during chasing a female, rapidly peak during mounting a female, and slightly increase during non-aggressive encounters with a male conspecific (Li et al., 2016). In contrast, aversive stimuli do not activate DR 5HT neurons (Li et al., 2016). In another study by (Dölen et al., 2013), conditional deletion of OxtR containing projections from the dorsal raphe to the nucleus accumbens (NAc) prevents social conditioned placed preference (CPP), indicating that presynaptic OxtRs on dorsal raphe axons terminals within the NAc are required for social reward. Histochemical data suggests a substantial innervation of NAc by DR 5HT-producing cells. Furthermore, socially rewarding interactions and

application of oxytocin induce long term depression in excitatory post synaptic currents in NAc medium spiny neurons (MSNs), which are similarly induced by a 5HT1B agonist and prevented by a 5HT1B antagonist application to the NAc (Dölen et al., 2013). Together these data show that DR serotonin neurons are active during socially rewarding interactions and their projections to the NAc are required for social reward (Dölen et al., 2013; Li et al., 2016). In theory, then, could BNST-Avp signal during male mating behaviors, but also during other socially rewarding interactions, convey a positive-valence specific signal to the DR serotonin neurons?

One interpretation of our data is that positive valence social interactions significantly increase DR Fos expression, at least in part, in Avpr1a neurons, and negative social interactions do not. Furthermore, we show that chemogenetic silencing of DR Avpr1a neurons decreases male-female and, surprisingly, increases in male-male social behaviors and causes no noticeable effect on aggression. The latter result contrasts with our hypothesis. At first, we speculated that chemogenetic inhibition of DR Avpr1a neurons may cause an increase in aggressive behavior due to reduced stimulation of the serotonin system. However, it seems that serotonin's effect on aggression might be independent of or only partly dependent on Avp-Avpr1a input. Overall, inhibition of Avpr1a neuronal output seems to increase male-male social behaviors but not aggression. (Rigney et al., 2020) found that application of an Avpr1a antagonist to the DR reduces urine marking by a male, but not female, subject exposed to a male stimulus, while causing no change to the onset of male-male aggression. Given that chemogenetic inhibition of DR Avpr1a neurons decreased male-female but increased male-male interactions, under normal conditions DR Avpr1a neurons may be responsible for forming a specific pattern of behavior in male mice

that favors interactions with a female stimulus, reconciling nicely with the Fos data of male subjects. As for female subjects, chemogenetic inhibition of DR Avpr1a neurons does not show any robust changes in social behaviors towards male or female stimuli.

5.2 Multiple Sub-Types of Avpr1a-Expressing Neurons are Found in the Dorsal

Raphe

Roughly half of the neurons expressing Fos following social interactions expressed Avpr1a. Although multiple studies have explored the phenotypes of GABAergic and serotonergic neurons in the DR (Challis et al., 2013; Rood & Beck, 2014), Avpr1a-expressing neurons represent an unexplored phenotype. In a recent study from our lab (Patel et al., 2022), RNAseq and in situ hybridization data suggest that there are multiple potential Avpr1a neuron phenotypes in the DR. RNAseq data from pooled cell samples contained counts of serotonin neuron markers (tryptophan hydroxylase and serotonin transporter), glutamate markers (vesicular glutamate transporter 2 and 3), and GABA markers (glutamate decarboxylase 1 and 2). In situ hybridization results show evidence for these same phenotypes (i.e., glutamate, GABA, and serotonin specific genes). Additionally, patch clamp studies (Patel et al., 2022) identified properties consistent with fast-spiking interneurons in other brain regions including short duration action potentials, rapid after-hyperpolarization (AHP), and high firing rates (Connors & Gutnick, 1990). Because most patched cells were located lateral to the midline, it is unlikely that any Avpr1a-expressing serotonin neurons were included in the cell phenotype data. Although we do not know the GABA/glutamate phenotype of recorded Avpr1a neurons, it is of note that almost all Avpr1a neurons recorded (40 of 44) had a fast AHP, which is not typically observed in

either DR serotonin neurons or DR Gad2 neurons (Aghajanian & Vandermaelen, 1982; Challis et al., 2013; Patel et al., 2022; Rood & Beck, 2014). It is possible that Avpr1a GABA neurons are distinct from other DR GABA neurons. In summary, DR Avpr1a neurons may be a heterogeneous population, hinting at distinct subpopulations of Avpr1a neurons that either participate in functionally discrete systems or signal to distinct neuron types (i.e., serotonin and non-serotonin) to coordinate specific aspects of behavior.

The fact that there are multiple distinct subtypes of Avpr1a neurons within the dorsal raphe underscores the physiological and behavioral complexity of the Avp system within the DR. Overall, the interneuron phenotype and anatomical positioning of Avpr1a neurons fits with the hypothesis that they relay signals from the BNST to nearby serotonin neurons but also possibly may exert influence non-serotonin cells.

5.3 Summary and Future Directions

Our data confirm the presence of Avpr1a-expressing neurons in the DR and identify multiple subtypes. Avpr1a neurons constitute about half of DR neurons activated during social interactions, more specifically during prosocial versus antagonistic interactions, in both male and female mice. DR Avpr1a neurons had characteristics of fast-spiking interneurons fitting with their predicted role in relaying an Avp-dependent excitatory signal from the BNST to serotonin neurons. Our chemogenetic study also revealed a significant role of the DR Avpr1a in favor of male-female and possibly female-female social behavior. How DR Avpr1a neurons accomplish this is still unclear. We believe that DR Avpr1a neurons, in part, accomplish the prosocial behavior patterning by exerting a glutamatergic influence on DR serotonin neurons. While we answered some critical questions about the

role of Avp-responsive cells in the DR, our findings in conjunction with recent studies in the field of social behavior raise some interesting questions to further investigate. Are the DR Avpr1a neurons activating DR serotonin neurons? What is the significance of discrete subtypes of Avpr1a neurons in the DR? Does Avp released from the BNST into other target brain regions have a similar impact on behavior as in the DR?

Evidence for an interaction between Avp and DR serotonin system stemmed from an electrophysiological study in which bath application of Avp on DR slices elicited EPSCs in serotonin neurons (Rood & Beck, 2014). Our data from Chapter 2 indicates that putative Avpr1a neurons exist not only in the DR but also in the PAG (and other nearby regions). Therefore, while the DR Avpr1a neurons are closest to the DR serotonin neurons, it is possible that bath application of Avp activates the DR serotonin neurons by the way of PAG (or other nearby regions containing) Avpr1a neurons instead. To directly answer this question, we could express a Cre-dependent optogenetic construct in the DR, PAG, or other nearby regions in Avpr1a-Cre mice and assess the impact of optogenetic activation of a given Avpr1a neuron population on the excitability of DR serotonin neurons using ex-vivo patch clamp electrophysiology.

RNAseq and ISH data indicate that Avpr1a neurons also contain markers for serotonin (Tph2 and SERT), glutamate (Vglut 2 and 3), and GABA (GAD 1 and 2). First, a simple ISH study in Avpr1a-Cre::RC-PTom mice would allow for the assessment of co-labeling of GABA or Glutamate markers with RFP (i.e., putative Avpr1a). This data would further add to the anatomic characterization of DR Avpr1a neurons. Furthermore, serotonin neurons are likely influenced by Avp in glutamate-dependent manner (Rood & Beck, 2014). This prompts further inquiry into the role of Avpr1a+GABA neurons. Could they be

responsible for normally dampening male-male interactions which enhanced upon chemogenetic inhibition of DR Avpr1a neurons? Using the latest INTERSECT technology (Fenno et al., 2020), we can begin to access subtypes of Avpr1a neurons within the DR and design gain-of-function and/or loss-of-function studies to determine the functional role of subtypes of Avpr1a neurons. These studies investigating subtype specific Avpr1a cells in the DR would be fruitful in adding to our understanding of the complex role of DR Avpr1a neurons uncovered by the studies in this dissertation.

References

- Aghajanian, G. K., & Vandermaelen, C. P. (1982). Intracellular recordings from serotonergic dorsal raphe neurons: pacemaker potentials and the effect of LSD. *Brain Res*, 238(2), 463-469. [https://doi.org/10.1016/0006-8993\(82\)90124-x](https://doi.org/10.1016/0006-8993(82)90124-x)
- Alenina, N., Kikic, D., Todiras, M., Mosienko, V., Qadri, F., Plehm, R., Boye, P., Vilianovitch, L., Sohr, R., Tenner, K., Hortnagl, H., & Bader, M. (2009). Growth retardation and altered autonomic control in mice lacking brain serotonin. *Proc Natl Acad Sci U S A*, 106(25), 10332-10337. <https://doi.org/10.1073/pnas.0810793106>
- Alexander, G. M., Rogan, S. C., Abbas, A. I., Armbruster, B. N., Pei, Y., Allen, J. A., Nonneman, R. J., Hartmann, J., Moy, S. S., Nicoletis, M. A., McNamara, J. O., & Roth, B. L. (2009). Remote control of neuronal activity in transgenic mice expressing evolved G protein-coupled receptors. *Neuron*, 63(1), 27-39. <https://doi.org/10.1016/j.neuron.2009.06.014>
- Ali, M. M., & Dwyer, D. S. (2010). Social network effects in alcohol consumption among adolescents. *Addict Behav*, 35(4), 337-342. <https://doi.org/10.1016/j.addbeh.2009.12.002>
- Angoa-Perez, M., Herrera-Mundo, N., Kane, M. J., Sykes, C. E., Anneken, J. H., Francescutti, D. M., & Kuhn, D. M. (2015). Brain serotonin signaling does not determine sexual preference in male mice. *PLoS One*, 10(2), e0118603. <https://doi.org/10.1371/journal.pone.0118603>
- Antoni, F. A. (1984). Novel ligand specificity of pituitary vasopressin receptors in the rat. *Neuroendocrinology*, 39(2), 186-188. <https://doi.org/10.1159/000123976>
- APA. (2022). *Diagnostic and statistical manual of mental disorders* (5 ed.). American Psychiatric Association. <https://doi.org/https://doi.org/10.1176/appi.books.9780890425787>
- Armbruster, B. N., Li, X., Pausch, M. H., Herlitze, S., & Roth, B. L. (2007). Evolving the lock to fit the key to create a family of G protein-coupled receptors potently activated by an inert ligand. *Proc Natl Acad Sci U S A*, 104(12), 5163-5168. <https://doi.org/10.1073/pnas.0700293104>
- Aste, N., Honda, S., & Harada, N. (2003). Forebrain Fos responses to reproductively related chemosensory cues in aromatase knockout mice. *Brain Res Bull*, 60(3), 191-200. [https://doi.org/10.1016/s0361-9230\(03\)00035-2](https://doi.org/10.1016/s0361-9230(03)00035-2)
- Azmitia, E. C., & Segal, M. (1978). An autoradiographic analysis of the differential ascending projections of the dorsal and median raphe nuclei in the rat. *J Comp Neurol*, 179(3), 641-667. <https://doi.org/10.1002/cne.901790311>

- Backman, C. M., Malik, N., Zhang, Y., Shan, L., Grinberg, A., Hoffer, B. J., Westphal, H., & Tomac, A. C. (2006). Characterization of a mouse strain expressing Cre recombinase from the 3' untranslated region of the dopamine transporter locus. *Genesis*, *44*(8), 383-390. <https://doi.org/10.1002/dvg.20228>
- Bamshad, M., Novak, M. A., & de Vries, G. J. (1994). Cohabitation alters vasopressin innervation and paternal behavior in prairie voles (*Microtus ochrogaster*). *Physiol Behav*, *56*(4), 751-758. [https://doi.org/10.1016/0031-9384\(94\)90238-0](https://doi.org/10.1016/0031-9384(94)90238-0)
- Bankir, L. (2001). Antidiuretic action of vasopressin: quantitative aspects and interaction between V1a and V2 receptor-mediated effects. *Cardiovasc Res*, *51*(3), 372-390. [https://doi.org/10.1016/s0008-6363\(01\)00328-5](https://doi.org/10.1016/s0008-6363(01)00328-5)
- Barofsky, A. L., Taylor, J., Tizabi, Y., Kumar, R., & Jones-Quartey, K. (1983). Specific neurotoxin lesions of median raphe serotonergic neurons disrupt maternal behavior in the lactating rat. *Endocrinology*, *113*(5), 1884-1893. <https://doi.org/10.1210/endo-113-5-1884>
- Bayless, D. W., Yang, T., Mason, M. M., Susanto, A. A. T., Lobdell, A., & Shah, N. M. (2019). Limbic Neurons Shape Sex Recognition and Social Behavior in Sexually Naive Males. *Cell*, *176*(5), 1190-1205 e1120. <https://doi.org/10.1016/j.cell.2018.12.041>
- Beitz, A. J., Shepard, R. D., & Wells, W. E. (1983). The periaqueductal gray-raphé magnus projection contains somatostatin, neurotensin and serotonin but not cholecystokinin. *Brain Res*, *261*(1), 132-137. [https://doi.org/10.1016/0006-8993\(83\)91292-1](https://doi.org/10.1016/0006-8993(83)91292-1)
- Benjamini, Y., & Hochberg, Y. (1995). Controlling the False Discovery Rate: A Practical and Powerful Approach to Multiple Testing. *Journal of the Royal Statistical Society. Series B (Methodological)*, *57*(1), 289-300. <http://www.jstor.org.ezproxy.rowan.edu/stable/2346101>
- Berman, M. E., Tracy, J. I., & Coccaro, E. F. (1997). The serotonin hypothesis of aggression revisited. *Clin Psychol Rev*, *17*(6), 651-665. [https://doi.org/10.1016/s0272-7358\(97\)00039-1](https://doi.org/10.1016/s0272-7358(97)00039-1)
- Bielsky, I. F., Hu, S. B., Ren, X., Terwilliger, E. F., & Young, L. J. (2005). The V1a vasopressin receptor is necessary and sufficient for normal social recognition: a gene replacement study. *Neuron*, *47*(4), 503-513. <https://doi.org/10.1016/j.neuron.2005.06.031>
- Bielsky, I. F., Hu, S. B., Szegda, K. L., Westphal, H., & Young, L. J. (2004). Profound impairment in social recognition and reduction in anxiety-like behavior in vasopressin V1a receptor knockout mice. *Neuropsychopharmacology*, *29*(3), 483-493. <https://doi.org/10.1038/sj.npp.1300360>
- Bobillier, P., Seguin, S., Petitjean, F., Salvat, D., Touret, M., & Jouvet, M. (1976). The raphe nuclei of the cat brain stem: a topographical atlas of their efferent projections as revealed by autoradiography. *Brain Res*, *113*(3), 449-486. [https://doi.org/10.1016/0006-8993\(76\)90050-0](https://doi.org/10.1016/0006-8993(76)90050-0)

- Borelli, K. G., Blanchard, D. C., Javier, L. K., Defensor, E. B., Brandao, M. L., & Blanchard, R. J. (2009). Neural correlates of scent marking behavior in C57BL/6J mice: detection and recognition of a social stimulus. *Neuroscience*, *162*(4), 914-923. <https://doi.org/10.1016/j.neuroscience.2009.05.047>
- Bowen, M. T., & McGregor, I. S. (2014). Oxytocin and vasopressin modulate the social response to threat: a preclinical study. *Int J Neuropsychopharmacol*, *17*(10), 1621-1633. <https://doi.org/10.1017/s1461145714000388>
- Branda, C. S., & Dymecki, S. M. (2004). Talking about a revolution: The impact of site-specific recombinases on genetic analyses in mice. *Dev Cell*, *6*(1), 7-28. [https://doi.org/10.1016/s1534-5807\(03\)00399-x](https://doi.org/10.1016/s1534-5807(03)00399-x)
- Buijs, R. M., & Swaab, D. F. (1979). Immuno-electron microscopical demonstration of vasopressin and oxytocin synapses in the limbic system of the rat. *Cell Tissue Res*, *204*(3), 355-365. <https://doi.org/10.1007/BF00233648>
- Buijs, R. M., & Van Heerikhuize, J. J. (1982). Vasopressin and oxytocin release in the brain--a synaptic event. *Brain Res*, *252*(1), 71-76. [https://doi.org/10.1016/0006-8993\(82\)90979-9](https://doi.org/10.1016/0006-8993(82)90979-9)
- Caldwell, H. K., Lee, H. J., Macbeth, A. H., & Young, W. S., 3rd. (2008). Vasopressin: behavioral roles of an "original" neuropeptide. *Prog Neurobiol*, *84*(1), 1-24. <https://doi.org/10.1016/j.pneurobio.2007.10.007>
- Carpenter, A. E., Jones, T. R., Lamprecht, M. R., Clarke, C., Kang, I. H., Friman, O., Guertin, D. A., Chang, J. H., Lindquist, R. A., Moffat, J., Golland, P., & Sabatini, D. M. (2006). CellProfiler: image analysis software for identifying and quantifying cell phenotypes. *Genome Biol*, *7*(10), R100. <https://doi.org/10.1186/gb-2006-7-10-r100>
- Castel, M., & Morris, J. F. (1988). The neurophysin-containing innervation of the forebrain of the mouse. *Neuroscience*, *24*(3), 937-966. [https://doi.org/10.1016/0306-4522\(88\)90078-4](https://doi.org/10.1016/0306-4522(88)90078-4)
- Challis, C., Boulden, J., Veerakumar, A., Espallergues, J., Vassoler, F. M., Pierce, R. C., Beck, S. G., & Berton, O. (2013). Raphe GABAergic neurons mediate the acquisition of avoidance after social defeat. *J Neurosci*, *33*(35), 13978-13988, 13988a. <https://doi.org/10.1523/JNEUROSCI.2383-13.2013>
- Chisholm, D., Sweeny, K., Sheehan, P., Rasmussen, B., Smit, F., Cuijpers, P., & Saxena, S. (2016). Scaling-up treatment of depression and anxiety: a global return on investment analysis. *Lancet Psychiatry*, *3*(5), 415-424. [https://doi.org/10.1016/S2215-0366\(16\)30024-4](https://doi.org/10.1016/S2215-0366(16)30024-4)
- Cicconet, M., Hochbaum, D. R., Richmond, D., & Sabatini, B. L. (2017). Bots for Software-Assisted Analysis of Image-Based Transcriptomics. *bioRxiv*, 172296. <https://doi.org/10.1101/172296>

- Coffield, J. A., Bowen, K. K., & Miletic, V. (1992). Retrograde tracing of projections between the nucleus submedius, the ventrolateral orbital cortex, and the midbrain in the rat. *J Comp Neurol*, *321*(3), 488-499. <https://doi.org/10.1002/cne.903210314>
- Collier, D. A., Stober, G., Li, T., Heils, A., Catalano, M., Di Bella, D., Arranz, M. J., Murray, R. M., Vallada, H. P., Bengel, D., Muller, C. R., Roberts, G. W., Smeraldi, E., Kirov, G., Sham, P., & Lesch, K. P. (1996). A novel functional polymorphism within the promoter of the serotonin transporter gene: possible role in susceptibility to affective disorders. *Mol Psychiatry*, *1*(6), 453-460. <https://www.ncbi.nlm.nih.gov/pubmed/9154246>
- Commons, K. G., Connolley, K. R., & Valentino, R. J. (2003). A neurochemically distinct dorsal raphe-limbic circuit with a potential role in affective disorders. *Neuropsychopharmacology*, *28*(2), 206-215. <https://doi.org/10.1038/sj.npp.1300045>
- Connors, B. W., & Gutnick, M. J. (1990). Intrinsic firing patterns of diverse neocortical neurons. *Trends Neurosci*, *13*(3), 99-104. [https://doi.org/10.1016/0166-2236\(90\)90185-d](https://doi.org/10.1016/0166-2236(90)90185-d)
- Correll, C. U., Lencz, T., & Malhotra, A. K. (2011). Antipsychotic drugs and obesity. *Trends Mol Med*, *17*(2), 97-107. <https://doi.org/10.1016/j.molmed.2010.10.010>
- Dantzer, R., Koob, G. F., Bluthé, R. M., & Le Moal, M. (1988). Septal vasopressin modulates social memory in male rats. *Brain Res*, *457*(1), 143-147. [https://doi.org/10.1016/0006-8993\(88\)90066-2](https://doi.org/10.1016/0006-8993(88)90066-2)
- de Vries, G. J., Buijs, R. M., & Sluiter, A. A. (1984). Gonadal hormone actions on the morphology of the vasopressinergic innervation of the adult rat brain. *Brain Res*, *298*(1), 141-145. [https://doi.org/10.1016/0006-8993\(84\)91157-0](https://doi.org/10.1016/0006-8993(84)91157-0)
- De Vries, G. J., & Panzica, G. C. (2006). Sexual differentiation of central vasopressin and vasotocin systems in vertebrates: different mechanisms, similar endpoints. *Neuroscience*, *138*(3), 947-955. <https://doi.org/10.1016/j.neuroscience.2005.07.050>
- De Vries, G. J., Wang, Z., Bullock, N. A., & Numan, S. (1994). Sex differences in the effects of testosterone and its metabolites on vasopressin messenger RNA levels in the bed nucleus of the stria terminalis of rats. *J Neurosci*, *14*(3 Pt 2), 1789-1794. <https://doi.org/10.1523/JNEUROSCI.14-03-01789.1994>
- De Wied, D. (1971). Long term effect of vasopressin on the maintenance of a conditioned avoidance response in rats. *Nature*, *232*(5305), 58-60. <https://doi.org/10.1038/232058a0>
- Delville, Y., De Vries, G. J., Schwartz, W. J., & Ferris, C. F. (1998). Flank-marking behavior and the neural distribution of vasopressin innervation in golden hamsters with suprachiasmatic lesions. *Behav Neurosci*, *112*(6), 1486-1501. <https://doi.org/10.1037//0735-7044.112.6.1486>

- Demotes-Mainard, J., Chauveau, J., Rodriguez, F., Vincent, J. D., & Poulain, D. A. (1986). Septal release of vasopressin in response to osmotic, hypovolemic and electrical stimulation in rats. *Brain Res*, *381*(2), 314-321. [https://doi.org/10.1016/0006-8993\(86\)90082-x](https://doi.org/10.1016/0006-8993(86)90082-x)
- Dölen, G., Darvishzadeh, A., Huang, K. W., & Malenka, R. C. (2013). Social reward requires coordinated activity of nucleus accumbens oxytocin and serotonin. *Nature*, *501*(7466), 179-184. <https://doi.org/10.1038/nature12518>
- Dong, H. W., Petrovich, G. D., & Swanson, L. W. (2001). Topography of projections from amygdala to bed nuclei of the stria terminalis. *Brain Res Brain Res Rev*, *38*(1-2), 192-246. [https://doi.org/10.1016/s0165-0173\(01\)00079-0](https://doi.org/10.1016/s0165-0173(01)00079-0)
- Egashira, N., Tanoue, A., Matsuda, T., Koushi, E., Harada, S., Takano, Y., Tsujimoto, G., Mishima, K., Iwasaki, K., & Fujiwara, M. (2007). Impaired social interaction and reduced anxiety-related behavior in vasopressin V1a receptor knockout mice. *Behav Brain Res*, *178*(1), 123-127. <https://doi.org/10.1016/j.bbr.2006.12.009>
- Erskine, M. S. (1985). Effects of paced coital stimulation on estrus duration in intact cycling rats and ovariectomized and ovariectomized-adrenalectomized hormone-primed rats. *Behav Neurosci*, *99*(1), 151-161. <https://doi.org/10.1037//0735-7044.99.1.151>
- Fenno, L. E., Ramakrishnan, C., Kim, Y. S., Evans, K. E., Lo, M., Vesuna, S., Inoue, M., Cheung, K. Y. M., Yuen, E., Pichamoorthy, N., Hong, A. S. O., & Deisseroth, K. (2020). Comprehensive Dual- and Triple-Feature Intersectional Single-Vector Delivery of Diverse Functional Payloads to Cells of Behaving Mammals. *Neuron*, *107*(5), 836-853.e811. <https://doi.org/10.1016/j.neuron.2020.06.003>
- Ferris, C. F., Melloni, R. H., Jr., Koppel, G., Perry, K. W., Fuller, R. W., & Delville, Y. (1997). Vasopressin/serotonin interactions in the anterior hypothalamus control aggressive behavior in golden hamsters. *J Neurosci*, *17*(11), 4331-4340. <https://www.ncbi.nlm.nih.gov/pubmed/9151749>
- Ferris, C. F., & Potegal, M. (1988). Vasopressin receptor blockade in the anterior hypothalamus suppresses aggression in hamsters. *Physiol Behav*, *44*(2), 235-239. [https://doi.org/10.1016/0031-9384\(88\)90144-8](https://doi.org/10.1016/0031-9384(88)90144-8)
- Franklin, K. B. J., & Paxinos, G. (2008). *The mouse brain in stereotaxic coordinates* (3rd ed.). Boston : Elsevier/Academic Press.
- Gagneten, S., Le, Y., Miller, J., & Sauer, B. (1997). Brief expression of a GFP cre fusion gene in embryonic stem cells allows rapid retrieval of site-specific genomic deletions. *Nucleic Acids Res*, *25*(16), 3326-3331. <https://doi.org/10.1093/nar/25.16.3326>
- Gainer, H., Sarne, Y., & Brownstein, M. J. (1977). Neurophysin biosynthesis: conversion of a putative precursor during axonal transport. *Science*, *195*(4284), 1354-1356. <https://doi.org/10.1126/science.65791>

- Gini, G., & Pozzoli, T. (2009). Association between bullying and psychosomatic problems: a meta-analysis. *Pediatrics*, *123*(3), 1059-1065. <https://doi.org/10.1542/peds.2008-1215>
- Gofflot, F., Wendling, O., Chartoire, N., Birling, M. C., Warot, X., & Auwerx, J. (2011). Characterization and Validation of Cre-Driver Mouse Lines. *Curr Protoc Mouse Biol*, *1*(1), 1-15. <https://doi.org/10.1002/9780470942390.mo100103>
- Gomez, J. L., Bonaventura, J., Lesniak, W., Mathews, W. B., Sysa-Shah, P., Rodriguez, L. A., Ellis, R. J., Richie, C. T., Harvey, B. K., Dannals, R. F., Pomper, M. G., Bonci, A., & Michaelides, M. (2017). Chemogenetics revealed: DREADD occupancy and activation via converted clozapine. *Science*, *357*(6350), 503-507. <https://doi.org/10.1126/science.aan2475>
- Grant, E. C., & Mackintosh, J. H. (1963). A comparison of the social postures of some common laboratory rodents. *Behaviour*, *21*, 246-259. <https://doi.org/10.1163/156853963X00185>
- Guenette, M. D., Giacca, A., Hahn, M., Teo, C., Lam, L., Chintoh, A., Arenovich, T., & Remington, G. (2013). Atypical antipsychotics and effects of adrenergic and serotonergic receptor binding on insulin secretion in-vivo: an animal model. *Schizophr Res*, *146*(1-3), 162-169. <https://doi.org/10.1016/j.schres.2013.02.023>
- Haas, S. A., & Schaefer, D. R. (2014). With a Little Help from My Friends? Asymmetrical Social Influence on Adolescent Smoking Initiation and Cessation. *J Health Soc Behav*, *55*(2), 126-143. <https://doi.org/10.1177/0022146514532817>
- Hatzenbuehler, M. L., McLaughlin, K. A., & Xuan, Z. (2012). Social networks and risk for depressive symptoms in a national sample of sexual minority youth. *Soc Sci Med*, *75*(7), 1184-1191. <https://doi.org/10.1016/j.socscimed.2012.05.030>
- Hendricks, T. J., Fyodorov, D. V., Wegman, L. J., Lelutiu, N. B., Pehek, E. A., Yamamoto, B., Silver, J., Weeber, E. J., Sweatt, J. D., & Deneris, E. S. (2003). Pet-1 ETS gene plays a critical role in 5-HT neuron development and is required for normal anxiety-like and aggressive behavior. *Neuron*, *37*(2), 233-247. [https://doi.org/10.1016/s0896-6273\(02\)01167-4](https://doi.org/10.1016/s0896-6273(02)01167-4)
- Hernando, F., Schoots, O., Lolait, S. J., & Burbach, J. P. (2001). Immunohistochemical localization of the vasopressin V1b receptor in the rat brain and pituitary gland: anatomical support for its involvement in the central effects of vasopressin. *Endocrinology*, *142*(4), 1659-1668. <https://doi.org/10.1210/endo.142.4.8067>
- Hill, E. M., Griffiths, F. E., & House, T. (2015). Spreading of healthy mood in adolescent social networks. *Proc Biol Sci*, *282*(1813), 20151180. <https://doi.org/10.1098/rspb.2015.1180>
- Ho, J. M., Murray, J. H., Demas, G. E., & Goodson, J. L. (2010). Vasopressin cell groups exhibit strongly divergent responses to copulation and male-male interactions in mice. *Horm Behav*, *58*(3), 368-377. <https://doi.org/10.1016/j.yhbeh.2010.03.021>

- Holmes, A., Yang, R. J., Lesch, K. P., Crawley, J. N., & Murphy, D. L. (2003). Mice lacking the serotonin transporter exhibit 5-HT(1A) receptor-mediated abnormalities in tests for anxiety-like behavior. *Neuropsychopharmacology*, 28(12), 2077-2088. <https://doi.org/10.1038/sj.npp.1300266>
- Holschbach, M. A., Vitale, E. M., & Lonstein, J. S. (2018). Serotonin-specific lesions of the dorsal raphe disrupt maternal aggression and caregiving in postpartum rats. *Behav Brain Res*, 348, 53-64. <https://doi.org/10.1016/j.bbr.2018.04.008>
- Inoue, Y. U., Miwa, H., Hori, K., Kaneko, R., Morimoto, Y., Koike, E., Asami, J., Kamijo, S., Yamada, M., Hoshino, M., & Inoue, T. (2022). Targeting Neurons with Functional Oxytocin Receptors: A Novel Set of Simple Knock-In Mouse Lines for Oxytocin Receptor Visualization and Manipulation. *eNeuro*, 9(1). <https://doi.org/10.1523/ENEURO.0423-21.2022>
- Jacobs, B. L., & Azmitia, E. C. (1992). Structure and function of the brain serotonin system. *Physiol Rev*, 72(1), 165-229. <https://doi.org/10.1152/physrev.1992.72.1.165>
- Jacobs, B. L., & Cohen, A. (1976). Differential behavioral effects of lesions of the median or dorsal raphe nuclei in rats: open field and pain-elicited aggression. *J Comp Physiol Psychol*, 90(1), 102-108. <https://doi.org/10.1037/h0077262>
- Jacobs, B. L., & Fornal, C. A. (1993). 5-HT and motor control: a hypothesis. *Trends Neurosci*, 16(9), 346-352. [https://doi.org/10.1016/0166-2236\(93\)90090-9](https://doi.org/10.1016/0166-2236(93)90090-9)
- Jard, S., Barberis, C., Audigier, S., & Tribollet, E. (1987). Neurohypophyseal hormone receptor systems in brain and periphery. *Prog Brain Res*, 72, 173-187. [https://doi.org/10.1016/s0079-6123\(08\)60206-x](https://doi.org/10.1016/s0079-6123(08)60206-x)
- Johansen, J. A., Clemens, L. G., & Nunez, A. A. (2008). Characterization of copulatory behavior in female mice: evidence for paced mating. *Physiol Behav*, 95(3), 425-429. <https://doi.org/10.1016/j.physbeh.2008.07.004>
- Johnson, A. E., Audigier, S., Rossi, F., Jard, S., Tribollet, E., & Barberis, C. (1993). Localization and characterization of vasopressin binding sites in the rat brain using an iodinated linear AVP antagonist. *Brain Res*, 622(1-2), 9-16. [https://doi.org/10.1016/0006-8993\(93\)90795-o](https://doi.org/10.1016/0006-8993(93)90795-o)
- Johnson, M. D., & Ma, P. M. (1993). Localization of NADPH diaphorase activity in monoaminergic neurons of the rat brain. *J Comp Neurol*, 332(4), 391-406. <https://doi.org/10.1002/cne.903320402>
- Kaidanovich-Beilin, O., Lipina, T., Vukobradovic, I., Roder, J., & Woodgett, J. R. (2011). Assessment of social interaction behaviors. *J Vis Exp*(48). <https://doi.org/10.3791/2473>

Kang, N., Baum, M. J., & Cherry, J. A. (2009). A direct main olfactory bulb projection to the 'vomeronasal' amygdala in female mice selectively responds to volatile pheromones from males. *Eur J Neurosci*, 29(3), 624-634. <https://doi.org/10.1111/j.1460-9568.2009.06638.x>

Kangasniemi, A. M., L.; Sereneo, M. (2019). *The ROI in workplace mental health programs: good for people, good for business. A blueprint for workplace mental health programs.*

Kim, C. K., Adhikari, A., & Deisseroth, K. (2017). Integration of optogenetics with complementary methodologies in systems neuroscience. *Nature Reviews Neuroscience*, 18(4), 222-235. <https://doi.org/10.1038/nrn.2017.15>

Kim, S. J., Young, L. J., Gonen, D., Veenstra-VanderWeele, J., Courchesne, R., Courchesne, E., Lord, C., Leventhal, B. L., Cook, E. H., Jr., & Insel, T. R. (2002). Transmission disequilibrium testing of arginine vasopressin receptor 1A (AVPR1A) polymorphisms in autism. *Mol Psychiatry*, 7(5), 503-507. <https://doi.org/10.1038/sj.mp.4001125>

Knafo, A., Israel, S., Darvasi, A., Bachner-Melman, R., Uzefovsky, F., Cohen, L., Feldman, E., Lerer, E., Laiba, E., Raz, Y., Nemanov, L., Gritsenko, I., Dina, C., Agam, G., Dean, B., Bornstein, G., & Ebstein, R. P. (2008). Individual differences in allocation of funds in the dictator game associated with length of the arginine vasopressin 1a receptor RS3 promoter region and correlation between RS3 length and hippocampal mRNA. *Genes Brain Behav*, 7(3), 266-275. <https://doi.org/10.1111/j.1601-183X.2007.00341.x>

Kollack-Walker, S., & Newman, S. W. (1995). Mating and agonistic behavior produce different patterns of Fos immunolabeling in the male Syrian hamster brain. *Neuroscience*, 66(3), 721-736. [https://doi.org/10.1016/0306-4522\(94\)00563-k](https://doi.org/10.1016/0306-4522(94)00563-k)

Krashes, M. J., Koda, S., Ye, C., Rogan, S. C., Adams, A. C., Cusher, D. S., Maratos-Flier, E., Roth, B. L., & Lowell, B. B. (2011). Rapid, reversible activation of AgRP neurons drives feeding behavior in mice. *J Clin Invest*, 121(4), 1424-1428. <https://doi.org/10.1172/jci46229>

Kunkhyen, T., McCarthy, E. A., Korzan, W. J., Doctor, D., Han, X., Baum, M. J., & Cherry, J. A. (2017). Optogenetic Activation of Accessory Olfactory Bulb Input to the Forebrain Differentially Modulates Investigation of Opposite versus Same-Sex Urinary Chemosignals and Stimulates Mating in Male Mice. *eNeuro*, 4(2). <https://doi.org/10.1523/ENEURO.0010-17.2017>

Land, H., Schutz, G., Schmale, H., & Richter, D. (1982). Nucleotide sequence of cloned cDNA encoding bovine arginine vasopressin-neurophysin II precursor. *Nature*, 295(5847), 299-303. <https://doi.org/10.1038/295299a0>

Langer, S. Z., Zarifian, E., Briley, M., Raisman, R., & Sechter, D. (1981). High-affinity binding of 3H-imipramine in brain and platelets and its relevance to the biochemistry of affective disorders. *Life Sci*, 29(3), 211-220. [https://doi.org/10.1016/0024-3205\(81\)90236-8](https://doi.org/10.1016/0024-3205(81)90236-8)

Lerch-Haner, J. K., Frierson, D., Crawford, L. K., Beck, S. G., & Deneris, E. S. (2008). Serotonergic transcriptional programming determines maternal behavior and offspring survival. *Nat Neurosci*, 11(9), 1001-1003. <https://doi.org/10.1038/nn.2176>

Lesch, K. P. (2007). Linking emotion to the social brain. The role of the serotonin transporter in human social behaviour. *EMBO Rep*, 8 Spec No(Suppl 1), S24-29. <https://doi.org/10.1038/sj.embor.7401008>

Li, L., Zhang, L.-Z., He, Z.-X., Ma, H., Zhang, Y.-T., Xun, Y.-F., Yuan, W., Hou, W.-J., Li, Y.-T., Lv, Z.-J., Jia, R., & Tai, F.-D. (2021). Dorsal raphe nucleus to anterior cingulate cortex 5-HTergic neural circuit modulates consolation and sociability. *eLife*, 10, e67638. <https://doi.org/10.7554/eLife.67638>

Li, Y., Zhong, W., Wang, D., Feng, Q., Liu, Z., Zhou, J., Jia, C., Hu, F., Zeng, J., Guo, Q., Fu, L., & Luo, M. (2016). Serotonin neurons in the dorsal raphe nucleus encode reward signals. *Nat Commun*, 7, 10503. <https://doi.org/10.1038/ncomms10503>

Li, Y. Q., Jia, H. G., Rao, Z. R., & Shi, J. W. (1990). Serotonin-, substance P- or leucine-enkephalin-containing neurons in the midbrain periaqueductal gray and nucleus raphe dorsalis send projection fibers to the central amygdaloid nucleus in the rat. *Neurosci Lett*, 120(1), 124-127. [https://doi.org/10.1016/0304-3940\(90\)90184-b](https://doi.org/10.1016/0304-3940(90)90184-b)

Lillesaar, C. (2011). The serotonergic system in fish. *J Chem Neuroanat*, 41(4), 294-308. <https://doi.org/10.1016/j.jchemneu.2011.05.009>

Lin, D. Y., Zhang, S. Z., Block, E., & Katz, L. C. (2005). Encoding social signals in the mouse main olfactory bulb. *Nature*, 434(7032), 470-477. <https://doi.org/10.1038/nature03414>

Liu, D., Rahman, M., Johnson, A., Tsutsui-Kimura, I., Pena, N., Talay, M., Logeman, B. L., Finkbeiner, S., Choi, S., Capo-Battaglia, A., Abdus-Saboor, I., Ginty, D. D., Uchida, N., Watabe-Uchida, M., & Dulac, C. (2023). A Hypothalamic Circuit Underlying the Dynamic Control of Social Homeostasis. *bioRxiv*, 2023.2005.2019.540391. <https://doi.org/10.1101/2023.05.19.540391>

Liu, Y., Jiang, Y., Si, Y., Kim, J. Y., Chen, Z. F., & Rao, Y. (2011). Molecular regulation of sexual preference revealed by genetic studies of 5-HT in the brains of male mice. *Nature*, 472(7341), 95-99. <https://doi.org/10.1038/nature09822>

Lolait, S. J., O'Carroll, A. M., Mahan, L. C., Felder, C. C., Button, D. C., Young, W. S., 3rd, Mezey, E., & Brownstein, M. J. (1995). Extrapituitary expression of the rat V1b vasopressin receptor gene. *Proc Natl Acad Sci U S A*, 92(15), 6783-6787. <https://doi.org/10.1073/pnas.92.15.6783>

- Lolait, S. J., O'Carroll, A. M., McBride, O. W., Konig, M., Morel, A., & Brownstein, M. J. (1992). Cloning and characterization of a vasopressin V2 receptor and possible link to nephrogenic diabetes insipidus. *Nature*, 357(6376), 336-339. <https://doi.org/10.1038/357336a0>
- Lowry, C. A., Evans, A. K., Gasser, P. J., Hale, M. W., Staub, D. R., & Shekhar, A. (2008). Topographic organization and chemoarchitecture of the dorsal raphe nucleus and the median raphe nucleus. In J. M. Monti, S. R. Pandi-Perumal, B. L. Jacobs, & D. J. Nutt (Eds.), *Serotonin and Sleep: Molecular, Functional and Clinical Aspects* (pp. 25-67). Birkhäuser Basel. https://doi.org/10.1007/978-3-7643-8561-3_2
- Lowry, C. A., Johnson, P. L., Hay-Schmidt, A., Mikkelsen, J., & Shekhar, A. (2005). Modulation of anxiety circuits by serotonergic systems. *Stress*, 8(4), 233-246. <https://doi.org/10.1080/10253890500492787>
- Lucki, I. (1998). The spectrum of behaviors influenced by serotonin. *Biol Psychiatry*, 44(3), 151-162. [https://doi.org/10.1016/s0006-3223\(98\)00139-5](https://doi.org/10.1016/s0006-3223(98)00139-5)
- Lund, C., Orkin, K., Witte, M. C. d., Davies, T., Haushofer, J., Bass, J. K., Bolton, P. A., Murray, S. R., Murray, L. K., Tol, W. A., Thornicroft, G., & Patel, V. (2018). Economic impacts of mental health interventions in low and middle-income countries: a systematic review and meta-analysis Authors.
- Lyon, K. A., Rood, B. D., Wu, L., Senft, R. A., Goodrich, L. V., & Dymecki, S. M. (2020). Sex-Specific Role for Dopamine Receptor D2 in Dorsal Raphe Serotonergic Neuron Modulation of Defensive Acoustic Startle and Dominance Behavior. *eNeuro*, 7(6). <https://doi.org/10.1523/ENEURO.0202-20.2020>
- Ma, P. M., Beltz, B. S., & Kravitz, E. A. (1992). Serotonin-containing neurons in lobsters: their role as gain-setters in postural control mechanisms. *J Neurophysiol*, 68(1), 36-54. <https://doi.org/10.1152/jn.1992.68.1.36>
- Machalova, A., Slais, K., Vrskova, D., & Sulcova, A. (2012). Differential effects of modafinil, methamphetamine, and MDMA on agonistic behavior in male mice. *Pharmacol Biochem Behav*, 102(2), 215-223. <https://doi.org/10.1016/j.pbb.2012.04.013>
- MacLaren, D. A., Browne, R. W., Shaw, J. K., Krishnan Radhakrishnan, S., Khare, P., Espana, R. A., & Clark, S. D. (2016). Clozapine N-Oxide Administration Produces Behavioral Effects in Long-Evans Rats: Implications for Designing DREADD Experiments. *eNeuro*, 3(5). <https://doi.org/10.1523/ENEURO.0219-16.2016>
- Madisen, L., Zwingman, T. A., Sunkin, S. M., Oh, S. W., Zariwala, H. A., Gu, H., Ng, L. L., Palmiter, R. D., Hawrylycz, M. J., Jones, A. R., Lein, E. S., & Zeng, H. (2010). A robust and high-throughput Cre reporting and characterization system for the whole mouse brain. *Nat Neurosci*, 13(1), 133-140. <https://doi.org/10.1038/nn.2467>

- Manvich, D. F., Webster, K. A., Foster, S. L., Farrell, M. S., Ritchie, J. C., Porter, J. H., & Weinshenker, D. (2018). The DREADD agonist clozapine N-oxide (CNO) is reverse-metabolized to clozapine and produces clozapine-like interoceptive stimulus effects in rats and mice. *Sci Rep*, 8(1), 3840. <https://doi.org/10.1038/s41598-018-22116-z>
- Martinez, L. A., & Petrulis, A. (2011). The bed nucleus of the stria terminalis is critical for sexual solicitation, but not for opposite-sex odor preference, in female Syrian hamsters. *Horm Behav*, 60(5), 651-659. <https://doi.org/10.1016/j.yhbeh.2011.08.018>
- Mayes, C. R., Watts, A. G., McQueen, J. K., Fink, G., & Charlton, H. M. (1988). Gonadal steroids influence neurophysin II distribution in the forebrain of normal and mutant mice. *Neuroscience*, 25(3), 1013-1022. [https://doi.org/10.1016/0306-4522\(88\)90054-1](https://doi.org/10.1016/0306-4522(88)90054-1)
- Meyer-Lindenberg, A., Domes, G., Kirsch, P., & Heinrichs, M. (2011). Oxytocin and vasopressin in the human brain: social neuropeptides for translational medicine. *Nat Rev Neurosci*, 12(9), 524-538. <https://doi.org/10.1038/nrn3044>
- Meyer-Lindenberg, A., Kolachana, B., Gold, B., Olsh, A., Nicodemus, K. K., Mattay, V., Dean, M., & Weinberger, D. R. (2009). Genetic variants in AVPR1A linked to autism predict amygdala activation and personality traits in healthy humans. *Mol Psychiatry*, 14(10), 968-975. <https://doi.org/10.1038/mp.2008.54>
- Michl, J., Scharinger, C., Zauner, M., Kasper, S., Freissmuth, M., Sitte, H. H., Ecker, G. F., & Pezawas, L. (2014). A multivariate approach linking reported side effects of clinical antidepressant and antipsychotic trials to in vitro binding affinities. *Eur Neuropsychopharmacol*, 24(9), 1463-1474. <https://doi.org/10.1016/j.euroneuro.2014.06.013>
- Miczek, K. A., Mos, J., & Olivier, B. (1989). Brain 5-HT and inhibition of aggressive behavior in animals: 5-HIAA and receptor subtypes. *Psychopharmacol Bull*, 25(3), 399-403. <https://www.ncbi.nlm.nih.gov/pubmed/2483273>
- Mieda, M., Ono, D., Hasegawa, E., Okamoto, H., Honma, K., Honma, S., & Sakurai, T. (2015). Cellular clocks in AVP neurons of the SCN are critical for interneuronal coupling regulating circadian behavior rhythm. *Neuron*, 85(5), 1103-1116. <https://doi.org/10.1016/j.neuron.2015.02.005>
- Montastruc, F., Palmaro, A., Bagheri, H., Schmitt, L., Montastruc, J. L., & Lapeyre-Mestre, M. (2015). Role of serotonin 5-HT_{2C} and histamine H₁ receptors in antipsychotic-induced diabetes: A pharmacoepidemiological-pharmacodynamic study in VigiBase. *Eur Neuropsychopharmacol*, 25(10), 1556-1565. <https://doi.org/10.1016/j.euroneuro.2015.07.010>
- Morel, A., O'Carroll, A. M., Brownstein, M. J., & Lolait, S. J. (1992). Molecular cloning and expression of a rat V_{1a} arginine vasopressin receptor. *Nature*, 356(6369), 523-526. <https://doi.org/10.1038/356523a0>

- Mosienko, V., Bert, B., Beis, D., Matthes, S., Fink, H., Bader, M., & Alenina, N. (2012). Exaggerated aggression and decreased anxiety in mice deficient in brain serotonin. *Transl Psychiatry*, 2(5), e122. <https://doi.org/10.1038/tp.2012.44>
- Moss, M. S., Glazer, E. J., & Basbaum, A. I. (1983). The peptidergic organization of the cat periaqueductal gray. I. The distribution of immunoreactive enkephalin-containing neurons and terminals. *J Neurosci*, 3(3), 603-616. <https://doi.org/10.1523/JNEUROSCI.03-03-00603.1983>
- Moy, S. S., Nadler, J. J., Perez, A., Barbaro, R. P., Johns, J. M., Magnuson, T. R., Piven, J., & Crawley, J. N. (2004). Sociability and preference for social novelty in five inbred strains: an approach to assess autistic-like behavior in mice. *Genes Brain Behav*, 3(5), 287-302. <https://doi.org/10.1111/j.1601-1848.2004.00076.x>
- Muzerelle, A., Scotto-Lomassese, S., Bernard, J. F., Soiza-Reilly, M., & Gaspar, P. (2016). Conditional anterograde tracing reveals distinct targeting of individual serotonin cell groups (B5-B9) to the forebrain and brainstem. *Brain Struct Funct*, 221(1), 535-561. <https://doi.org/10.1007/s00429-014-0924-4>
- Niederkofler, V., Asher, T. E., Okaty, B. W., Rood, B. D., Narayan, A., Hwa, L. S., Beck, S. G., Miczek, K. A., & Dymecki, S. M. (2016). Identification of Serotonergic Neuronal Modules that Affect Aggressive Behavior. *Cell Rep*, 17(8), 1934-1949. <https://doi.org/10.1016/j.celrep.2016.10.063>
- Oliver, G., & Schafer, E. A. (1895). The Physiological Effects of Extracts of the Suprarenal Capsules. *J Physiol*, 18(3), 230-276. <https://doi.org/10.1113/jphysiol.1895.sp000564>
- Ostrowski, N. L., Lolait, S. J., & Young, W. S., 3rd. (1994). Cellular localization of vasopressin V1a receptor messenger ribonucleic acid in adult male rat brain, pineal, and brain vasculature. *Endocrinology*, 135(4), 1511-1528. <https://doi.org/10.1210/endo.135.4.7925112>
- Ottersen, O. P. (1981). Afferent connections to the amygdaloid complex of the rat with some observations in the cat. III. Afferents from the lower brain stem. *J Comp Neurol*, 202(3), 335-356. <https://doi.org/10.1002/cne.902020304>
- Pagani, J. H., Zhao, M., Cui, Z., Avram, S. K., Caruana, D. A., Dudek, S. M., & Young, W. S. (2015). Role of the vasopressin 1b receptor in rodent aggressive behavior and synaptic plasticity in hippocampal area CA2. *Mol Psychiatry*, 20(4), 490-499. <https://doi.org/10.1038/mp.2014.47>
- Pankevich, D. E., Baum, M. J., & Cherry, J. A. (2004). Olfactory sex discrimination persists, whereas the preference for urinary odorants from estrous females disappears in male mice after vomeronasal organ removal. *J Neurosci*, 24(42), 9451-9457. <https://doi.org/10.1523/JNEUROSCI.2376-04.2004>

- Patel, T. N., Caiola, H. O., Mallari, O. G., Blandino, K. L., Goldenthal, A. R., Dymecki, S. M., & Rood, B. D. (2022). Social Interactions Increase Activation of Vasopressin-Responsive Neurons in the Dorsal Raphe. *Neuroscience*, *495*, 25-46. <https://doi.org/10.1016/j.neuroscience.2022.05.032>
- Paul, E. D., Hale, M. W., Lukkes, J. L., Valentine, M. J., Sarchet, D. M., & Lowry, C. A. (2011). Repeated social defeat increases reactive emotional coping behavior and alters functional responses in serotonergic neurons in the rat dorsal raphe nucleus. *Physiol Behav*, *104*(2), 272-282. <https://doi.org/10.1016/j.physbeh.2011.01.006>
- Petit, J. M., Luppi, P. H., Peyron, C., Rampon, C., & Jouvet, M. (1995). VIP-like immunoreactive projections from the dorsal raphe and caudal linear raphe nuclei to the bed nucleus of the stria terminalis demonstrated by a double immunohistochemical method in the rat. *Neurosci Lett*, *193*(2), 77-80. [https://doi.org/10.1016/0304-3940\(95\)11669-n](https://doi.org/10.1016/0304-3940(95)11669-n)
- Preibisch, S., Saalfeld, S., & Tomancak, P. (2009). Globally optimal stitching of tiled 3D microscopic image acquisitions. *Bioinformatics*, *25*(11), 1463-1465. <https://doi.org/10.1093/bioinformatics/btp184>
- Prichard, Z. M., Mackinnon, A. J., Jorm, A. F., & Easta, S. (2007). AVPR1A and OXTR polymorphisms are associated with sexual and reproductive behavioral phenotypes in humans. Mutation in brief no. 981. Online. *Hum Mutat*, *28*(11), 1150. <https://doi.org/10.1002/humu.9510>
- Raam, T., & Hong, W. (2021). Organization of neural circuits underlying social behavior: A consideration of the medial amygdala. *Curr Opin Neurobiol*, *68*, 124-136. <https://doi.org/10.1016/j.conb.2021.02.008>
- Raisman, R., Briley, M., & Langer, S. Z. (1979). Specific tricyclic antidepressant binding sites in rat brain. *Nature*, *281*(5727), 148-150. <https://doi.org/10.1038/281148a0>
- RCoreTeam. (2022). *R: A language and environment for statistical computing*. In R Foundation for Statistical Computing.
- Reichling, D. B., & Basbaum, A. I. (1990). Contribution of brainstem GABAergic circuitry to descending antinociceptive controls: I. GABA-immunoreactive projection neurons in the periaqueductal gray and nucleus raphe magnus. *J Comp Neurol*, *302*(2), 370-377. <https://doi.org/10.1002/cne.903020213>
- Ren, J., Friedmann, D., Xiong, J., Liu, C. D., Ferguson, B. R., Weerakkody, T., DeLoach, K. E., Ran, C., Pun, A., Sun, Y., Weissbourd, B., Neve, R. L., Huguenard, J., Horowitz, M. A., & Luo, L. (2018). Anatomically Defined and Functionally Distinct Dorsal Raphe Serotonin Sub-systems. *Cell*, *175*(2), 472-487.e420. <https://doi.org/10.1016/j.cell.2018.07.043>
- Rigney, N., Beaumont, R., & Petrulis, A. (2020). Sex differences in vasopressin 1a receptor regulation of social communication within the lateral habenula and dorsal raphe of mice. *Horm Behav*, *121*, 104715. <https://doi.org/10.1016/j.yhbeh.2020.104715>

- Rigney, N., de Vries, G. J., & Petrulis, A. (2023a). Modulation of social behavior by distinct vasopressin sources. *Front Endocrinol (Lausanne)*, *14*, 1127792. <https://doi.org/10.3389/fendo.2023.1127792>
- Rigney, N., de Vries, G. J., & Petrulis, A. (2023b). Sex differences in afferents and efferents of vasopressin neurons of the bed nucleus of the stria terminalis and medial amygdala in mice. *Horm Behav*, *154*, 105407. <https://doi.org/10.1016/j.yhbeh.2023.105407>
- Rigney, N., Whylings, J., de Vries, G. J., & Petrulis, A. (2021). Sex Differences in the Control of Social Investigation and Anxiety by Vasopressin Cells of the Paraventricular Nucleus of the Hypothalamus. *Neuroendocrinology*, *111*(6), 521-535. <https://doi.org/10.1159/000509421>
- Rigney, N., Whylings, J., Mieda, M., de Vries, G., & Petrulis, A. (2019). Sexually Dimorphic Vasopressin Cells Modulate Social Investigation and Communication in Sex-Specific Ways. *eNeuro*, *6*(1). <https://doi.org/10.1523/ENEURO.0415-18.2019>
- Rigney, N., Zbib, A., de Vries, G. J., & Petrulis, A. (2022). Knockdown of sexually differentiated vasopressin expression in the bed nucleus of the stria terminalis reduces social and sexual behaviour in male, but not female, mice. *J Neuroendocrinol*, *34*(9), e13083. <https://doi.org/10.1111/jne.13083>
- Rodd, Z. A., Engleman, E. A., Truitt, W. A., Burke, A. R., Molosh, A. I., Bell, R. L., & Hauser, S. R. (2022). CNO Administration Increases Dopamine and Glutamate in the Medial Prefrontal Cortex of Wistar Rats: Further Concerns for the Validity of the CNO-activated DREADD Procedure. *Neuroscience*, *491*, 176-184. <https://doi.org/10.1016/j.neuroscience.2022.03.028>
- Rood, B. D., & Beck, S. G. (2014). Vasopressin indirectly excites dorsal raphe serotonin neurons through activation of the vasopressin1A receptor. *Neuroscience*, *260*, 205-216. <https://doi.org/10.1016/j.neuroscience.2013.12.012>
- Rood, B. D., & De Vries, G. J. (2011). Vasopressin innervation of the mouse (*Mus musculus*) brain and spinal cord. *J Comp Neurol*, *519*(12), 2434-2474. <https://doi.org/10.1002/cne.22635>
- Rood, B. D., Murray, E. K., Laroche, J., Yang, M. K., Blaustein, J. D., & De Vries, G. J. (2008). Absence of progesterone receptors alters distribution of vasopressin fibers but not sexual differentiation of vasopressin system in mice. *Neuroscience*, *154*(3), 911-921. <https://doi.org/10.1016/j.neuroscience.2008.03.087>
- Rood, B. D., Stott, R. T., You, S., Smith, C. J., Woodbury, M. E., & De Vries, G. J. (2013). Site of origin of and sex differences in the vasopressin innervation of the mouse (*Mus musculus*) brain. *J Comp Neurol*, *521*(10), 2321-2358. <https://doi.org/10.1002/cne.23288>

Saito, M., Sugimoto, T., Tahara, A., & Kawashima, H. (1995). Molecular cloning and characterization of rat V1b vasopressin receptor: evidence for its expression in extra-pituitary tissues. *Biochem Biophys Res Commun*, 212(3), 751-757. <https://doi.org/10.1006/bbrc.1995.2033>

SAMHSA. (2022). *Key substance use and mental health indicators in the United States: Results from the 2021 National Survey on Drug Use and Health*. <https://www.samhsa.gov/data/report/2021-nsduh-annual-national-report>

Santini, Z. I., Becher, H., Jorgensen, M. B., Davidsen, M., Nielsen, L., Hinrichsen, C., Madsen, K. R., Meilstrup, C., Koyanagi, A., Stewart-Brown, S., McDaid, D., & Koushede, V. (2021). Economics of mental well-being: a prospective study estimating associated health care costs and sickness benefit transfers in Denmark. *Eur J Health Econ*, 22(7), 1053-1065. <https://doi.org/10.1007/s10198-021-01305-0>

Sauer, B. (1993). Manipulation of transgenes by site-specific recombination: use of Cre recombinase. *Methods Enzymol*, 225, 890-900. [https://doi.org/10.1016/0076-6879\(93\)25056-8](https://doi.org/10.1016/0076-6879(93)25056-8)

Schotte, A., Janssen, P. F., Megens, A. A., & Leysen, J. E. (1993). Occupancy of central neurotransmitter receptors by risperidone, clozapine and haloperidol, measured ex vivo by quantitative autoradiography. *Brain Res*, 631(2), 191-202. [https://doi.org/10.1016/0006-8993\(93\)91535-z](https://doi.org/10.1016/0006-8993(93)91535-z)

Shapiro, L. E., & Dewsbury, D. A. (1990). Differences in affiliative behavior, pair bonding, and vaginal cytology in two species of vole (*Microtus ochrogaster* and *M. montanus*). *J Comp Psychol*, 104(3), 268-274. <https://doi.org/10.1037/0735-7036.104.3.268>

Shewey, L. M., & Dorsa, D. M. (1988). V1-type vasopressin receptors in rat brain septum: binding characteristics and effects on inositol phospholipid metabolism. *J Neurosci*, 8(5), 1671-1677. <https://doi.org/10.1523/JNEUROSCI.08-05-01671.1988>

ShIPLEY, M. T., McLean, J. H., & Behbehani, M. M. (1987). Heterogeneous distribution of neurotensin-like immunoreactive neurons and fibers in the midbrain periaqueductal gray of the rat. *J Neurosci*, 7(7), 2025-2034. <https://doi.org/10.1523/JNEUROSCI.07-07-02025.1987>

Siafis, S., Tzachanis, D., Samara, M., & Papazisis, G. (2018). Antipsychotic Drugs: From Receptor-binding Profiles to Metabolic Side Effects. *Curr Neuropharmacol*, 16(8), 1210-1223. <https://doi.org/10.2174/1570159X15666170630163616>

Simpson, K. L., Waterhouse, B. D., & Lin, R. C. (2003). Differential expression of nitric oxide in serotonergic projection neurons: neurochemical identification of dorsal raphe inputs to rodent trigeminal somatosensory targets. *J Comp Neurol*, 466(4), 495-512. <https://doi.org/10.1002/cne.10912>

- Smith, A. S., Williams Avram, S. K., Cymerblit-Sabba, A., Song, J., & Young, W. S. (2016). Targeted activation of the hippocampal CA2 area strongly enhances social memory. *Mol Psychiatry*, *21*(8), 1137-1144. <https://doi.org/10.1038/mp.2015.189>
- Smith, K. S., Bucci, D. J., Luikart, B. W., & Mahler, S. V. (2016). DREADDS: Use and application in behavioral neuroscience. *Behavioral Neuroscience*, *130*, 137-155. <https://doi.org/10.1037/bne0000135>
- Stanton, S. C., Campbell, L., & Loving, T. J. (2014). Energized by love: thinking about romantic relationships increases positive affect and blood glucose levels. *Psychophysiology*, *51*(10), 990-995. <https://doi.org/10.1111/psyp.12249>
- Stemmelin, J., Lukovic, L., Salome, N., & Griebel, G. (2005). Evidence that the lateral septum is involved in the antidepressant-like effects of the vasopressin V1b receptor antagonist, SSR149415. *Neuropsychopharmacology*, *30*(1), 35-42. <https://doi.org/10.1038/sj.npp.1300562>
- Stephens, L. R., & Logan, S. D. (1986). Arginine-vasopressin stimulates inositol phospholipid metabolism in rat hippocampus. *J Neurochem*, *46*(2), 649-651. <https://doi.org/10.1111/j.1471-4159.1986.tb13016.x>
- Szot, P., Bale, T. L., & Dorsa, D. M. (1994). Distribution of messenger RNA for the vasopressin V1a receptor in the CNS of male and female rats. *Brain Res Mol Brain Res*, *24*(1-4), 1-10. [https://doi.org/10.1016/0169-328x\(94\)90111-2](https://doi.org/10.1016/0169-328x(94)90111-2)
- Terranova, J. I., Song, Z., Larkin, T. E., 2nd, Hardcastle, N., Norvelle, A., Riaz, A., & Albers, H. E. (2016). Serotonin and arginine-vasopressin mediate sex differences in the regulation of dominance and aggression by the social brain. *Proc Natl Acad Sci U S A*, *113*(46), 13233-13238. <https://doi.org/10.1073/pnas.1610446113>
- Terranova, M. L., & Laviola, G. (2005). Scoring of social interactions and play in mice during adolescence. *Curr Protoc Toxicol*, *Chapter 13*, Unit13.10. <https://doi.org/10.1002/0471140856.tx1310s26>
- Thompson, R. R., George, K., Walton, J. C., Orr, S. P., & Benson, J. (2006). Sex-specific influences of vasopressin on human social communication. *Proc Natl Acad Sci U S A*, *103*(20), 7889-7894. <https://doi.org/10.1073/pnas.0600406103>
- Tong, W. H., Abdulai-Saiku, S., & Vyas, A. (2021). Medial Amygdala Arginine Vasopressin Neurons Regulate Innate Aversion to Cat Odors in Male Mice. *Neuroendocrinology*, *111*(6), 505-520. <https://doi.org/10.1159/000508862>
- Tsuji, T., Allchorne, A. J., Zhang, M., Tsuji, C., Tobin, V. A., Pineda, R., Raftogianni, A., Stern, J. E., Grinevich, V., Leng, G., & Ludwig, M. (2017). Vasopressin casts light on the suprachiasmatic nucleus. *J Physiol*, *595*(11), 3497-3514. <https://doi.org/10.1113/JP274025>

- Turiault, M., Parnaudeau, S., Milet, A., Parlato, R., Rouzeau, J. D., Lazar, M., & Tronche, F. (2007). Analysis of dopamine transporter gene expression pattern -- generation of DAT-iCre transgenic mice. *FEBS J*, *274*(14), 3568-3577. <https://doi.org/10.1111/j.1742-4658.2007.05886.x>
- Turner, M. R., & Pallone, T. L. (1997). Vasopressin constricts outer medullary descending vasa recta isolated from rat kidneys. *Am J Physiol*, *272*(1 Pt 2), F147-151. <https://doi.org/10.1152/ajprenal.1997.272.1.F147>
- Vaccari, C., Lolait, S. J., & Ostrowski, N. L. (1998). Comparative distribution of vasopressin V1b and oxytocin receptor messenger ribonucleic acids in brain. *Endocrinology*, *139*(12), 5015-5033. <https://doi.org/10.1210/endo.139.12.6382>
- van Kerkhof, L. W., Trezza, V., Mulder, T., Gao, P., Voorn, P., & Vanderschuren, L. J. (2014). Cellular activation in limbic brain systems during social play behaviour in rats. *Brain Struct Funct*, *219*(4), 1181-1211. <https://doi.org/10.1007/s00429-013-0558-y>
- Veenema, A. H. (2009). Early life stress, the development of aggression and neuroendocrine and neurobiological correlates: what can we learn from animal models? *Front Neuroendocrinol*, *30*(4), 497-518. <https://doi.org/10.1016/j.yfrne.2009.03.003>
- Vertes, R. P., & Crane, A. M. (1997). Distribution, quantification, and morphological characteristics of serotonin-immunoreactive cells of the suprallemniscal nucleus (B9) and pontomesencephalic reticular formation in the rat. *J Comp Neurol*, *378*(3), 411-424. [https://doi.org/10.1002/\(sici\)1096-9861\(19970217\)378:3<411::aid-cne8>3.0.co;2-6](https://doi.org/10.1002/(sici)1096-9861(19970217)378:3<411::aid-cne8>3.0.co;2-6)
- Veyrac, A., Wang, G., Baum, M. J., & Bakker, J. (2011). The main and accessory olfactory systems of female mice are activated differentially by dominant versus subordinate male urinary odors. *Brain Res*, *1402*, 20-29. <https://doi.org/10.1016/j.brainres.2011.05.035>
- Vooijs, M., Jonkers, J., & Berns, A. (2001). A highly efficient ligand-regulated Cre recombinase mouse line shows that LoxP recombination is position dependent. *EMBO Rep*, *2*(4), 292-297. <https://doi.org/10.1093/embo-reports/kve064>
- Walum, H., Westberg, L., Henningsson, S., Neiderhiser, J. M., Reiss, D., Igl, W., Ganiban, J. M., Spotts, E. L., Pedersen, N. L., Eriksson, E., & Lichtenstein, P. (2008). Genetic variation in the vasopressin receptor 1a gene (AVPR1A) associates with pair-bonding behavior in humans. *Proc Natl Acad Sci U S A*, *105*(37), 14153-14156. <https://doi.org/10.1073/pnas.0803081105>
- Wang, Z., Ferris, C. F., & De Vries, G. J. (1994). Role of septal vasopressin innervation in paternal behavior in prairie voles (*Microtus ochrogaster*). *Proc Natl Acad Sci U S A*, *91*(1), 400-404. <https://doi.org/10.1073/pnas.91.1.400>
- Wassink, T. H., Piven, J., Vieland, V. J., Pietila, J., Goedken, R. J., Folstein, S. E., & Sheffield, V. C. (2004). Examination of AVPR1a as an autism susceptibility gene. *Mol Psychiatry*, *9*(10), 968-972. <https://doi.org/10.1038/sj.mp.4001503>

- Waterhouse, B. D., Border, B., Wahl, L., & Mihailoff, G. A. (1993). Topographic organization of rat locus coeruleus and dorsal raphe nuclei: distribution of cells projecting to visual system structures. *J Comp Neurol*, 336(3), 345-361. <https://doi.org/10.1002/cne.903360304>
- Waterhouse, B. D., Mihailoff, G. A., Baack, J. C., & Woodward, D. J. (1986). Topographical distribution of dorsal and median raphe neurons projecting to motor, sensorimotor, and visual cortical areas in the rat. *J Comp Neurol*, 249(4), 460-476, 478-481. <https://doi.org/10.1002/cne.902490403>
- Wersinger, S. R., Caldwell, H. K., Christiansen, M., & Young, W. S., 3rd. (2007). Disruption of the vasopressin 1b receptor gene impairs the attack component of aggressive behavior in mice. *Genes Brain Behav*, 6(7), 653-660. <https://doi.org/10.1111/j.1601-183X.2006.00294.x>
- Wersinger, S. R., Caldwell, H. K., Martinez, L., Gold, P., Hu, S. B., & Young, W. S., 3rd. (2007). Vasopressin 1a receptor knockout mice have a subtle olfactory deficit but normal aggression. *Genes Brain Behav*, 6(6), 540-551. <https://doi.org/10.1111/j.1601-183X.2006.00281.x>
- Wersinger, S. R., Ginns, E. I., O'Carroll, A. M., Lolait, S. J., & Young, W. S., 3rd. (2002). Vasopressin V1b receptor knockout reduces aggressive behavior in male mice. *Mol Psychiatry*, 7(9), 975-984. <https://doi.org/10.1038/sj.mp.4001195>
- Wersinger, S. R., Kelliher, K. R., Zufall, F., Lolait, S. J., O'Carroll, A. M., & Young, W. S., 3rd. (2004). Social motivation is reduced in vasopressin 1b receptor null mice despite normal performance in an olfactory discrimination task. *Horm Behav*, 46(5), 638-645. <https://doi.org/10.1016/j.yhbeh.2004.07.004>
- WHO. (2022). *World mental health report: transforming mental health for all*.
- Whylings, J., Rigney, N., de Vries, G. J., & Petrulis, A. (2021). Reduction in vasopressin cells in the suprachiasmatic nucleus in mice increases anxiety and alters fluid intake. *Horm Behav*, 133, 104997. <https://doi.org/10.1016/j.yhbeh.2021.104997>
- Wolke, D., & Lereya, S. T. (2014). Bullying and parasomnias: a longitudinal cohort study. *Pediatrics*, 134(4), e1040-1048. <https://doi.org/10.1542/peds.2014-1295>
- Wolke, D., & Lereya, S. T. (2015). Long-term effects of bullying. *Arch Dis Child*, 100(9), 879-885. <https://doi.org/10.1136/archdischild-2014-306667>
- Yates, F. E., Russell, S. M., Dallman, M. F., Hodge, G. A., McCann, S. M., & Dhariwal, A. P. (1971). Potentiation by vasopressin of corticotropin release induced by corticotropin-releasing factor. *Endocrinology*, 88(1), 3-15. <https://doi.org/10.1210/endo-88-1-3>

Yirmiya, N., Rosenberg, C., Levi, S., Salomon, S., Shulman, C., Nemanov, L., Dina, C., & Ebstein, R. P. (2006). Association between the arginine vasopressin 1a receptor (AVPR1a) gene and autism in a family-based study: mediation by socialization skills. *Mol Psychiatry*, *11*(5), 488-494. <https://doi.org/10.1038/sj.mp.4001812>

Young, L. J., Nilsen, R., Waymire, K. G., MacGregor, G. R., & Insel, T. R. (1999). Increased affiliative response to vasopressin in mice expressing the V1a receptor from a monogamous vole. *Nature*, *400*(6746), 766-768. <https://doi.org/10.1038/23475>

Young, W. S., Li, J., Wersinger, S. R., & Palkovits, M. (2006). The vasopressin 1b receptor is prominent in the hippocampal area CA2 where it is unaffected by restraint stress or adrenalectomy. *Neuroscience*, *143*(4), 1031-1039. <https://doi.org/10.1016/j.neuroscience.2006.08.040>

Zhuang, X., Masson, J., Gingrich, J. A., Rayport, S., & Hen, R. (2005). Targeted gene expression in dopamine and serotonin neurons of the mouse brain. *J Neurosci Methods*, *143*(1), 27-32. <https://doi.org/10.1016/j.jneumeth.2004.09.020>

Appendix

Figures & Tables

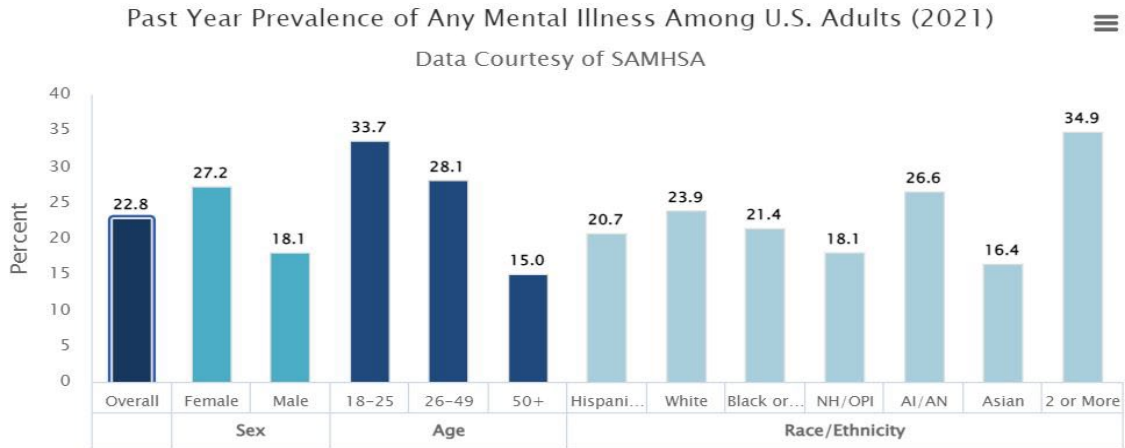


Figure A1.1 Prevalence of mental illness among US adults in 2021. NH/OPI = Native Hawaiian / Other Pacific Islander. AI/AN = American Indian / Alaskan Native. Adapted from Substance Abuse and Mental Health Services Administration (SAMHSA, 2022).

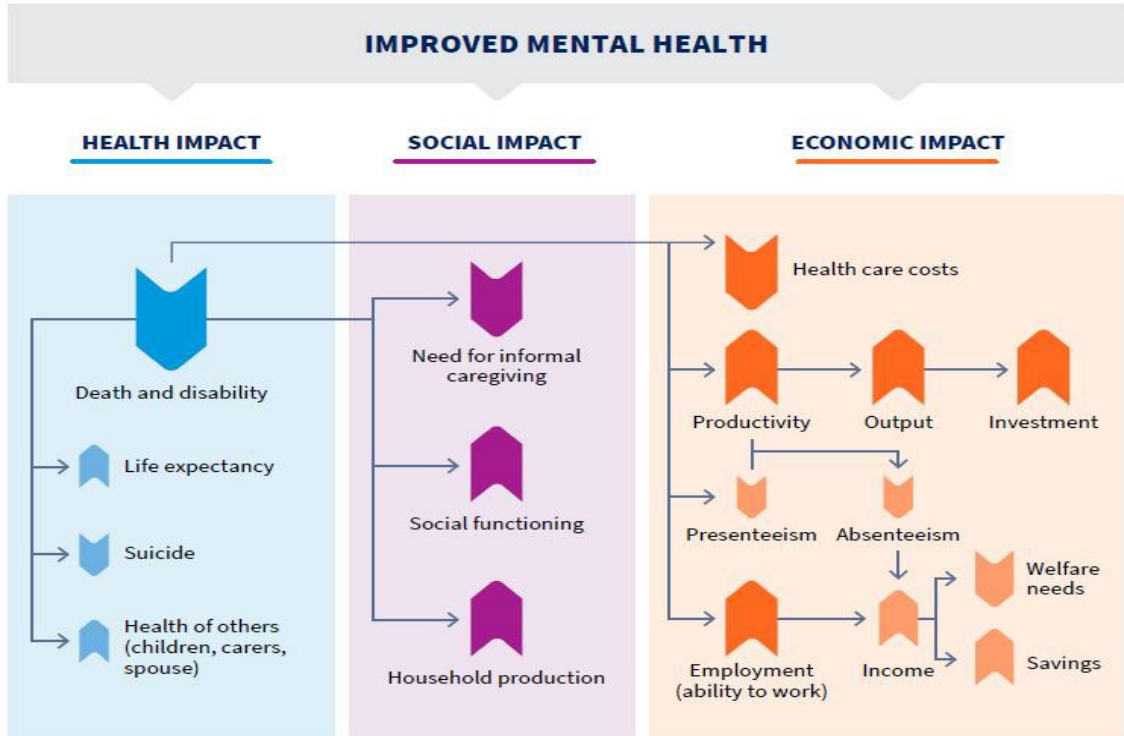


Figure A1. 2 Flowchart of social and economic benefits of investing in mental health. Figure adapted from (WHO, 2022).

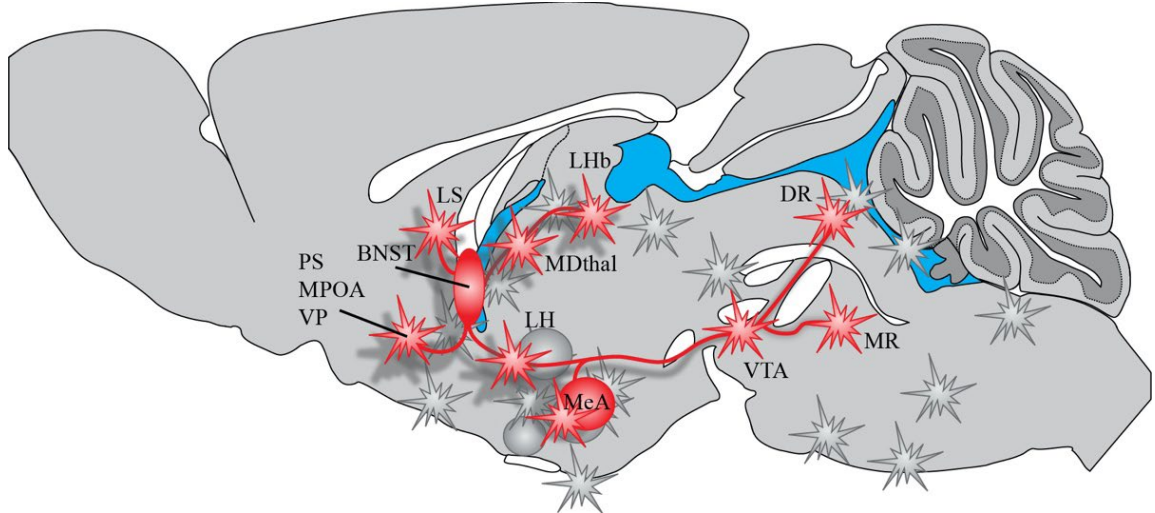


Figure A1. 3 Schematic of a sagittal section through the midline of a mouse brain depicts the BNST and MeA Avp nuclei and their projection sites. Gray spherical objects represent other Avp nuclei (SCN, PVN, and SON) and their projections are also in gray. PS = Parastrial Nucleus; MPOA = Medial Preoptic Area; VP = Ventral Pallidum; BNST = Bed Nucleus Stria Terminalis; LS = Lateral Septum; LH = Lateral Septum; MDthal = Mediodorsal Thalamus; LHb = Lateral Habenula; VTA = Ventral Tegmental Nucleus; MR = Median Raphe; DR = Dorsal Raphe; SCN = Suprachiasmatic Nucleus; PVN = Paraventricular Nucleus; SON = Supraoptic Nucleus. Adapted from data published in (Rood et al., 2013).

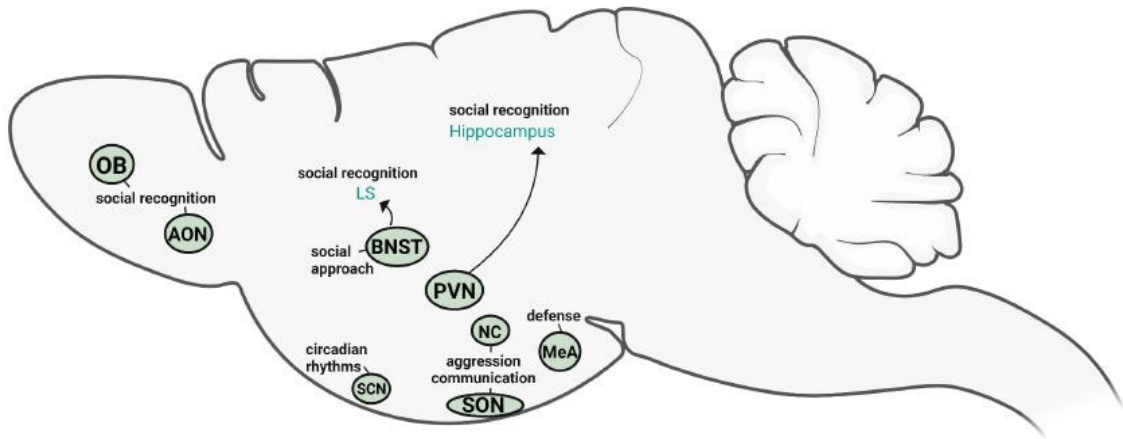


Figure A1. 4 Sources of vasopressin relevant for social behavior based on direct evidence. Figure adapted from a published review by (Rigney et al., 2023a).

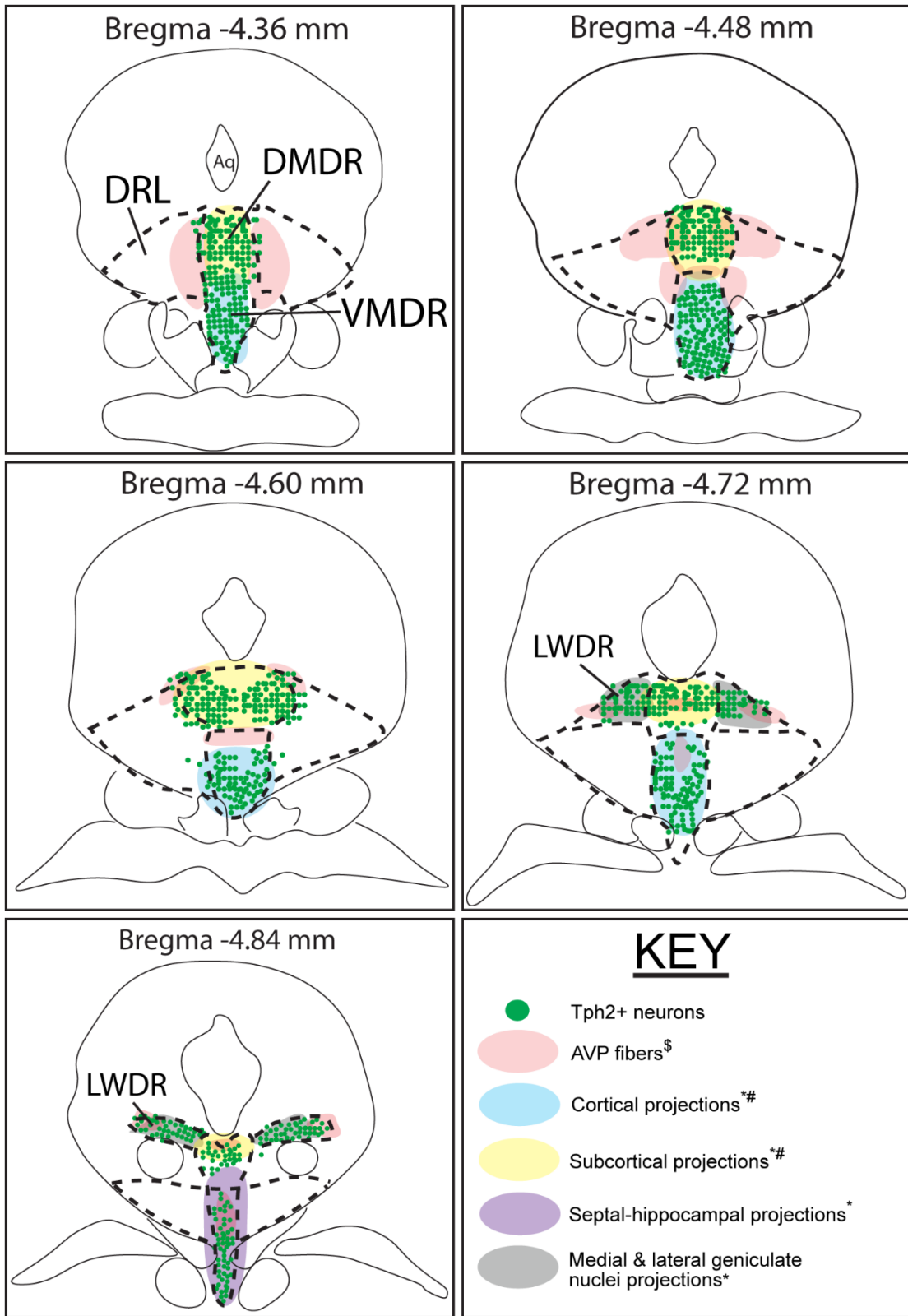


Figure A1. 5 DR consists of serotonin neurons topographically organized within subfields. The schematic displays coronal sections of the mouse DR, with rostral-caudal levels ranging from -4.36 to -4.84 mm. Anatomical boundaries of the DR (as indicated by dashed black lines) were drawn according to those in the mouse atlas published by (Franklin & Paxinos, 2008). Serotonin neurons are displayed as green circles and colored objects represent Avp fiber distribution and serotonin efferent projections (as denoted in the “KEY” panel). Figure created using data from several studies denoted by the following symbols in the Key panel: * (Muzerelle et al., 2016); # (Ren et al., 2018); \$ (Rood & De Vries, 2011; Rood et al., 2013). Aq = cerebral aqueduct; DRL = lateral dorsal raphe; DMDR = dorsomedial dorsal raphe; VMDR = ventromedial dorsal raphe; LWDR = lateral wings dorsal raphe.

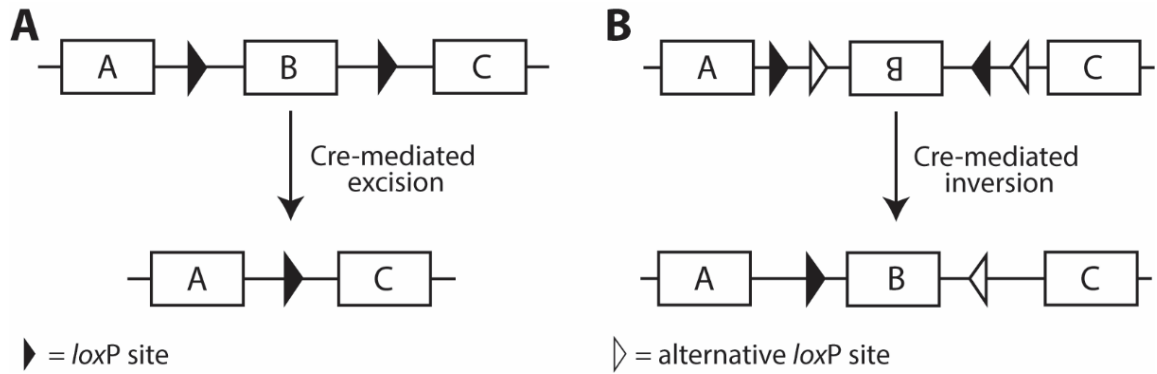


Figure A2. 1 Schematic of recombination reactions mediated by Cre recombinase. **A.** Target sites (loxP) oriented directly (i.e., in the same direction) produces an excision of “B”, intervening genetic region. **B.** In contrast, target sites (loxP and alternative loxP) oriented inversely (i.e., in the opposing direction) causes an inversion of intervening region.

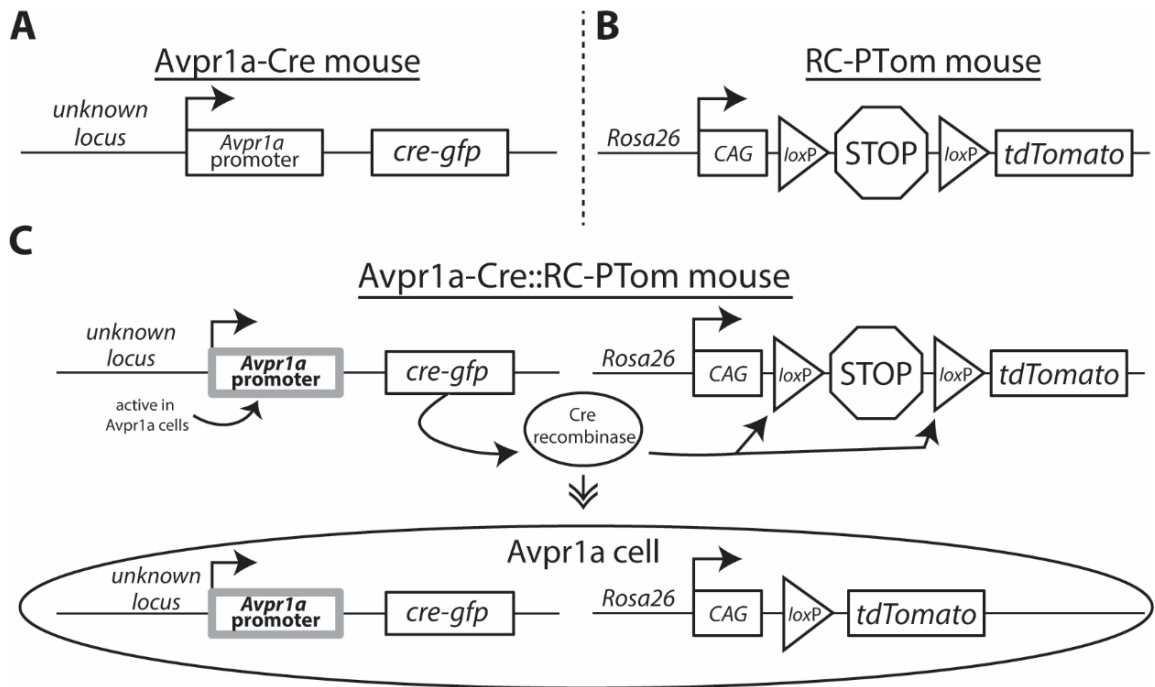


Figure A2. 2 Schematic of transgenic mouse lines used throughout this manuscript. **A.** Avpr1a-Cre mouse contains an allele with cre-gfp driven by the Avpr1a promoter upstream. **B.** RC-PTom mouse contains a construct consisting of CAG promoter followed by a “STOP” cassette flanked by loxP sites followed by tdTomato red fluorescent protein gene in the rosa26 locus. **C.** In progenies of Avpr1a-Cre and RC-PTom mating pair with both transgenes, Cre recombinase mediates excision of the STOP cassette from the RC-PTom allele within cells with active Avpr1a promoter.

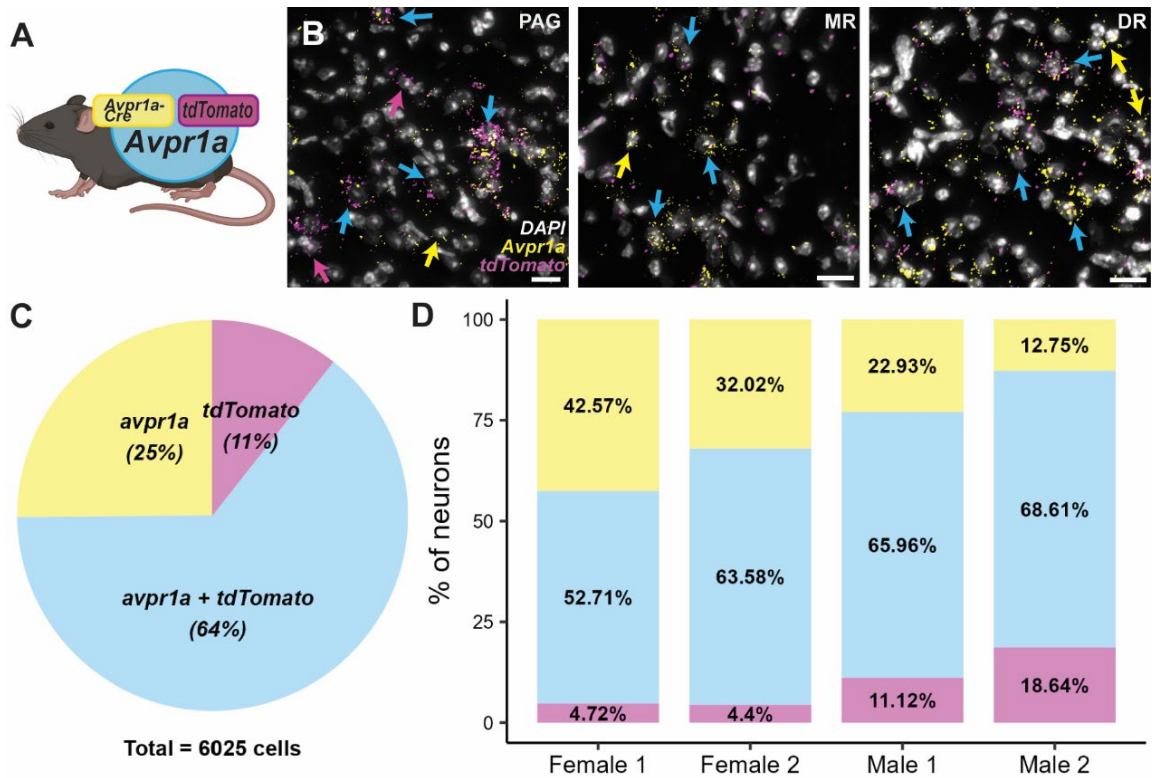


Figure A2. 3 In situ hybridization indirectly shows Cre recombinase expression is specific to *Avpr1a* expressing cells in *Avpr1a-Cre::RC-PTom* mice. **A.** Illustration of *Avpr1a-Cre::RC-PTom* mouse model. **B.** ISH representative images from PAG (left), MR (middle), and DR (right) show that majority of *Avpr1a* (yellow) and TdTomato (magenta) puncta are co-localized (light blue arrows). Some single labeled *Avpr1a* (yellow arrows) and TdTomato (magenta arrows) puncta are also observed. **C.** Pie chart shows percentages of cells with *Avpr1a* (yellow), TdTomato (magenta), or co-localized (light blue) puncta. **D.** Stacked bar chart displays data from C separated by each animal in the experiment. PAG = Periaqueductal gray. MR = Median Raphe. DR = Dorsal raphe.

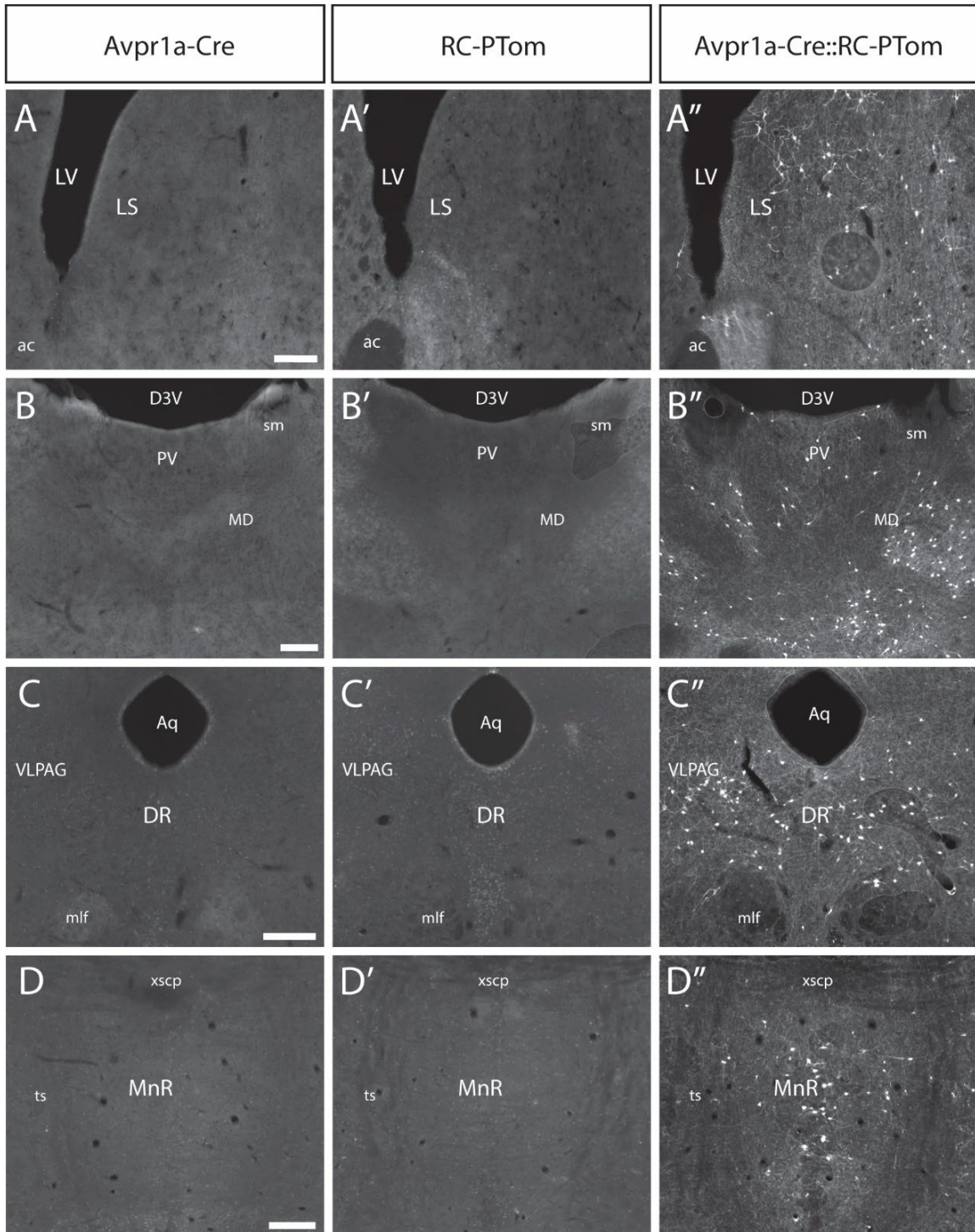


Figure A2. 4 TdTomato protein expression is driven by Cre-recombinase function within putative Avpr1a neurons. Paired images show anatomically matched brain sections from Avpr1a-Cre (**A**, **B**, **C**, **D**), RC-PTom (**A'**, **B'**, **C'**, **D'**), and Avpr1a-Cre::RC-PTom (**A''**, **B''**, **C''**, **D''**) mice. Scale bars = 200 μ M. Several regions that receive BNST vasopressin innervation are displayed: the LS (**A**, **A'**, **A''**; bregma = 0.74), thalamus (**B**, **B'**, **B''**; bregma = -0.6), DR (**C**, **C'**, **C''**; bregma = -4.48), and MR (**D**, **D'**, **D''**; bregma = -4.48). LV = lateral ventricle. ac = anterior commissure. LS = lateral septum. D3V = dorsal 3rd ventricle. MD = mediodorsal thalamus. sm = stria medullaris. PV = paraventricular thalamus. Aq = cerebral aqueduct. mlf = medial longitudinal fasciculus. DR = dorsal raphe. VLPAG = ventrolateral periaqueductal gray. xscp = decussation of superior cerebellar peduncle. ts = tectospinal tract. MnR = Median Raphe.

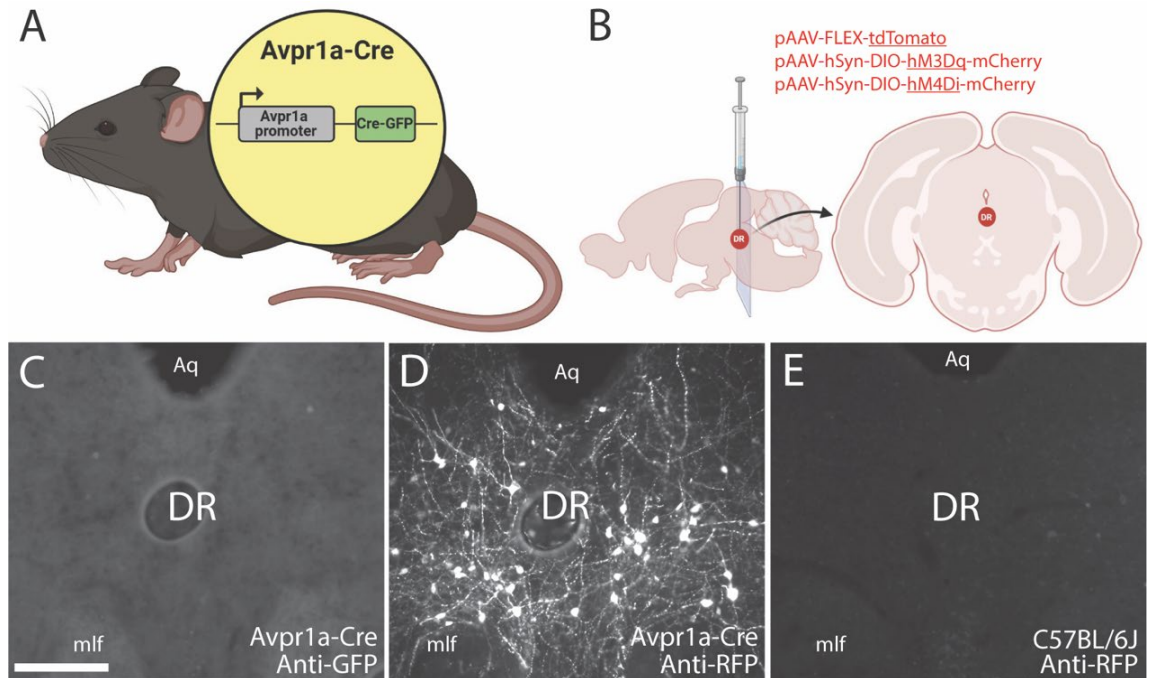


Figure A2.5 Expression of viral vectors with Cre-dependent constructs in adult Avpr1a-Cre but not C57BL/6J mice. **A.** Illustration of Avpr1a-Cre mouse in which Cre-GFP expression is driven by an Avpr1a promoter. **B.** Representation of stereotaxic injection of three viral vectors containing Cre-dependent constructs into the mouse dorsal raphe. Immunohistochemistry shows RFP positive cells (**D**) but no GFP positive cells (**C**) in Avpr1a-Cre mice. **E.** displays absence of RFP positive cells in dorsal raphe of wildtype mice. Scale bar = 200 μ M. DR = dorsal raphe. Aq = Aqueduct. mlf = medial longitudinal fasciculus. Graphics in (**A**) and (**B**) made with BioRender.com.

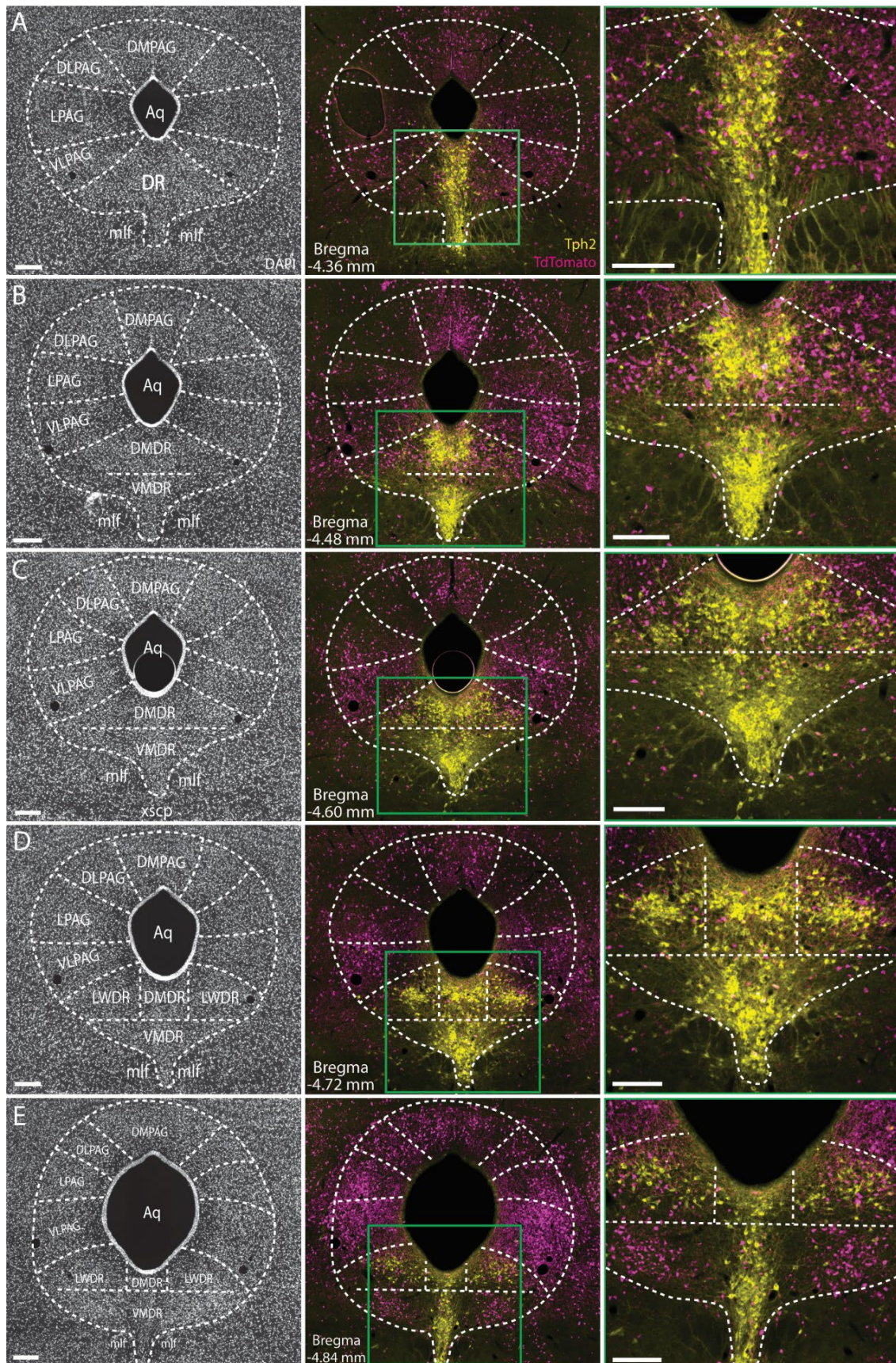


Figure A2. 6 Immunohistochemistry of DR sections from Avpr1a-Cre::RC-PTom mouse shows organization of putative Avpr1a (TdTomato) and Serotonin (Tph2) neurons throughout the rostro-caudal extent of the DR. **A-E.** display dorsal raphe sections from rostral DR (AP from bregma = -4.36 mm) to caudal DR (AP from bregma = -4.84 mm). Nuclei (DAPI) are visualized in the first (**left**) column and used to annotate anatomical regions adapted from (Franklin & Paxinos, 2008). Second (**middle**) column displays combination of regional outlines and immunostaining. The green rectangle in the second column represents the DR region magnified and viewed in the third (**right**) column. Scale bars = 200 μ m. DMPAG = dorsomedial periaqueductal gray. DLPAG = dorsolateral periaqueductal gray. LPAG = lateral periaqueductal gray. VLPAG = ventrolateral periaqueductal gray. DR = dorsal raphe. DMDR = dorsomedial dorsal raphe. VMDR = ventromedial dorsal raphe. LWDR = lateral wings dorsal raphe. Aq = aqueduct. mlf = medial longitudinal fasciculus. xscp = decussation of superior cerebral peduncle.

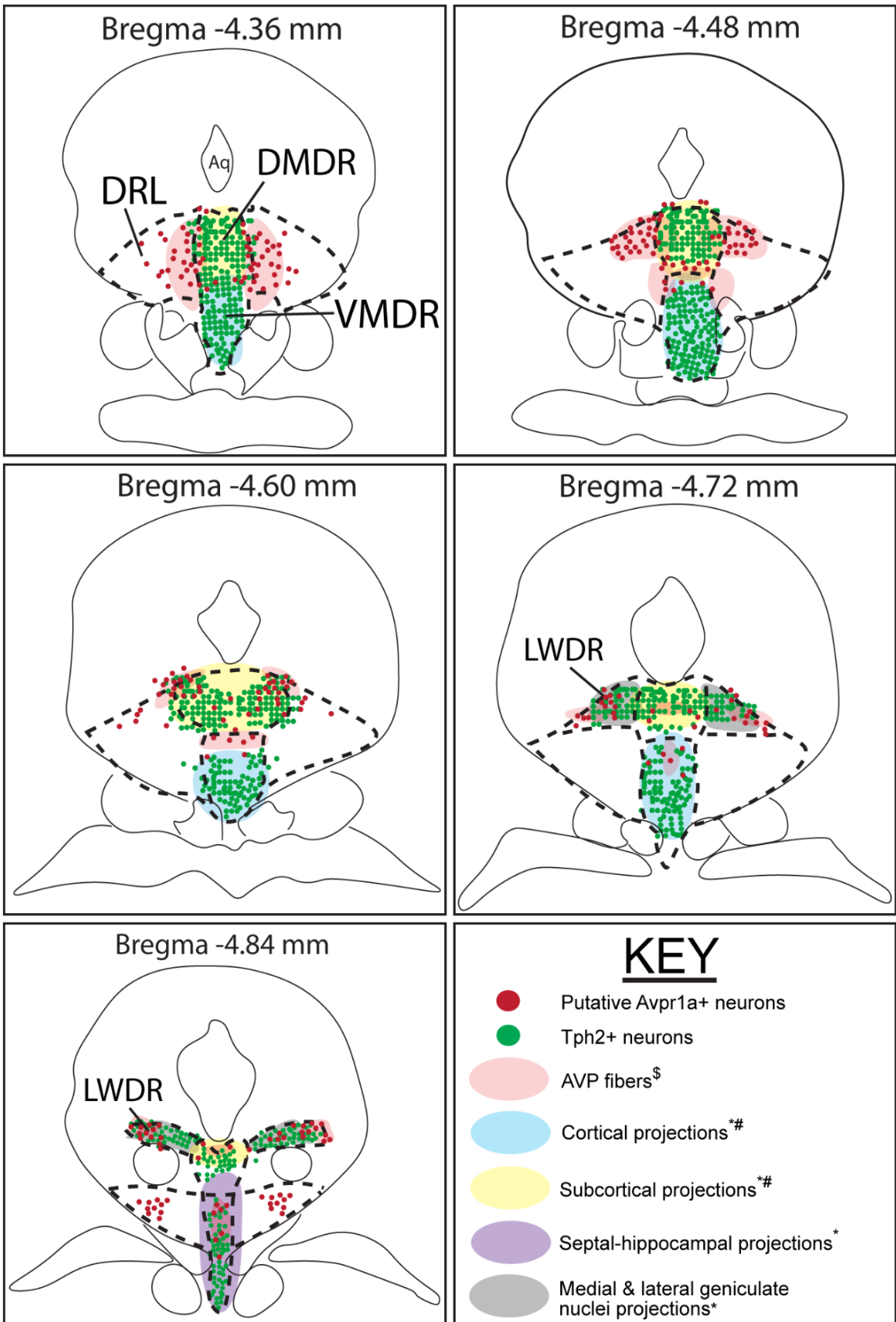


Figure A2. 7 Organization of serotonin and Avpr1a neurons within the DR. The schematic displays coronal sections of the mouse DR, with rostral-caudal levels ranging from -4.36 to -4.84 mm. Anatomical boundaries of the DR (as indicated by dashed black lines) were drawn according to those in the mouse atlas published by (Franklin & Paxinos, 2008). Serotonin neurons are displayed as green circles, putative Avpr1a neurons are displayed as red circles, and colored objects represent Avp-ir fiber distribution and neuronal projection sites (as denoted in the “KEY” panel). Figure created using data from several studies denoted by the following symbols in the Key panel: * (Muzerelle et al., 2016); # (Ren et al., 2018); \$ (Rood & De Vries, 2011; Rood et al., 2013). Aq = cerebral aqueduct; DRL = lateral dorsal raphe; DMDR = dorsomedial dorsal raphe; VMDR = ventromedial dorsal raphe; LWDR = lateral wings dorsal raphe.

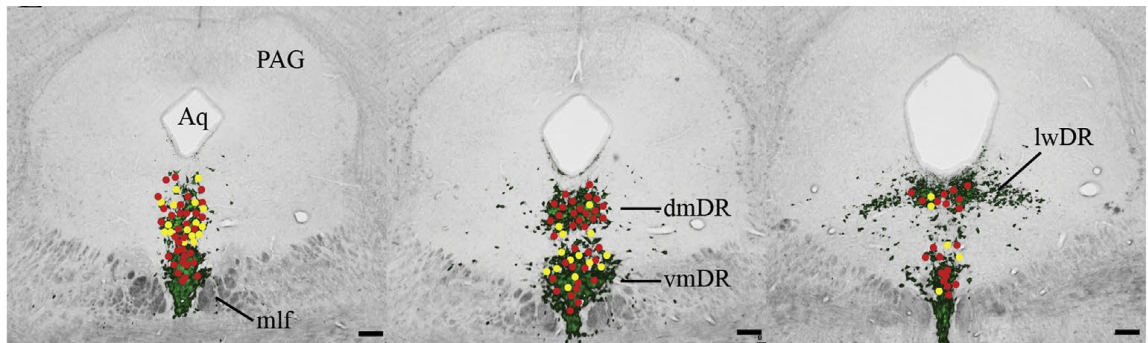


Figure A2. 8 Serotonin neurons display excitatory post synaptic currents (PSC) in response to bath application of AVP in the DR. Recordings were made from 122 serotonin neurons spread across the rostral to caudal extent of the ventromedial (vm) and dorsomedial (dm) subfields of the DR. Most AVP-responsive neurons were located rostrally in the dmDR and upper part of the vmDR. The relative locations of recorded cells are shown with yellow dots indicating neurons that had an increase in PSC frequency >1 Hz following AVP administration and red dots indicating a response less than 1 Hz or a decrease in PSC frequency. Scale bars in the bottom right corner of all images are equal to 100 μm . Aq=cerebral aqueduct; lwDR=later wings of the DR; mlf=medial longitudinal fasciculus; PAG=periaqueductal gray. Figure adapted from (Rood & Beck, 2014).

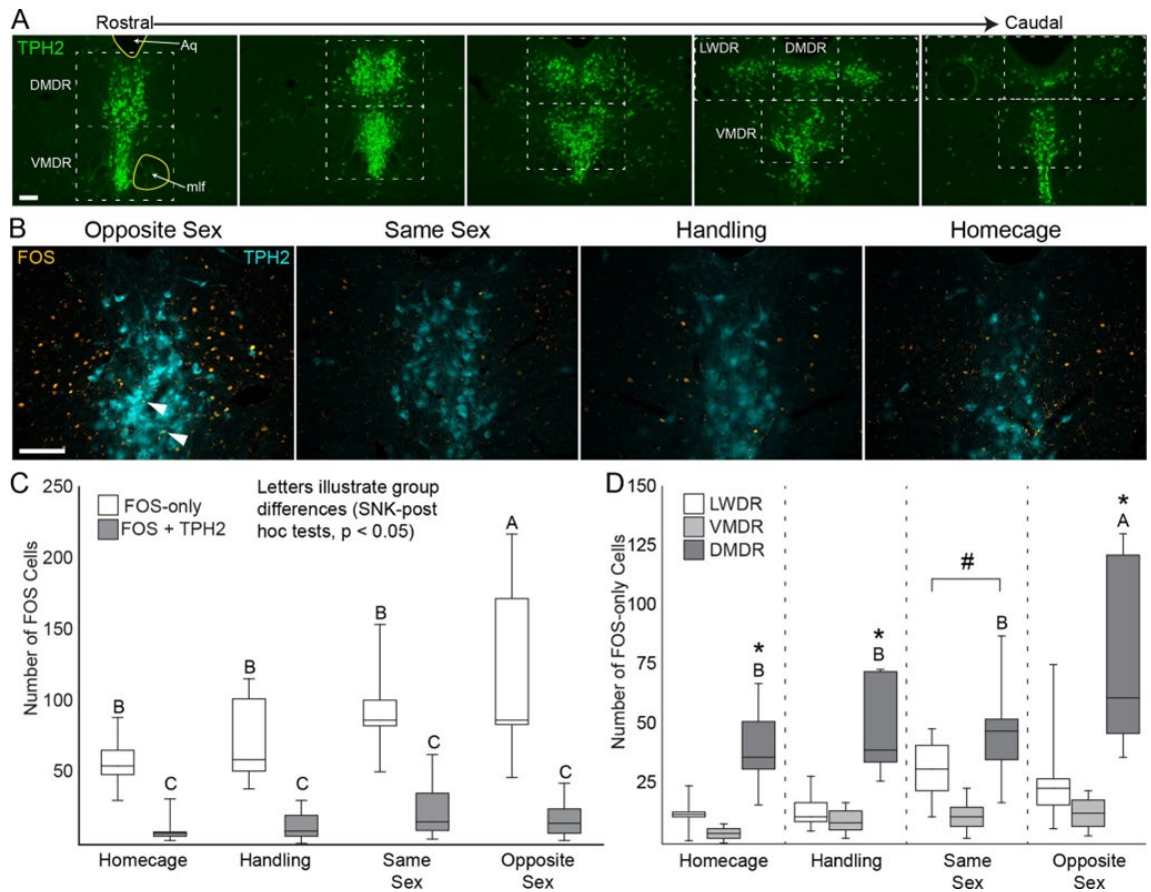


Figure A3. *1* Fos expression increases in dorsal raphe of male mice exposed to a female mouse. **A.** Representative images illustrate the rostral to caudal sections of the dorsal raphe chosen for analysis and the approximate region analyzed (dotted squares). Aq = cerebral aqueduct, DMDR = dorsomedial part of dorsal raphe, LWDR = lateral wings of DR, mlf = medial longitudinal fasciculus, VMDR = ventromedial part of DR. **B.** Representative images of the rostral dorsomedial region illustrate Fos cells (orange) surrounding serotonin neurons (blue, stained for Tph2) in the brain of a male subject exposed to a female (Opposite Sex), a male (Same Sex), an empty cage (Handling), or no stimulus (Homecage). **C.** Total Fos cell counts collapsed across the raphe for serotonin and non-serotonin neurons. Letters indicate results of SNK post-hoc tests ($p < 0.05$). **D.** Analysis of Fos-only cells by region. Letters indicate significant Treatment differences for the DMDR; there were no Treatment differences in VMDR or LWDR. (*) For Homecage, Handling, and Opposite Sex groups, DMDR had more Fos cells than VMDR or LWDR. (#) For Same Sex group, DMDR and LWDR were significantly different from VMDR, but not each other. All box plots include the median (line), 25–75 quartiles (box), and 5–95 percentiles (whisker). Adapted from (Patel et al., 2022).

Table A3. 1*Analysis of Non-Social Behaviors. Adapted From (Patel et al., 2022)*

Behavior	TREATMENT			Statistics	
Digging	Opposite Sex	Same Sex	Handling	SEX	$F(1,24) = 2.1$, $p = 0.16$
	Male	3.4 ± 2.1	4.7 ± 3.1	TREATMENT	$F(2,24) = 0.42$, $p = 0.65$
	Female	12 ± 8.3	20.4 ± 15.2	SEX × TREATMENT	$F(2,24) = 0.38$, $p = 0.69$
Exploring	Opposite Sex	Same Sex	Handling	SEX	$F(1,24) = 0.01$, $p = 0.92$
	Male	567.6 ± 45.1	519.6 ± 49	TREATMENT	$F(2,24) = 0.42$, $p = 0.66$
	Female	566.9 ± 51.2	506.9 ± 97.9	SEX × TREATMENT	$F(2,24) = 0.01$, $p = 0.99$
Grooming	Opposite Sex	Same Sex	Handling	SEX	$F(1,24) = 0.25$, $p = 0.62$
	Male	69.8 ± 30.6	291.1 ± 66.6	TREATMENT	$F(2,24) = 11.07$, $p < 0.001$
	Female	111.1 ± 28	327.1 ± 87.5	SEX × TREATMENT	$F(2,24) = 0.14$, $p = 0.87$
Rearing	Opposite Sex	Same Sex	Handling	SEX	$F(1,24) = 1.09$, $p = 0.31$
	Male	122 ± 42	149.4 ± 49.9	TREATMENT	$F(2,24) = 0.37$, $p = 0.69$
	Female	174.5 ± 56.6	225 ± 65	SEX × TREATMENT	$F(2,24) = 0.36$, $p = 0.7$

Mean (in seconds) ± standard errors are shown for male and female subjects ($n = 5$ per group) in Opposite Sex, Same Sex, and Handling groups for non-social behaviors including digging, exploring, grooming, and rearing. Results of 2-factor ANOVA (SEX × TREATMENT) are shown for each behavior in right hand column. Total test period was 20 min. or 1200 s.

Table A3. 2*Analysis of Social Behaviors. Adapted From (Patel et al., 2022)*

Behavior	TREATMENT		Statistics	
Allo-grooming	Opposite Sex	Same Sex	SEX	$F(1,16) = 0.61$, $p = 0.45$
	Male	20.9 ± 9.3	TREATMENT	$F(1,16) = 1.09$, $p = 0.31$
	Female	109.5 ± 93.9	SEX × TREATMENT	$F(1,16) = 1.16$, $p = 0.3$
Investigating	Opposite Sex	Same Sex	SEX	$F(1,16) = 0.03$, $p = 0.86$
	Male	134.7 ± 36.5	TREATMENT	$F(1,16) = 0.08$, $p = 0.79$
	Female	105.1 ± 13.3	SEX × TREATMENT	$F(1,16) = 0.69$, $p = 0.42$
Chasing	Opposite Sex	Same Sex	SEX	$F(1,16) = 1.66$, $p = 0.21$
	Male	135.5 ± 45.2	TREATMENT	$F(1,16) = 0.61$, $p = 0.45$
	Female	74.8 ± 20.2	SEX × TREATMENT	$F(1,16) = 0.45$, $p = 0.51$
Fighting	Opposite Sex	Same Sex	SEX	$F(1,16) = 0.98$, $p = 0.34$
	Male	27.3 ± 22.2	TREATMENT	$F(1,16) = 1.3$, $p = 0.27$
	Female	2.3 ± 2	SEX × TREATMENT	$F(1,16) = 1.5$, $p = 0.24$
Mounting	Opposite Sex	Same Sex		
	Male	0 ± 0		
	Female	0 ± 0		

Mean (in seconds) ± standard errors are shown for male and female subjects ($n = 5$ per group) in Opposite Sex and Same Sex groups for social behaviors including allo-grooming, investigating, chasing, fighting, and mounting. Results of 2-factor ANOVA (SEX × TREATMENT) are shown for each behavior except mounting in right hand column. Total test period was 20 min. or 1200 s.

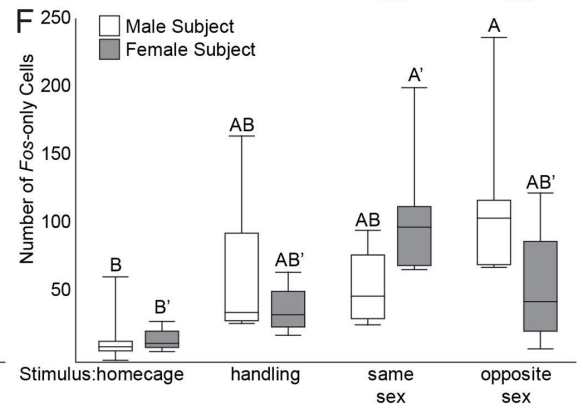
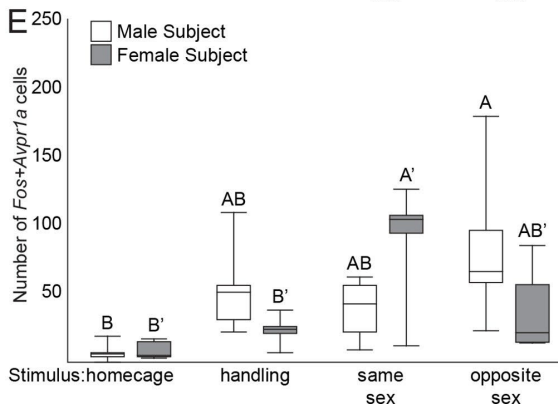
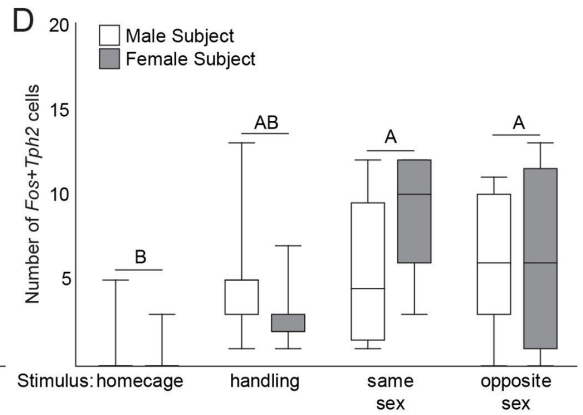
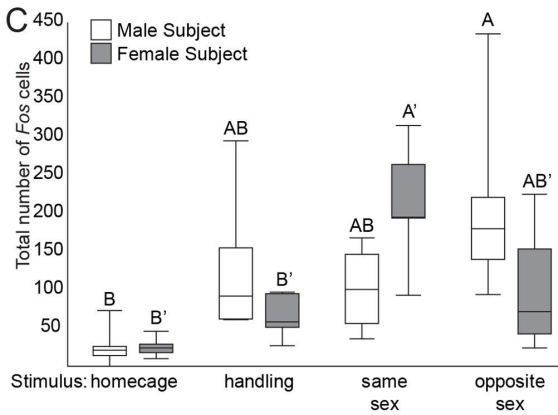
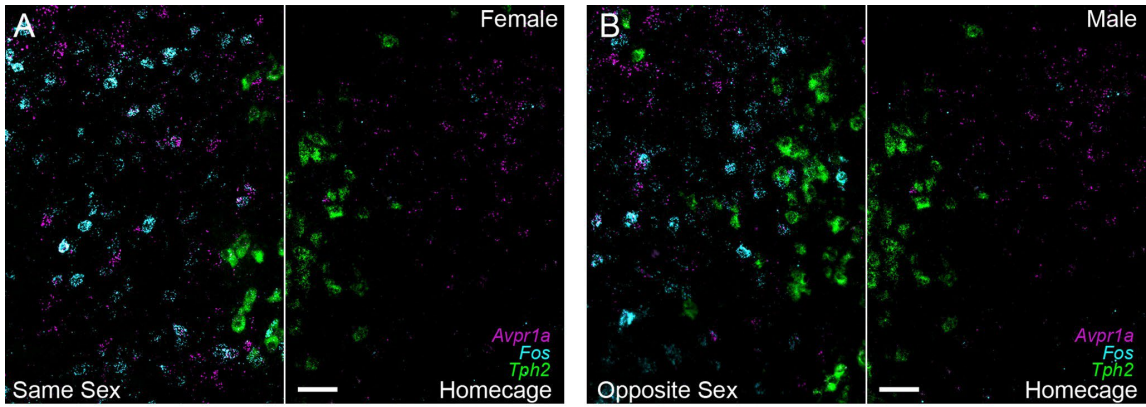


Figure A3. 2 Interaction with a female increases fos expression in both male and female subjects. **A.** Representative photomicrograph from a female subject exposed to a female stimulus (left) or no stimulus (right) and **B.** a male subject exposed to a female stimulus (left) or no stimulus (right); Tph2 (green), Avpr1a (magenta), and Fos (cyan). Scale bar = 50 μm . **C.** Total number of Fos-expressing cells in male and female subjects in Same and Opposite Sex social stimulus groups and Handling and Homecage control groups. **D- F.** show the number of Fos expressing cells for different cell phenotypes including Fos + Tph2 (**D**), Fos + Avpr1a (**E**), and Fos-only (**F**; did not have Tph2 or Avpr1a puncta). For analyses (**C**, **E**, and **F**), there were significant interactions between SEX and TREATMENT and letters indicate significant differences between TREATMENT groups separately for male and female (‘) subjects based on SNK post-hoc tests ($p < 0.05$). For the analysis in (**D**), there was only a significant effect of TREATMENT; thus, letters indicate TREATMENT differences collapsed across SEX based on SNK post-hoc tests ($p < 0.05$). All box plots include the median (line), 25–75 quartiles (box), and 5–95 percentiles (whisker). Adapted from (Patel et al., 2022).

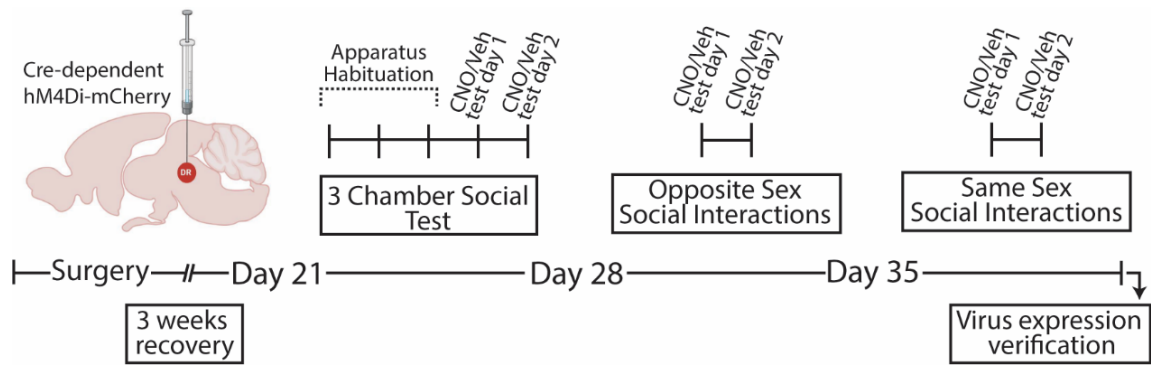


Figure A4. 1 Schematic of experimental timeline for chapter 4.

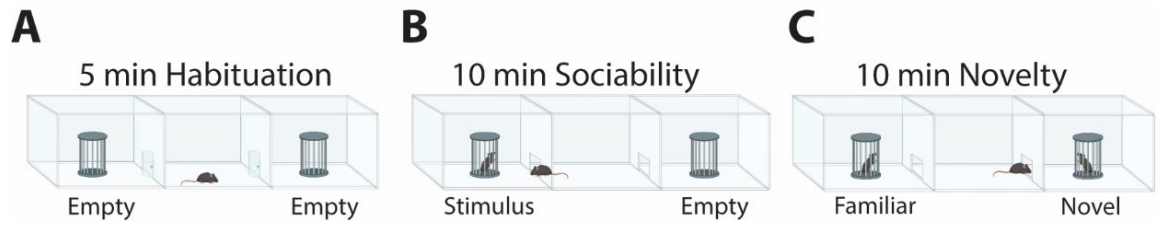


Figure A4. 2 Schematic of the three-chamber social test. **A.** 5 min Habituation stage **B.** 10 min Sociability stage. **C.** 10 min Novelty stage. *Made with Biorender.com*

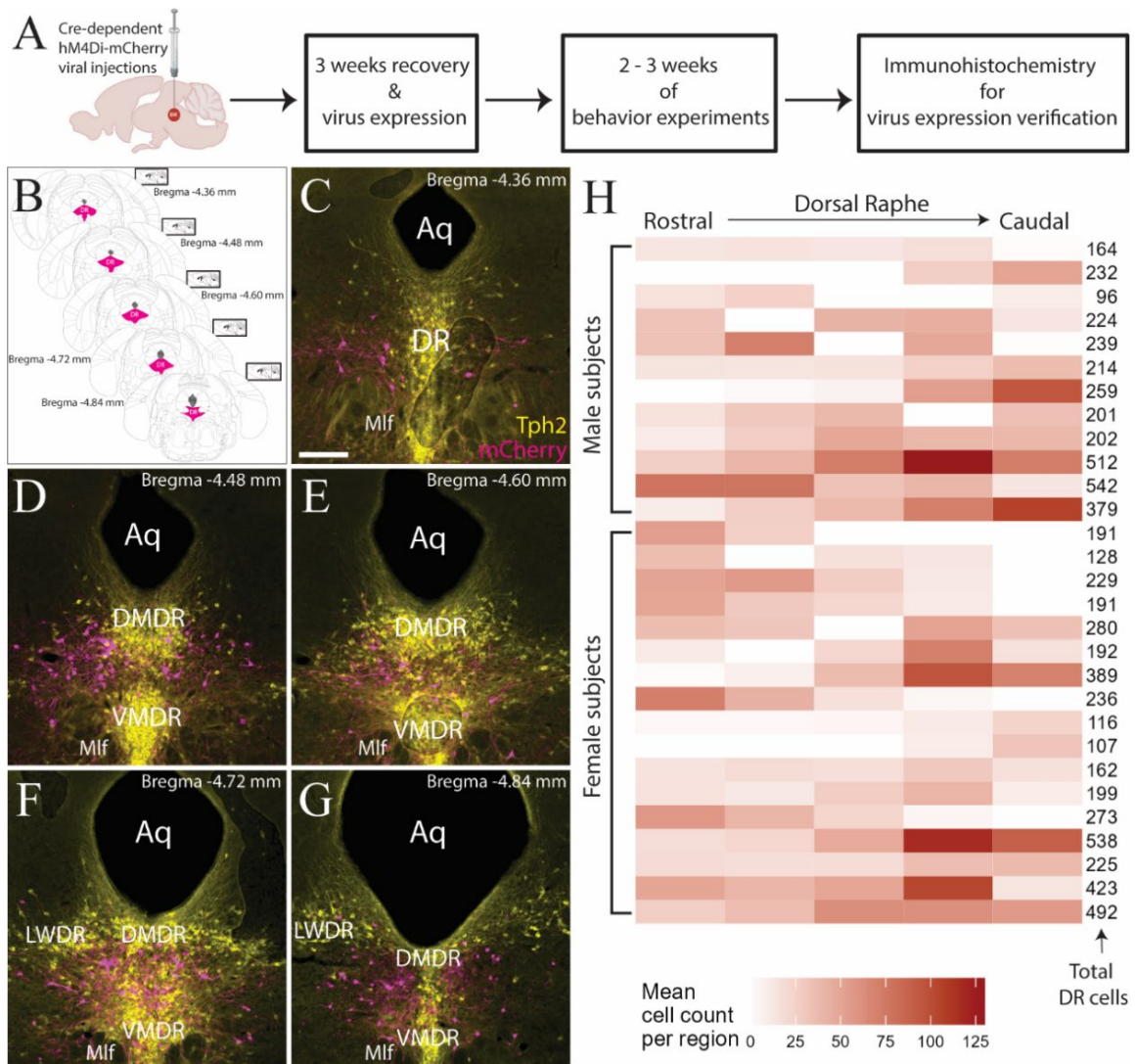


Figure A4. 3 Immunohistochemistry shows expression of red fluorescent protein as a marker to verify Cre-dependent hM4Di viral injection accuracy and spread in the DR of *Avpr1a-Cre* mice. **A.** Schematic displays a general timeline of this chapter's experiments, starting with viral injections to behavior experiments to virus expression verification. **B.** Rostral to caudal (from Bregma -4.36 to -4.84 mm) atlas sections of the DR expected to contain the virus expression (magenta fill). **C-G.** display representative images from immunohistochemistry used to detect mCherry (magenta) and Tph2 (yellow; Serotonin marker) from sections along the rostro-caudal extent of the DR. Scale bar = 200 μ M. **H.** Heatmap characterizes virus expression (mean mCherry-positive cell count) through rostro-caudal regions of DR in animals (each row; 12 males, 17 females) with successful DR injections. Aq = cerebral aqueduct. DR = dorsal raphe. DMDR = dorsomedial dorsal raphe. VM DR = ventromedial dorsal raphe. LWDR = lateral wing DR. Mlf = medial longitudinal fasciculus.

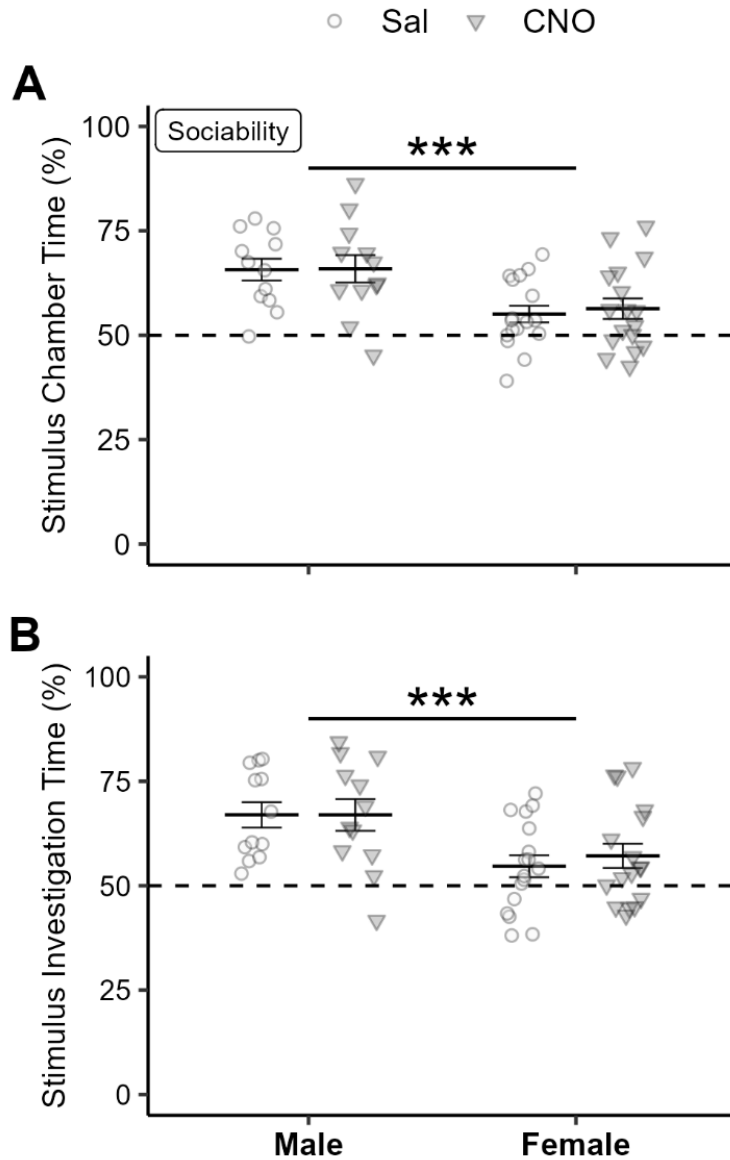


Figure A4.4 Male mice, compared to female mice, show greater sociability for a female stimulus in the three-chamber social test. Baseline sex differences in time spent in the chamber with a female stimulus (A) and time spent directly investigating the stimulus (B) were observed. Drug treatment (Sal or CNO) had no observable effect. Dashed lines represent 50% mark, above which is considered preference toward sociability. Data shown as mean \pm SEM. *** $p \leq 0.001$, main effect of sex.

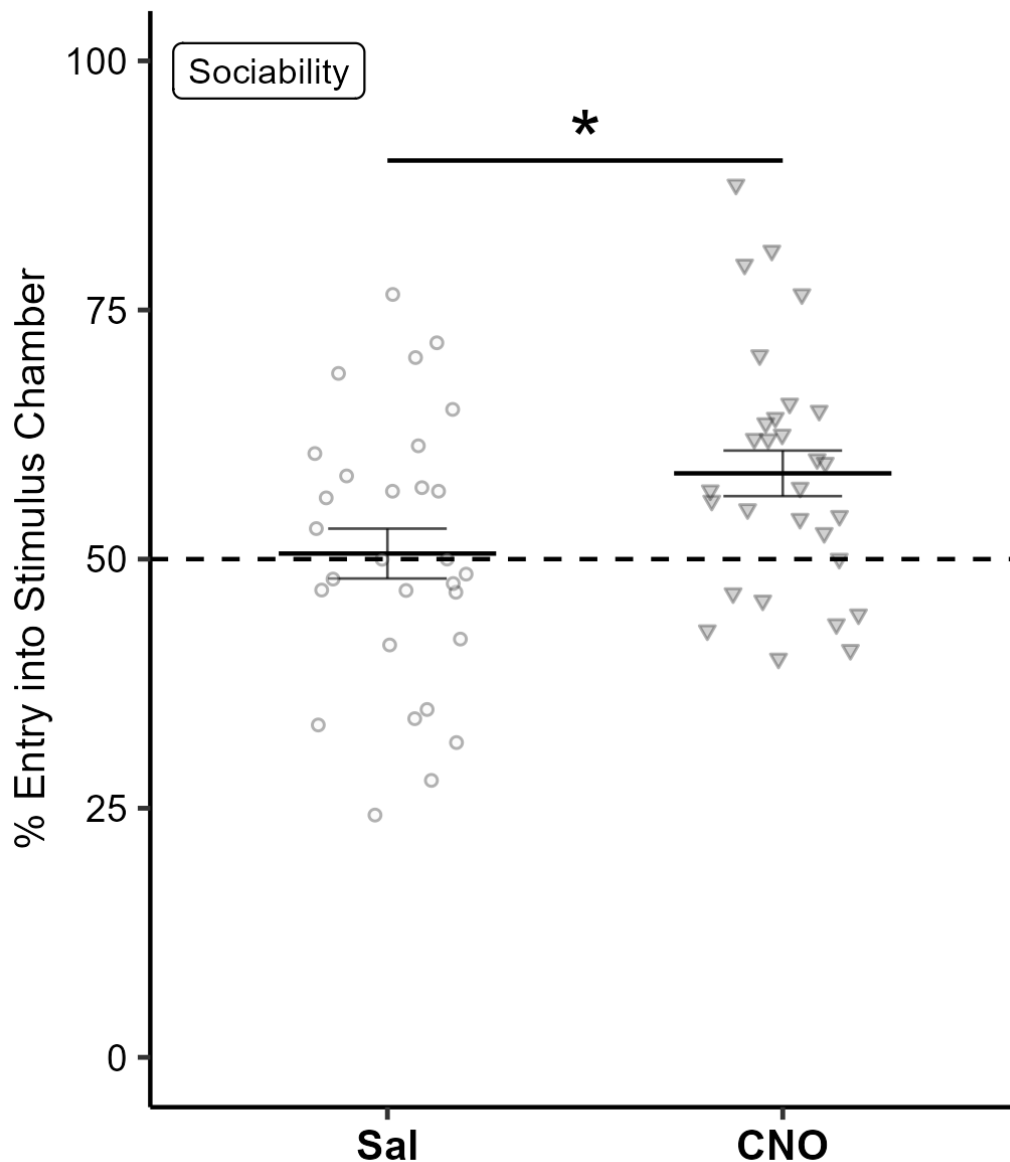


Figure A4. 5 CNO treatment in Avpr1a-Cre mice with chemogenetic inhibition of the DR Avpr1a neurons increases the percentage of entries into the stimulus chamber (vs. the empty chamber) in the three-chamber social test. **A.** depicts the effect of CNO treatment on percentage of entry into the stimulus chamber irrespective of sex. * $p \leq 0.05$, main effect of Drug. Dashed line represents 50% mark, above which is considered preference toward sociability. CNO treatment divergently impacts the number of entries into the stimulus (**B**) and empty chamber (**C**). Data shown as mean \pm SEM.

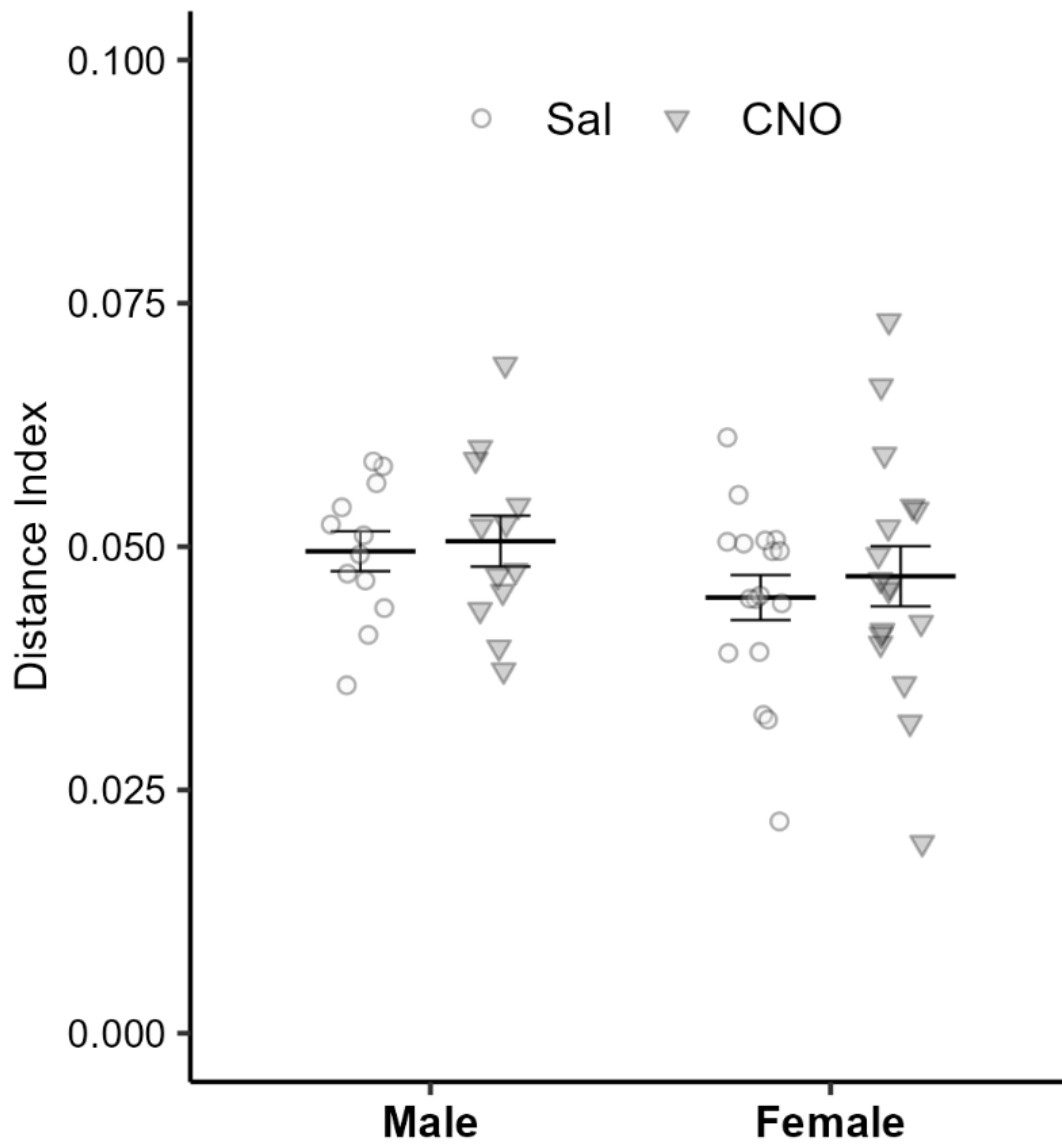


Figure A4. 6 Distance traveled does not differ due to chemogenetic inhibition of the DR Avpr1a neurons. Distance index (distance traveled / duration of test) calculated to normalize for variation in duration of test between a few subjects. Two way ANOVA (between-subject factor: Sex; within-subject factor: Drug) revealed no main effects or interaction.

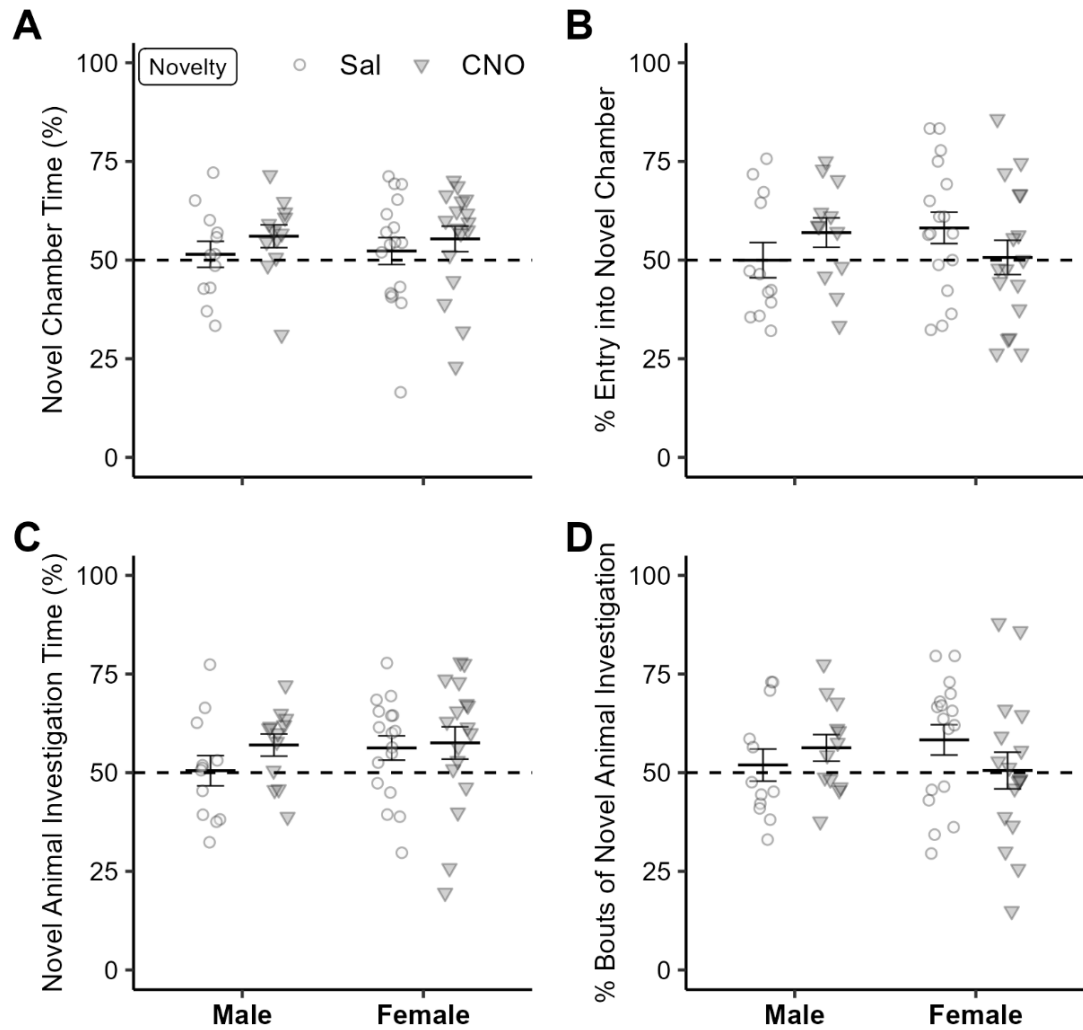


Figure A4.7 Novelty preference does not alter in response to CNO treatment or sex in *Avpr1a-Cre* mice with chemogenetic inhibition of the DR *Avpr1a* neurons. Percentage of time spent in the novel chamber (**A**), entries into the novel chamber (**B**), time spent investigating the novel animal (**C**), and bouts of investigating the novel animal (**D**) in response to CNO or Saline treatment by male and female mice are displayed. Two-way ANOVA with Sex as between-subjects and Drug as within-subjects factors revealed no significant main effects or interactions. Data shown as mean \pm SEM. Dashed lines represent 50% mark, above which is considered preference toward novelty.

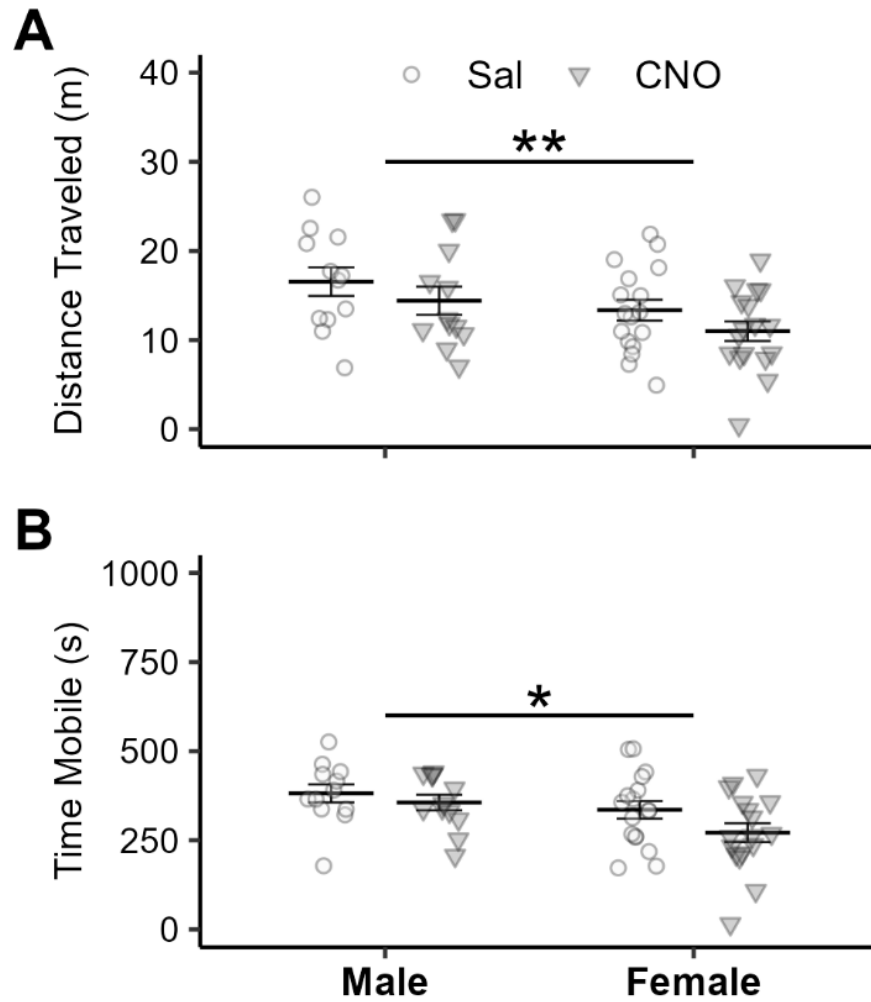


Figure A4.8 Male mice display a higher level of locomotor activity than female mice in a social interaction apparatus. General locomotion assessed by measuring distance traveled (**A**) and total mobility time (**B**). ** $p \leq 0.01$ and * $p \leq 0.05$ denote significant main effect of sex. Data shown as mean \pm SEM.

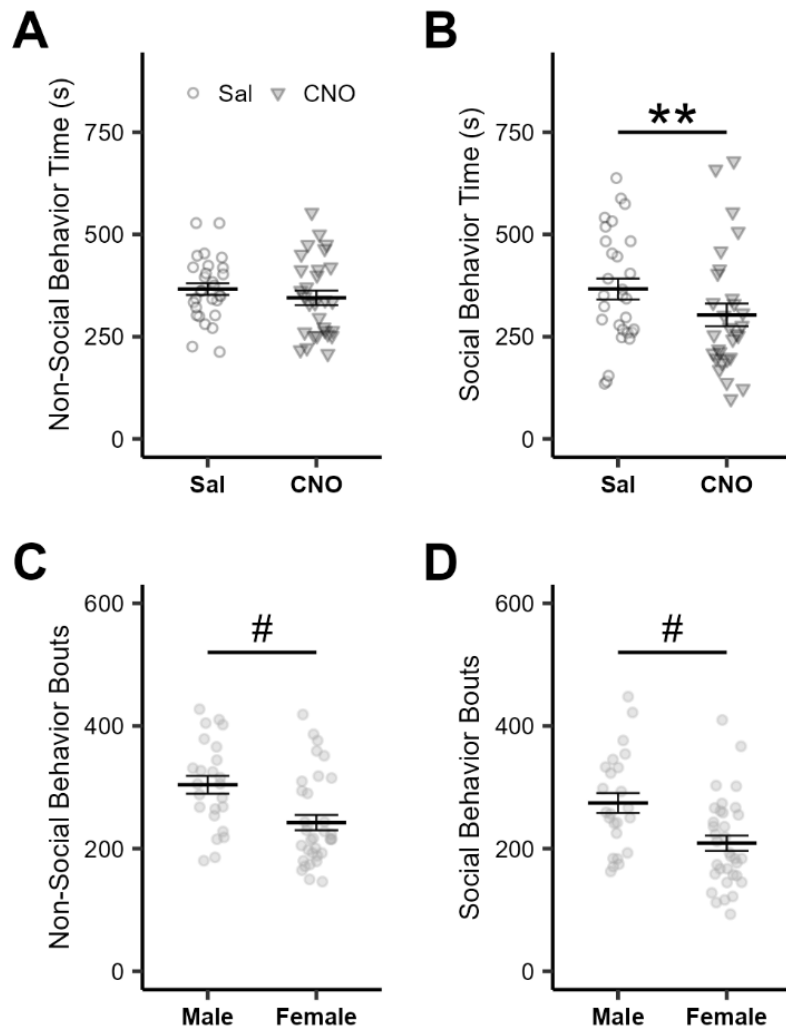


Figure A4.9 Chemogenetic silencing of DR Avpr1a neurons reduces social behavior in both males and females while interacting with a female stimulus. Non-social behavior time (**A**) and social behavior time (**B**) are displayed in response to treatment. Non-social (**C**) and social (**D**) behavior bouts are shown by sex. Two-way ANOVA with Sex (between) and Drug (within) factors was performed. ** $p \leq 0.01$, significant main effect of Drug. # $p \leq 0.05$, significant main effect of Sex. Data shown as mean \pm SEM.

Table A4. 1*Analysis of Social Behaviors During an Interaction with a Female Stimulus*

Social Behavior	Saline	CNO	Statistics		
			Sex	Drug	Sex x Drug
Female	387.1 ± 34.8	336.1 ± 43.9	$F_{1,27} = 1.721,$ $p = 0.201$	$F_{1,27} = 8.971,$ $p = 0.006$	$F_{1,27} = 0.460,$ $p = 0.503$
Male	337.7 ± 37.5	256.9 ± 21.1			
Head to Head Sniffing					
Female	104 ± 11.8	103.1 ± 15.9	$F_{1,27} = 0.231,$ $p = 0.634$	$F_{1,27} = 0.017,$ $p = 0.897$	$F_{1,27} = 0.0002,$ $p = 0.988$
Male	95.7 ± 12.1	94.5 ± 10.7			
Head to Rear Sniffing					
Female	84.3 ± 10.4	70 ± 11.2	$F_{1,27} = 7.715,$ $p = 0.010$	$F_{1,27} = 8.636,$ $p = 0.007$	$F_{1,27} = 0.566,$ $p = 0.458$
Male	125.8 ± 7.3	101.6 ± 9.5			
Following					
Female	13 ± 4.1	11.3 ± 3.2	$F_{1,27} = 27.554,$ $p = 1.56 \times 10^{-5}$	$F_{1,27} = 5.969,$ $p = 0.021$	$F_{1,27} = 4.469,$ $p = 0.044$
Male	58.2 ± 10.2	34.7 ± 6.2			
Allogrooming					
Female	18.8 ± 6.8	26.2 ± 13.3	$F_{1,27} = 0.353,$ $p = 0.557$	$F_{1,27} = 0.002,$ $p = 0.966$	$F_{1,27} = 0.753,$ $p = 0.393$
Male	19.9 ± 10.1	11.8 ± 5.6			
Huddling					
Female	135.3 ± 28	85.2 ± 20.1	$F_{1,27} = 10.130,$ $p = 0.004$	$F_{1,27} = 4.000,$ $p = 0.056$	$F_{1,27} = 0.315,$ $p = 0.579$
Male	35.9 ± 29.6	7.7 ± 2.1			
Mounting					
Female	0 ± 0	0 ± 0	$F_{1,27} = 15.563,$ $p = 0.0005$	$F_{1,27} = 0.016,$ $p = 0.899$	$F_{1,27} = 0.016,$ $p = 0.899$
Male	62.3 ± 17.9	59.7 ± 25.9			
Fighting					
Female	0.2 ± 0.1	0.2 ± 0.2	$F_{1,27} = 0.187,$ $p = 0.669$	$F_{1,27} = 1.022,$ $p = 0.321$	$F_{1,27} = 0.865,$ $p = 0.361$
Male	0.1 ± 0.1	0.5 ± 0.4			

Mean (in seconds) ± SEM are shown for Avpr1a-Cre male (n = 12) and female (n = 17) subjects injected with cre-dependent hM4Di virus and treated with CNO or Saline. Results of two-factor ANOVA (Sex (between) x Treatment (within)) are shown for each behavior in the right hand column. The total test period was 20 min or 1200 s.

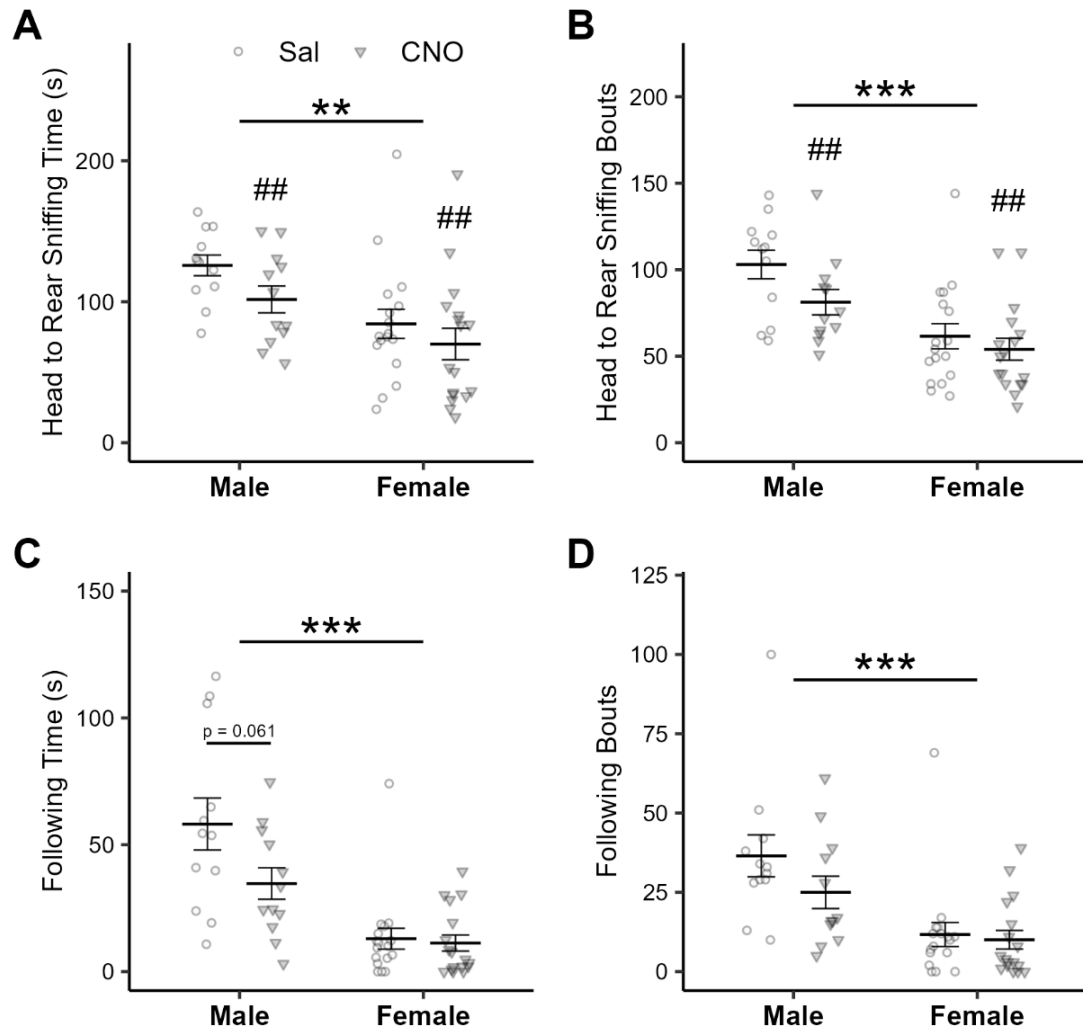


Figure A4.10 Chemogenetic inhibition of DR Avpr1a neurons decreases head to rear investigative and following behavior in males and females exposed to a female stimulus. Head to rear sniffing time (A) and bouts (B), and following behavior time (C) and bouts (D) in both male and female subjects by saline and CNO treatment groups. Results of 2-factor ANOVA shown. ** $p \leq 0.01$ and *** $p \leq 0.001$ denote significant main effect of sex. ## $p \leq 0.01$ mark significant main effect of Drug. Data shown as mean \pm SEM.

Table A4. 2*Analysis of Nonsocial Behaviors During an Interaction with a Female Stimulus*

	Saline	CNO	Statistics		
Non Social Behavior			Sex	Drug	Sex x Drug
Female	362.2 ± 21.2	319.5 ± 22.5	F _{1,27} = 2.006, p = 0.168	F _{1,27} = 0.702, p = 0.410	F _{1,27} = 1.701, p = 0.203
Male	372 ± 17.5	381.3 ± 26.6			
Grooming					
Female	176.1 ± 22.8	131.2 ± 14.3	F _{1,27} = 13.082, p = 0.001	F _{1,27} = 0.428, p = 0.519	F _{1,27} = 2.894, p = 0.100
Male	72 ± 13.2	92 ± 22.5			
Rearing					
Female	62.8 ± 8.3	71 ± 11.6	F _{1,27} = 9.470, p = 0.005	F _{1,27} = 0.002, p = 0.967	F _{1,27} = 1.125, p = 0.298
Male	116.6 ± 10.7	109 ± 16.2			
Exploring					
Female	123.3 ± 11.1	117.2 ± 10.9	F _{1,27} = 10.312, p = 0.003	F _{1,27} = 0.256, p = 0.617	F _{1,27} = 0.027, p = 0.871
Male	183.3 ± 18.6	180.3 ± 21.1			

Mean (in seconds) ± SEM are shown for Avpr1a-Cre male (n = 12) and female (n = 17) subjects injected with cre-dependent hM4Di virus and treated with CNO or Saline. Results of two-factor ANOVA (Sex (between) x Treatment (within)) are shown for each behavior in the right hand column. The total test period was 20 min or 1200 s.

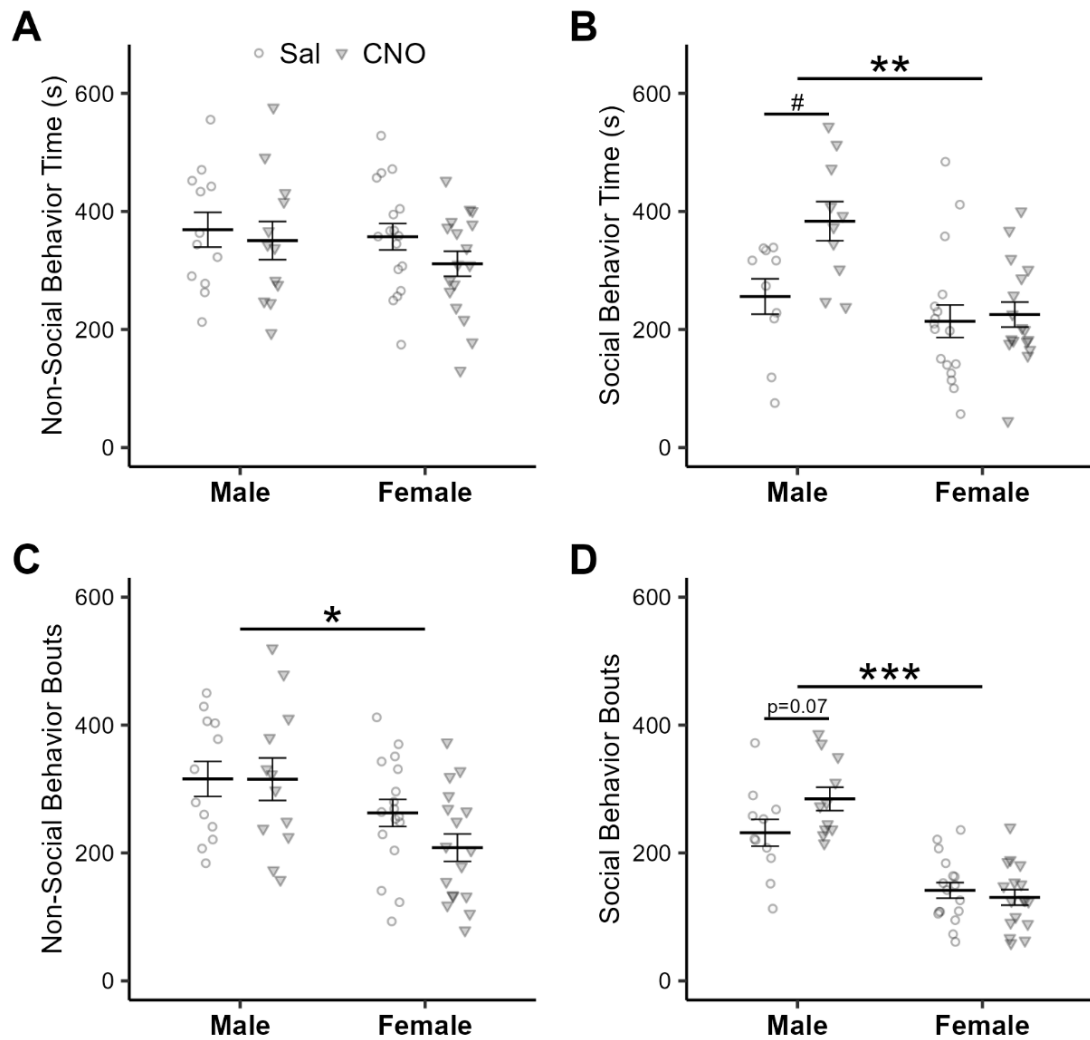


Figure A4. 11 Chemogenetic silencing of DR Avpr1a neurons increases social behavior in mice interacting with a male stimulus. Non-social behavior time (A) and social behavior time (B) are displayed in response to treatment for both male and female subjects. Non-social (C) and social (D) behavior bouts are shown. Two-way ANOVA with Sex (between) and Drug (within) factors was performed. * $p \leq 0.05$, ** $p \leq 0.01$, and *** $p \leq 0.001$, significant main effect of sex. # $p \leq 0.05$, post-hoc t-test (BH adjustment). Data shown as mean \pm SEM.

Table A4. 3*Analysis of Social Behaviors During an Interaction with a Male Stimulus*

	Saline	CNO	Statistics		
			Sex	Treatment	Sex x Treatment
Social Behavior					
Female	213.9 ± 27.5	225.2 ± 21.2	F _{1,25} = 11.404, p = 0.002	F _{1,25} = 6.539, p = 0.017	F _{1,25} = 4.588, p = 0.042
Male	255.9 ± 30.0	383.5 ± 33.2			
Head to Head Sniffing					
Female	72.9 ± 5.9	66.4 ± 7.2	F _{1,27} = 9.091, p = 0.006	F _{1,27} = 0.072, p = 0.790	F _{1,27} = 1.638, p = 0.212
Male	115.6 ± 19	125.6 ± 20			
Head to Rear Sniffing					
Female	45.2 ± 7.1	42.3 ± 6.4	F _{1,27} = 21.687, p = 7.66x10 ⁻⁰⁵	F _{1,27} = 0.280, p = 0.601	F _{1,27} = 0.786, p = 0.383
Male	84.3 ± 11.9	95.6 ± 11.7			
Following					
Female	7.9 ± 2.3	5.3 ± 1.5	F _{1,27} = 10.745, p = 0.003	F _{1,27} = 0.114, p = 0.739	F _{1,27} = 0.155, p = 0.697
Male	29.4 ± 9.3	29.6 ± 8.6			
Allogrooming					
Female	0.7 ± 0.3	1.2 ± 0.6	F _{1,27} = 15.918, p = 0.0005	F _{1,27} = 1.443, p = 0.240	F _{1,27} = 1.313, p = 0.262
Male	40.9 ± 20.2	62.6 ± 17.3			
Huddling					
Female	9.4 ± 3.2	18.9 ± 5.1	F _{1,27} = 5.041, p = 0.033	F _{1,27} = 1.868, p = 0.183	F _{1,27} = 1.091, p = 0.306
Male	30.5 ± 8.4	31.8 ± 8			
Mounting					
Female	0.3 ± 0.3	0.1 ± 0.1			
Male	0 ± 0	0 ± 0			
Fighting					
Female	0 ± 0	0.1 ± 0.1	F _{1,27} = 12.317, p = 0.002	F _{1,27} = 3.797, p = 0.062	F _{1,27} = 3.830, p = 0.061
Male	39.2 ± 16	12.4 ± 5.9			

Mean (in seconds) ± SEM are shown for Avpr1a-Cre male (n = 12, except for n=10 in social behavior time analysis) and female (n = 17) subjects injected with cre-dependent hM4Di virus and treated with CNO or Saline. Results of two-factor ANOVA (Sex (between) x Treatment (within)) are shown for each behavior in the right hand column. The total test period was 20 min or 1200 s.

Table A4. 4*Analysis of Nonsocial Behaviors During an Interaction with a Male*

	Saline	CNO		Statistics	
Non Social Behavior			Sex	Treatment	Sex x Treatment
Female	357.1 ± 22.5	311.4 ± 21.2	$F_{1,27} = 0.692,$ $p = 0.413$	$F_{1,27} = 2.524,$ $p = 0.124$	$F_{1,27} = 0.460,$ $p = 0.503$
Male	368.9 ± 29.5	350.6 ± 32.4			
Grooming					
Female	97.6 ± 14.5	108.6 ± 19.2	$F_{1,27} = 0.0002,$ $p = 0.989$	$F_{1,27} = 0.286,$ $p = 0.597$	$F_{1,27} = 1.560,$ $p = 0.222$
Male	116.5 ± 21.8	89.1 ± 12			
Rearing					
Female	106.5 ± 13.3	85.9 ± 11.5	$F_{1,27} = 0.016,$ $p = 0.899$	$F_{1,27} = 1.994, p = 0.402$	$F_{1,27} = 0.402,$ $p = 0.531$
Male	102.8 ± 23.6	95 ± 20			
Exploring					
Female	153 ± 10.4	116.9 ± 13.5	$F_{1,27} = 1.672,$ $p = 0.207$	$F_{1,27} = 0.901,$ $p = 0.351$	$F_{1,27} = 6.845,$ $p = 0.014$
Male	149.6 ± 14.9	166.5 ± 19.7			

Mean (in seconds) ± SEM are shown for Avpr1a-Cre male (n = 12) and female (n = 17) subjects injected with cre-dependent hM4Di virus and treated with CNO or Saline. Results of two-factor ANOVA (Sex (between) x Treatment (within)) are shown for each behavior in the right hand column. The total test period was 20 min or 1200 s.